The University Of Sheffield.

The Role of Tribbles-3 in Inflammation and Metabolism

Jihan Mesfer Meshref Al-Ghamdi

Registration Number: 080236041

Supervisors:

Dr. Endre Kiss-Toth

Dr. Victoria C Ridger

Prof. Paul G Hellewell

Cardiovascular Science (CVS)

1435-2014

Abstract

There are different studies on the impact of tribbles (TRIBs) on immunity, metabolic, and cardiovascular diseases. Interestingly, the current study identified TRIB3 as a gene that may be involved in the development of hyperlipidemia, inflammatory diseases and insulin sensitivity. Hence our interest in the mechanisms by which TRIB3 may regulate specific aspects of lipid homeostasis, blood glucose level and neutrophil function. It was found that neutrophil chemotaxis towards KC and fMLP, was dependent upon on p38 MAPK and PI3K, which could be controlled by TRIB3. TRIB3 regulates cytokine production, as absence of TRIB3 increased murine interleukin-13 (IL-13) level in thioglycollate-induced peritonitis significantly. Genetic deletion of TRIB3 prevented the increase in circulating leukocyte levels considerably, increased neutrophil migration towards the peritoneum; elevated neutrophil levels persisted in thioglycollate-induced peritonitis. These data supported the theory that TRIB3 deficiency and high fat diet (HFD) have an effect on leukocyte count in peritoneum and blood. However, their effect is varied and appeared to depend on a range of factors. Furthermore, in combination they increased murine weight gain. The project also proved that the effect of TRIB3 knockout on weight was gender specific, as TRIB3-/- males on chow, weighed significantly more than C57B6 mice but this effect was not observed in females. TRIB3 may also increase cell mitosis of murine adipose tissue on HFD. In addition to this, the results confirmed what has previously been published with regards to TRIB3 maintaining normal blood glucose level. TRIB3 was also able to control lipid homeostasis and this is a novel discovery, as knocking out TRIB3 reduced cholesterol and HDL levels significantly in murine blood on HFD. A critical question raised by these results is whether TRIB3 can be used as a treatment for insulin resistance, inflammatory and metabolic diseases. Further studies on TRIB3 need to be conducted to evaluate its multiple-functions, for instance molecular mechanisms of its action on signaling pathways, leukocyte chemotaxis, lipid homeostasis and insulin sensitivity.

Table of Contents

Table of Figures

Abbreviations

ACC	**Acetyl coenzyme A carboxylase**
Akt2	**RAC-beta serine/threonine-protein kinase**
ANOVA	**Analysis of variance**
AP-1	**Activator protein 1**
aPKC	**atypical protein kinase C**
ApoE	**Apolipoprotein E**
ATF	**Activating transcription factor**
BCR	**B Cell antigen receptor**
BSA	**Bovine serum albumin**
BW	**Body weight**
C/EBPs	**CCAAT/enhancer-binding proteins**
CBA	**Cytometric bead array**
CCR1	**C-C chemokine receptor type 1**
CD11b	**Cluster of differentiation molecule 11B**
CD28	**Cluster of differentiation 28**
COP1	**Caspase recruitment domain-containing protein 16**
CPB	**Cardiopulmonary bypass**
CVD	**Cardiovascular disease**
DMSO	**Dimethyl sulfoxide**
DNA-PK	**DNA-dependent kinase**
DW	**Distilled water**
EDTA	**Ethylenediaminetetraacetic acid**
EGF	**Epidermal growth factor**
ERK	**Extracellular signal-regulated kinase**
ESL1	**E-selectin-ligand-1**
EtBr	**Ethidium bromide**
FBS	**Formalin buffered saline**
FKHR	**Forkhead in rhabdomyosarcoma**
fMLP	**Formyl-methionyl-leucyl-phenylalanine**
FSC	**Forward scatter**
GADD153	**Growth arrest and DNA damage transcription factor 153**
GMCSF	**Granulocyte-macrophage colony-stimulating factor**
GPCR	**G protein-coupled receptor**
Grb2	**Growth factor receptor-bound protein 2**
GSK3B	**Glycogen synthase kinase 3 beta**
GTT	**Glucose tolerance test**
H & E	**Hematoxylin and eosin**
H_2O_2	**Hydrogen peroxide**
HBP	**High blood pressure**
HDL	**High-density lipoprotein**
HEPES	**4-(2-Hydroxyethyl)-1-piperazineethanesulfonic acid**
HepG2	**Hepatocellular carcinoma, human**

HFD	**High fat diet**
HGF	**Hepatocyte growth factor**
HRP	**Horseradish peroxidase**
HTRIBs	**Human tribbles homologues**
IBD	**Inflammatory bowel disease**
ICAM-1	**Intercellular adhesion molecule-1**
IFN	**Interferon**
IGF	**Insulin-like growth factor**
IL-1, 4, 8, 12, 13, 17 & 17A	**Interleukin-1, 4, 8, 12, 13, 17 & 17A**
ILK	**Integrin-linked kinase**
IP	**Immunoprecipitation**
ITT	**Insulin tolerance test**
JNK	**C-Jun N-terminal kinase**
KC	**Keratinocyte-derived cytokine, the murine homolog of GRO-α**
LDL	**Low-density lipoprotein**
LFA-1	**Lymphocyte function antigen-1**
LPL	**Lipoprotein lipase**
LPS	**Lipopolysaccharide**
LTB4	**Leukotriene B4**
MAC-1	**Macrophage-1 antigen**
MAPK	**Mitogen-activated protein kinase**
MAPKAPKs, -2, -3 and -5	**Mitogen-activated protein kinase-activated protein kinase**
MAPKK/MKK	**MAPK kinase**
MAPKKK/MKKK	**MAPK kinase kinase**
MCP-1	**Monocyte chemotactic protein 1**
Mdm2	**Mouse double minute 2 homolog**
MIP-1a, -1b or 2	**Macrophage inflammatory protein 1 alpha, 1 beta or 2**
MKPs	**MAPK phosphatises**
MNK1	**MAPK-interacting kinase 1**
MRP-14	**Myeloid-related protein-14**
mTOR	**Mammalian target of rapamycin**
MW	**Molecular weight**
Na_3VO_4	**Sodium orthovanadate**
NaCl	**Sodium chloride**
NaF	**Sodium fluoride**
NFkB	**Nuclear factor kappa-light-chain-enhancer of activated B cells**
NGF	**Nerve growth factor**
NO	**Nitric oxide**
P70S6K	**Serine/threonine kinase**
PAF	**Platelet activating factor**
PBS	**Phosphate buffer saline**
PDGF	**Platelet-derived growth factor**
PDK1	**Phosphoinositide-dependent kinase 1**
PDK2	**Pyruvate dehydrogenase kinase, isozyme 2**
PGC-1	**Peroxisome proliferator-activated (PPAR)-γ coactivator-1**
PH	**Pleckstrin homology**

PI3K	**Phosphoinositide 3-kinase**
PIP	**Phosphatidylinositol 3-phosphate**
PIP2	**Phosphatidylinositol-4,5-bisphosphate**
PIP3	**Phosphatidylinositol-3,4,5-trisphosphate**
PKB	**Protein kinase B**
PKC	**Protein kinase C**
PMA	**Phorbol 12-myristate 13-acetate**
PMSF	**Phenylmethylsulfonyl fluoride**
PPAR	**Peroxisome proliferator-activated receptor**
PSGL-1	**P-selectin glycoprotein ligand-1**
PTX	**Pertussis toxin**
RA	**Rheumatoid arthritis**
RhoB	**Ras homolog gene family, member B**

Chapter 1: Introduction

1.1 Infection, inflammation and signal transduction

Infectious disease is the pathological state resulting from the harmful colonisation of host cells by a pathogenic microorganism. Infection can lead to subsequent tissue injury, which at times may be fatal. Inflammation, however, is the response of the host to infection, injury or irritants, symptoms of which can be swelling, fever, and erythema. It is a protective attempt via a complex biological response of the organism and initiates tissue healing processes.

Acute inflammation represents the initial response to detrimental stimuli by serving to deliver mediators of leukocytes and proteins to the injured site. The inflammatory response is propagated and matured by a cascade of biochemical events involving the local vascular and immune system, as well as different cells within the injured tissue. As the detrimental stimuli are removed, the host returns to a normal state. If the detrimental stimuli cannot be quickly removed, the consequence may be chronic inflammation. Chronic inflammation is recognised by prolonged low-grade damage to cells by the inflammatory process propagated through signal transduction.

Signal transduction is a rapid process involving the binding of ligands and extracellular signalling molecules to plasma membrane receptors on the surface of the cell in order to stimulate intracellular processes. It requires multiple enzymes to carry out a sequential order of biochemical reactions inside the cell. The enzymes are activated by second messengers, which then activate a signalling system. Signal transduction leads to various effects including cellular proliferation and apoptosis [1], alterations in metabolic processes [2], the switching on and off of genes [3] and activation of transcription factors. Newly produced proteins or mRNAs will,

in turn, induce the expression of other genes, leading to a complex cellular response. Thus, a stimulus can lead to new groups of genes being expressed, promoting for example the recruitment of neutrophils, which will be discussed in depth further in the thesis, to sites of infection stimulated by the products of bacteria. A transcriptional program is often defined as the set and order of changes in gene expression that are stimulated in response to specific stimuli [4].

1.2 Development of atherosclerosis is driven by multiple factors, including inflammation, hyperlipidaemia and metabolic syndromes.

Atherosclerosis is thickening of the arteries, which occurs when fatty substances such as cholesterol accumulate in the artery walls and build up plaques (hard structures). Later, plaques may obstruct the arteries and lead to further complications. Artery wall thickening frequently occurs with aging, as with age plaque increases, hence, narrowing arteries and causing further thickening. Plaque formation requires smooth muscle cells, leukocytes, diverse inflammation and immunity response, for example cytokines [5]. Lesion starts as a fatty streak then may become a plaque, which have a lipid core and a fibrous cap.

Study by Cook *et al* in 2006 found that nitric oxide (NO) may have an essential role in the atherosclerotic pathogenesis [6]. Acute coronary syndromes and ischaemic stroke atherosclerotic are a consequence of rupturing a plaque leading to thrombosis with arterial obstruction.

These 'vulnerable plaques' may be widespread and yet may not produce stenosis or ischaemia, therefore are an underlying threat. This type of plaque causes acute clinical presentations such

as acute coronary syndrome and cerebrovascular events, whereas a more stable and stenotic plaque will produce a more chronic clinical picture such as stable angina. These concepts of widespread and vulnerable plaques have implications for management, reinforcing the importance to treat cardiovascular disease (CVD).

1.2.1 Lipid metabolism, inflammation and atherogenesis

Lipogenesis involves conversion of acetyl CoA to fat, which is then stored in the body. Fat is then broken down to produce energy either when the glycogen store is depleted or during starvation when there is no readily available glucose. Excess fat in the body leads to hyperlipidemia.

Hyperlipidemia and inflammation are considered as risk factors for atherosclerosis development [7]. This section will show interactions between dyslipidemia and inflammatory processes leading to atherosclerosis development. Atherogenesis commences with inflammatory cell recruitment to the tunica intima [8]. Activation of endothelial cells leads to expression of leukocyte adhesion molecules, which cause monocytes to adhere to the intima. This results in the expression of scavenger receptors, allowing the uptake of modified low-density lipoprotein (LDL). Cholesterol deposits result in collections of lipid-laden macrophages that form atheromatous plaques. These macrophages produce reactive oxygen species, pro-inflammatory mediators, and tissue factor pro-coagulants that augment local inflammation and encourage thrombotic complications [9].

Various studies indicate that neutrophils (the first white blood cell (WBC) that migrates to the location of inflammation) may have an essential role in human atherosclerosis. Diverse lines of evidence have demonstrated a relationship between increased circulating leukocytes and high

cardiovascular risk [10], [11]. In this situation, neutrophils predominate [12]. Moreover, circulating neutrophils have been shown to be activated in a number of conditions associated with increased risk of atherosclerosis, for example type II diabetes [13], hyperlipidemia [14], obesity [15], HBP (high blood pressure) [16], smoking-dependent vascular inflammation [17]. Naruko *et al* reported that in acute coronary syndromes the predominance is for neutrophils in human lesions [18] and Zernecke *et al* in 2008 have published supporting evidence on the importance of neutrophils in developing atherosclerotic lesions in mice [19]. Baetta *et al* in 2010 showed neutrophils could cause atherogenesis and atheroprogression [20]. Therefore, increased circulating neutrophils are a familiar marker for predicting cardiovascular events, regardless of disease status.

1.2.2 Interactions between inflammation and lipid metabolism

High circulating levels of modified lipoproteins (chylomicrons, very-low-density lipoprotein (VLDL) and LDL) trigger a hepatic inflammatory response through increased uptake by Kupffer cells [21], [22], promoting atherosclerosis. This is probably due to increased circulating proinflammatory mediators. Oxidized phospholipids promote endothelial cell dysfunction. Lysophosphatidylcholine (their derivative compound) may be involved in this step as they up-regulate metalloproteinase. Also oxidized phospholipids may be involved in atherosclerotic lesion progression, particularly those becoming vulnerable and unstable. Possibly, oxysterols and 4-hydroxy-2-nonenal have a main function in the inflammation-driven formation of atheroma. They are both critically implicated in foam cell formation via CD36 scavenger receptor net overexpression and in up-regulating macrophage–smooth muscle cell cross talk, essentially via an overexpression of the transforming growth factor-β (TGF-β) profibrogenic cytokine. Interestingly, cholesteryl linoleate oxidation product 9-oxononanoyl

cholesterol seems able to increase TGF-β and TGF-β receptors steady-state levels in macrophage lineage cells. Oxysterols, and potentially other free aldehydic products for instance 4-hydroxy-2-nonenal have a fundamental function in the process resulting in atherosclerotic plaque instability and rupture due to their ability to up-regulate macrophage metalloproteinase-9 expression and activity, as well as their noticeable proapoptotic influence. In comparison, constitutive levels of tissue inhibitor of metalloproteinase 1 (TIMP-1) and TIMP-2 (its particular inhibitors) are not changed. Furthermore, arachidonic acid oxidation derivatives have major functions in vascular tone modulation and vascular remodeling, essentially by controlling cell proliferation, platelet function, and matrix deposition [22]. Activation of nuclear factor kappa-light-chain-enhancer of activated B cells (NFκB) in hepatocytes enhances atherosclerotic lesion development considerably [23]. Also increased levels of plasma serum amyloid A (SAA) post feeding of cholesterol is accompanied with atherosclerosis [24]. Vascular inflammation as mentioned in 1.2.1. can also be induced by these lipoproteins [25].

In mice, hypercholesterolemia decreases binding and survival of regulatory T-cells in vessel wall, which disturbs the balance between T-cell subsets, resulting in a proinflammatory atmosphere locally [26]. A decrease in plasma cholesterol level restores the imbalance [26]. The content of macrophages found within plaque is also modified and the activity of hepatic and aortic NFκB and plasma SAA levels are reduced [27]. Furthermore, high-density lipoprotein (HDL) may be involved in decreasing vascular inflammation (as it has an anti-inflammatory function) and decreases the expression of vascular cell adhesion molecule 1 (VCAM-1) and intercellular adhesion molecule 1 (ICAM-1) in aortic wall of rabbits [28].

1.3 Cellular and molecular aspects of vascular inflammation

1.3.1 Neutrophils

Neutrophil granulocytes are an essential part of the immune system [29]. Representing 40-75% of leukocytes, they are the most abundant circulating WBC in humans with a standard normal range of 2.5–7.5 x 10^9/l, around 1:1000 of the erythrocyte concentration. They are small cells, approximately 9-10 μm in diameter with a nucleus composed of 2-5 lobes. They contain lots of storage granules in the cytoplasm and very few mitochondria. They use glycogen from which they derive almost all of their energy. These types of cells are terminally differentiated with a lifetime of 5.4 and 0.75 days in human and mice circulation respectively [30]. Neutrophil derives its name from the 'neutral' pink stain obtained on H&E (hematoxylin and eosin) staining.

1.3.2 Phagocytosis

Neutrophils internalise foreign substances or microorganisms, as they are phagocytic, forming a phagosome into which hydrolytic enzymes and reactive oxygen species are released. "Respiratory burst" has been used as a term for the consumption of oxygen during the production of these reactive oxygen species, although this term is not directly related to energy production or respiration per se. However, whilst phagocytosis of pathogens by neutrophils is a fundamental step in host defence, it contributes to tissue damage when overwhelmed.

1.3.3 Leukocyte adhesion cascade

Leukocyte margination (extravasation) from the blood vessels into inflamed tissue requires multi-adhesive stages. The process comprises: capture, rolling, slow rolling, firm adhesion and transmigration [31]. The principle mode of action of this cascade is displayed in figure 1.1.

Capture or tethering and rolling are the initial contact between a leukocyte and the activated endothelial cells. It occurs after extravasation during the inflammatory response when the endothelium is activated [32]. Selectins and their ligands are largely mediating the capture step [32].

While E- and P-selectins are expressed by activated endothelium, the L-selectin is expressed on most leukocytes. Further to the interaction that occurs between L-selectin and endothelial selectins, the P-selectin glycoprotein ligand-1 (PSGL-1) expressed on leukocytes is an essential ligand of the 3 selectins. The binding of PSGL-1 with P- and E-selectins contributes to the leukocytes-endothelium interaction, whereas the binding of PSGL-1 with L-selectin assists in leukocyte-leukocyte interaction [33]. Furthermore, there are other glycoproteins for example CD44 or E-selectin-ligand-1 (ESL1) that can bind to selectins, in the case of E-selectin. For initial leukocyte capture PSGL-1 is required, while ESL1 is required for the conversion to slower and more stable rolling [34]. Eventually, CD44 regulates the rolling speed and intervenes in the PSGL-1 and L-selectin polarization [34].

Selectins stimulate different signalling cascades such as MAPK (Mitogen-activated protein kinase) or Ras pathway [35]. In addition, PSGL-1 stimulates various signalling cascades, leading to an increase in the expression of diverse molecules which may have a role in the next stage of the margination [36].

Rolling slows down the flowing leukocytes [37]. Binding between the E-, P- or L-selectin and their ligands for instance PSGL-1 mediates the temporary rolling interactions between leukocytes and activated endothelium [37]. In addition to the capture and rolling, slow rolling requires P-selectin-PSGL-1 and E-selectin-PSGL-1 interactions [38], [39].

In slow rolling, integrins in particular β2-integrin lymphocyte function antigen-1 (LFA-1) promote firm adhesion from rolling [40], [41]. Signals from chemokines convert the low affinity selectin-dependent interaction to high affinity integrin-mediated firm arrest of leukocytes to the activated endothelium [42] for example cluster of differentiation molecule 11B (CD11b) also known as macrophage-1 antigen (MAC-1), leukocyte integrin, interacts with the immunoglobulin superfamily ICAM-1, its corresponding endothelial receptor [43], [44].

Following firm arrest, leukocytes crawl on the endothelium utilising MAC-1 and LFA-1 integrins [45] until they find a suitable place for transendothelial migration. This occurs either in a transcellular (via the endothelial cell body) or a paracellular (at the intercellular connections) fashion [46], [47]. The reason for the use of one pathway over the other remains unclear. The preference could be related to the level of the endothelium proinflammatory stimulation [48].

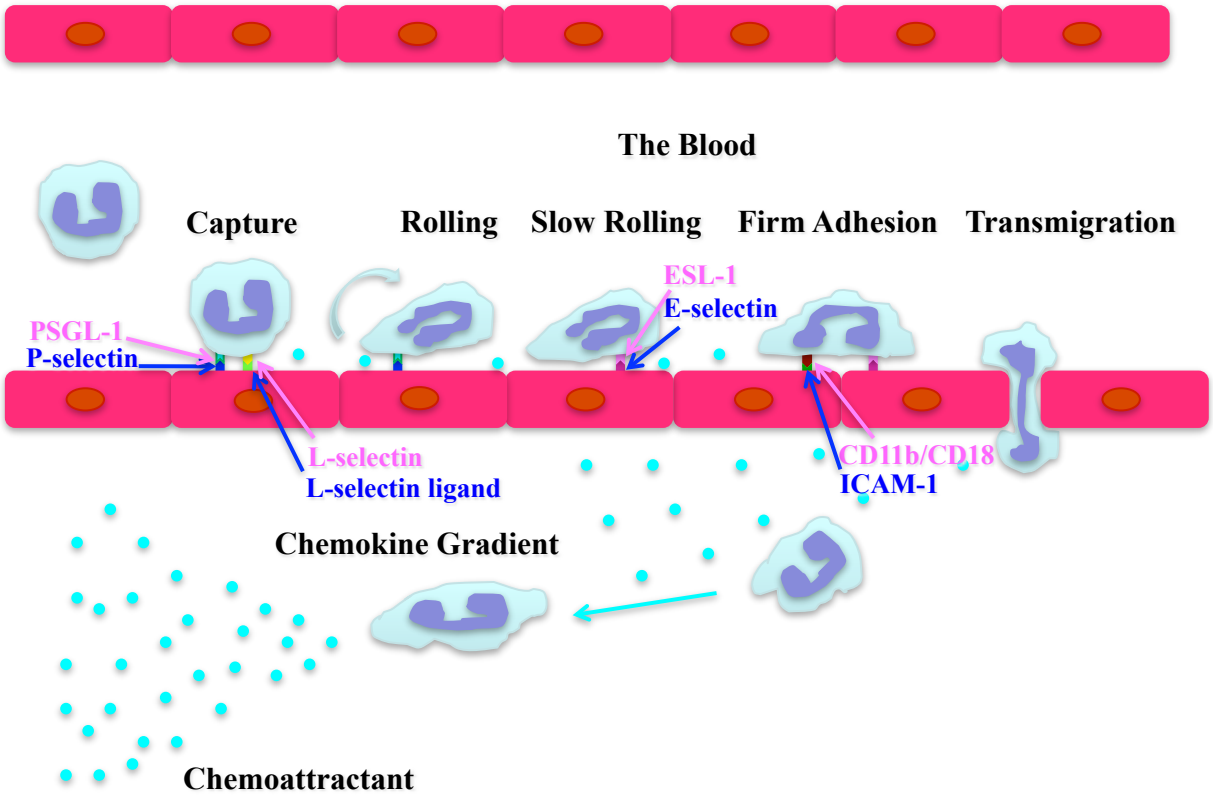

Figure 1. 1: Neutrophil adhesion cascade for chemotaxis

Neutrophil response to chemoattractants released by microbes or other cells of the immune system are required to pass through the stages of the adhesion cascade (capturing from flowing blood, rolling, slow rolling and then adhere firmly to the endothelial cells before transmigrating through blood-vessel walls) to migrate to the site of infection or damaged tissues. These stages occur by expressing particular adhesion molecules on the surface of neutrophil and endothelial cells.

1.3.4 Chemotaxis

Chemotaxis is a directional movement of inflammatory cells, such as neutrophils, in response to a chemical stimulation.

Neutrophils, through their cell membrane receptors, are capable of recognizing chemical gradients of materials such as C5a and IL-8 (CXCL8), which act as attractants. These cells rapidly aggregate at infected and injured sites, due to being highly mobile, attracted by chemokines that are expressed by mast cells, macrophages, epithelium and endothelium when activated. It has been shown that neutrophils react during the first hour after damage to the body. These are the classic characteristics of acute inflammation. Neutrophil cells are attracted to bacterial and endogenous chemoattractant signals. First of all, upon cell damage and/or infection, neutrophils stick to endothelial cells in response to the presence of chemokines at the endothelial interface. Next, they move out of the vessels attracted by other chemokines, which are secreted by nearby macrophages and other serosal cells [49], [50]. Then neutrophils follow end target chemoattractants, complement molecules and bacterial fragments, once in the vicinity of the infectious place. It has been noted that neutrophils face lots of chemoattractants on the way and the existence of a hierarchy of chemokines seems logical. Certainly, it is true that in the presence of many different chemoattractants, these cells give priority to end target chemoattractants like N-formylmethionine leucyl-phenylalanine (fMLP) and C5a which emerge from infected sites, rather than to intermediary chemoattractants such as leukotriene B4 (LTB4) and IL-8 which occur on the path to sites of infection even at high levels of intermediary chemoattractants [49], [51], [52], [53], [54].

Under agarose assays have shown that end target chemoattractants work essentially by activating the p38 MAPK pathway. However, the PI3K (Phosphatidylinositide 3-kinase)/Akt (also known as Protein Kinase B, PKB) cascade works alongside intermediary

chemoattractants [49]. In the presence of competing end target and intermediary chemoattractants, neutrophils show considerable reduction of Akt activation. Since activation of the p38 MAPK cascade inhibits the PI3K/Akt cascade in neutrophils, these processes confirm the hierarchical dominance of end target chemoattractants over intermediary ones. The preferential trafficking of these cells towards end target chemoattractants occurs even at 1/1000th of intermediary signals [49]. End target molecules do not need chemotactic characteristics, because LPS (lipopolysaccharide, p38 MAPK activator) inhibits Akt and consequently prevents movement to intermediary chemoattractants. On the other hand, p38 MAPK inhibitors have been observed to make cells have a preference for migration towards intermediary chemoattractants rather than towards end target ones (because inhibition of p38 MAPK leads to a notable increase in the activity of PI3K/Akt). Consequently, this leads to the drawing out of neutrophils from a location of end target chemoattractant surroundings to intermediary ones [49]. The receptors for chemoattractants are the seven-transmembrane helix receptor family [55], [56], although these chemoattractants have various structures. It has been shown that these receptors, once activated, broadcast signals to G proteins that lead to fast cytoskeletal rearrangements and chemotaxis via activation of downstream processes [57].

Activation of the PI3K cascade is one of the most important processes of neutrophil chemotaxis [58]. Chemotactic receptors use the p110γ isoform (despite isoforms of PI3K being multiple) for downstream actions, which include formation of phosphatidylinositol 3,4,5-triphosphate (PIP3) from membrane phospholipid phosphatidylinositol 4,5-biphosphate (PIP2). This leads to the activation of Akt, by phosphorylation. This is demonstrated by the defects in chemotaxis, which occur in p110γ deficient mice, induced by chemotactic receptor activation, showing neither phosphorylation nor activation of Akt [49]. Certainly, in humans and mice the p38 MAPK has a very necessary function in the chemotaxis of neutrophil cells [59], [60]. This process remains activated in p110 deficient mice, which may explain the accumulation of

neutrophil cells at the site of inflammation [61]. However, various aspects related to these pathways are still vague, such as if the p38 MAPK and PI3K/Akt cascades are overlapping, opposing or complementary to each other [49].

1.3.5 Neutrophil apoptosis

A balance of intracellular death and survival cascades controls neutrophil apoptosis and determines neutrophil fate. Neutrophils undergo apoptosis even in the absence of extracellular stimuli. This is named spontaneous/constitutive programed cell death. Under most conditions, pro-survival and pro-apoptosis cues are received by neutrophils. The balance of these signals seems to detect the net influence [62].

Neutrophils are fast recruited to infectious/injured sites. They have a role in initiation and progression of the inflammatory response. In addition to their several defence mechanisms that destroy pathogens, they are also able to make damage to the surrounding tissue [29]. Neutrophils are supposed to go through constitutive apoptosis, once the pathogens are removed [63]. Apoptosis makes neutrophils not respond to extracellular stimuli, resulting in expression of “eat-me” signals. Therefore, they can be recognized and removed by macrophages in the spleen, bone marrow and Kupffer cells in the liver [64], [65], [63], [66], hence restricting their potentially detrimental effects.

1.3.6 Neutrophils and vascular disease

It has been observed that after ischemic injury, neutrophils play a role after myocardial infarction [67] and cerebral ischemia [68]. There is evidence of a pathogenic function for

neutrophils. Within a day of symptom onset, they accumulate at sites of ischemia in the brain [68]. However, in myocardial infarction they also promote healing and scar formation as they play an essential role in myocardial ischemia–reperfusion. Initiation of the inflammatory-like response occurs through interactions between adhesion molecules on neutrophils and coronary vascular endothelium. Organic NO-donor agents that interdict neutrophil responses may be cardioprotective [69]. It is also noted, that there is a strong correlation between the risk of acute myocardial infarction and peripheral-blood neutrophil count [70]. Sleep restriction predisposes to cardiovascular disease as it increases WBC counts, mainly neutrophils [71].

In the various intermediate and advanced stages of atherosclerosis, the existence of neutrophils has been noted. In atherosclerotic lesions, neutrophils adhere to the lesional cap and in the adventitial layer [72]. Activation of neutrophils might lead to platelet activation and subsequently cause thrombosis in coronary arteries with atherosclerosis [67]. In addition, a study published by Tuttle *et al* suggested that platelets and neutrophils have a greater chance of being activated in diabetic women than diabetic men. They may play a role in thrombosis/inflammation and the severity of coronary heart disease [73]. It has also been observed that platelets [74] and neutrophils [75] are activated during cardiopulmonary bypass (CPB). It has been proposed that hyperinsulinaemia might accelerate atherosclerosis by directly stimulating neutrophil migration through MAPK activation [76].

The involvement of neutrophils in vascular diseases has been outlined above. Possible contribution of neutrophils in atherogenesis has been highlighted. However, as neutrophils also promote healing in myocardial infarction, it may be possible to utilise this function for treatment purposes.

1.4 Signalling pathways

1.4.1 Signal transduction mediated by mitogen-activated protein kinase (MAPK) cascade

The MAPK cascade represents one of the major signal transduction pathways that respond to extracellular stimuli such as mitogens (chemical substances that trigger mitosis causing cell division), and then controls diverse activities of cells, for example cellular proliferation [77], gene expression, growth, mitosis, differentiation, inflammatory responses, chemical and physical stress and cell survival/apoptosis [78]. On the other hand, the MAPK cascade is dys-regulated in various diseases, such as cancer, inflammatory, and immunological disorders. Therefore, it is an important target for therapy [77].

It has been recognized that mammalian cells have at least 14 genes encoding for mitogen-activated protein kinase kinase kinases (MAPKKKs), seven mitogen-activated protein kinase kinases (MAPKKs), and 12 MAPKs [77]. 'MAPK cascade' refers to any three kinase cascades activated by sequentially phosphorylating each other in response to various stimuli. For example, stress on a cell, growth factors, adherence of a cell, neurotransmitters, and cytokines can all lead to a diverse range of physiological responses.

Generally, the scheme of the MAPK cascade is composed of three kinase/phosphatase cycles, constructed into a three-tiered pathway. This pathway consists of a MAPK activated through phosphorylation by a MAPKK/MKK, which is phosphorylated by a MAPKKK/MKKK [79]. However, MAPKs are inactivated by a phosphatase family called MAPK phosphatases (MKPs) [80], [79], which plays an important role in regulation of MAPK through a phosphorylation cascade [81].

It has been documented that most MAPK cascade stimulators begin signalling by stimulating cell surface receptors that congregate into a receptor signalling complex. Then they activate a MAPKKK through a small GTPase [79]. The signalling process within the MAPK-cascade module seems to be fairly specific, which is common with a linear structure. However, there is a large body of literature demonstrating cross talk between the different MAPK pathways. For instance, it has been proposed that during apoptosis extracellular signal-regulated kinase (ERK) pathway activity is suppressed by c-Jun N-terminal kinase (JNK)/p38 kinases [82]. The number of MAPK effectors is vast and varied, including protein kinases, cytoskeletal proteins, and transcription factors. As a result of activation, MAPK can translocate into the nucleus and regulate gene transcription via its effect on the structure of chromatin and modifying of transcription factor activity [83], [79].

MAPKs have been uncovered as the essential regulators of pro-inflammatory cytokines, controlling, for example, the production of IL-1, IL-12, and tumor necrosis factor (TNF). In addition, MAPKs play very important roles in signal transduction pathways through the T-cell receptor/cluster of differentiation 28 (TCR/CD28) and toll-like receptor (TLR), B cell antigen receptor (BCR), and IL-1, IL-17, and TNF-α receptors [84], [85], [86] and chemoattractants (eg. fMLP) [49].

MAPK cascades have been studied widely, from yeast to humans. It has been discovered that there are three MAPK families in mammalian cells [77], [87]:

- Classical MAPK, known as ERK.
- JNK/SAPK (stress-activated protein kinase).
- P38 MAPK.

Cross talk between MAPK pathways are illustrated in the following figure, which demonstrates the essential components of these processes.

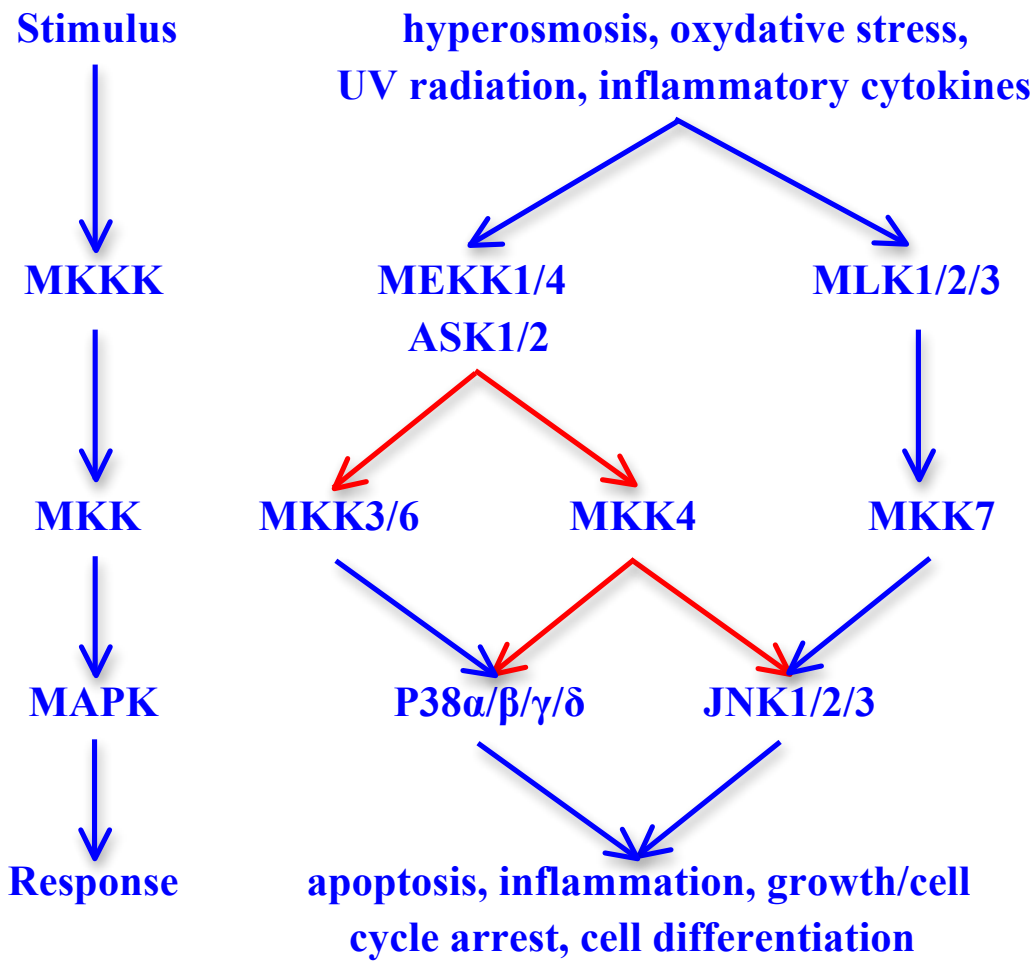

Figure 1. 2: Cross talk between different MAPK pathways

Activation of MAPKKKs leads to the phosphorylation of MAPKKs and ultimately to the activation of three MAPK families; extracellular signal-regulated kinase (ERK), C-Jun N-terminal kinase/stress-activated protein kinase (JNK/SAPK), and P38 MAPK. The MAPK cascades regulate diverse cellular, physiological and developmental processes, including apoptosis and differentiation. Red arrows are to show the crosstalk.

1.4.1.1 ERK cascade

The Raf-MEK-ERK cascade is one of the most well-documented MAPK signalling pathways. It has been reported that the activation of receptor tyrosine kinases (RTKs) and tyrosine kinase receptors enhances the stimulation of these MAPKs [77]. For instance, signalling proteins linking epidermal growth factor receptors to MAPK activation contain guanine nucleotide exchange protein (an adaptor protein Grb2), a small GTP binding protein, Sos, $p21^{ras}$, a sequence of protein kinase cascades, involving MAPKKK, c-RAF-1, and MAPKK (for example MEK1 and MEK2). MEKs phosphorylate ERK1 and ERK2 (p44 MAPK and p42 MAPK, respectively), therefore increasing their activity [88], [77]. The activated ERKs enter the nucleus and fulfil various functions such as activation of transcription factors, altering gene expression to stimulate mitosis, differentiation or growth [77]. It has been observed that whilst the ERK pathway has a minor function in the microbicidal activity of neutrophils, it is essential in regulating the migration of neutrophils in response to fMLP [89]. A further study by Katsube *et al* in 2008 found that activation of the ERK cascade in human neutrophils upon exposure to calpain inhibitors is followed by active migration of neutrophils (chemotaxis) [90].

1.4.1.2 JNK cascade

JNK α, β, and γ are encoded by three genes with 12 conceivable isoforms [91], [77]. Many MAPKKKs stimulate the JNK family, including the ASK group, MLKs, the MEKK group, TAKI, and Tpl2 [92], [77]. JNK can interact with c-Jun through its NH2-terminal activation domain and phosphorylate it on Ser-63 and Ser-73. c-Jun/c-fos combination forms activating protein-1 (AP-1) transcription factor [93], [94]. Therefore, it starts a positive feedback loop. There are different substrates for JNK, for instance NFAT4, DPC4, Elk-1, c-Jun, Sap-1a, p53, and activating transcription factor 2 (ATF-2) [95], [77]. As a result of activation of these

factors, there is an increased expression of c-Fos protein and a further increase in the level of AP-1. In addition, JNK phosphorylates JunB, JunD, and the Ets-related transcription factor PEA3 as well [96], [97], [77]. JNK stimulation is associated with proliferation, differentiation and apoptosis [77]. A study by Katsube *et al* reported that activation of the JNK cascade in human neutrophils upon exposure to calpain inhibitors is followed by active migration of neutrophils [90]. A further study by Kato suggested that JNK isoforms are involved in tumour necrosis factor α (TNFα)-induced neutrophil apoptosis and granulocyte-macrophage colony-stimulating factor (GMCSF)-mediated anti-apoptotic effect on human neutrophils, as well as in TNFα-induced and GMCSF-induced superoxide release [98].

1.4.1.3 p38

Stress on cells (including UV irradiation, high osmotic stress, heat shock, protein synthesis inhibitors), lipopolysaccharide, proinflammatory cytokines (for example TNF-α and IL-1) and specific mitogens activate the mammalian p38 MAPK families. At least four isoforms of p38 have been discovered (p38α, β, γ, and δ). MAPKK SKK3 (MKK6) can phosphorylate all of these isoforms. However, some p38 isoforms can be phosphorylated by other MAPKKs. p38α, γ, and δ can be activated by MKK3, whereas only p38α can be activated by MKK4 [77]. p38δ is essential for Interferon (IFN) signalling, in which it directs both the phosphorylation and the activation of cytosolic phospholipase A2. It has been observed that IFNα or γ stimulation of p38 MAPK also leads to the phosphorylation of Ser 727 of the transcription factor Stat1 [99]. The transcription factors Growth Arrest and DNA Damage transcription factor 153 (GADD153), Sap-1a, and ATF-2 can also be phosphorylated by p38 [100]. Moreover, NF-κB-dependent transcription can be regulated by p38 after its entrance into the nucleus. Interestingly, specific p38 isoforms stimulate non-transcription factor targets like the

MAPKAPKs (mitogen-activated protein kinase-activated protein kinases), -2, -3 and -5 and MNK1 (MAPK-interacting kinase 1), a related protein. P38 MAPK has a number of roles in inflammation, proliferation, differentiation, development, survival, apoptosis, as well as stress responses [77]. Katsube *et al* reported that activation of the p38 cascade in human neutrophils upon exposure to calpain inhibitors is followed by active migration of neutrophils [90]. In addition, previous findings demonstrated that in human neutrophils Myeloid-Related Protein-14 (MRP-14) is a potential mediator of p38-dependent functional responses [101]. Furthermore, a study by Browning *et al* examined the effects of NO on human neutrophils in the stimulation of p38 by LPS found that NO is sufficient to cause an increase in phosphorylation of p38 [102].

1.4.2 Signal transduction mediated by phosphoinositide 3-kinase (PI3K) cascade

The lipid kinase, PI3K, is a family of enzymes organized into 3 classes [103]; class I (catalytic p110 subunits and p85 adaptors) [104], class II (>200 kDa, characterized by a C-terminal containing a C2 domain) [104] and class III (homologous to the archetypal Vps34p characterized in Saccharomyces cerevisiae [104].

PI3K is activated by:

- Diverse forms of cellular stress, for example swelling of the cell or oxidative stress.
- Diverse hormones like insulin, platelet-derived growth factor (PDGF), epidermal growth factor (EGF), hepatocyte growth factor (HGF), insulin-like growth factor (IGF) and nerve growth factor (NGF).
- Ras activation.

- Signals coming from binding of receptors with the extracellular matrix molecules.
- Chemokines; neutrophils prefer to migrate towards the intermediary chemoattractants via PI3K/Akt (as discussed earlier).

This lipid kinase phosphorylates plasma membrane phosphatidylinositols, the 3rd OH group of the inositol [105], for instance generating PIP3 from PIP2. This PIP3 recruits protein kinases at the plasma membrane. These kinases like phosphoinositide-dependent kinase 1 (PDK1) and Akt bind with their pleckstrin homology-(PH)-domain to PIP3. Akt needs full activation through its phosphorylation at Thr-308 by PDK1 and at Ser-473 by PDK2 [106]. PDK1 further activates atypical protein kinase C (aPKC) and Serine/threonine-protein kinase (SGK), which alongside with Akt, phosphorylates a broad range of cellular signalling molecules that have a function in:

- Cell growth regulation [107], cellular proliferation [107], cell cycle, including serine/threonine kinase (p70S6K), forkhead box protein O1 (FKHR), mammalian target of rapamycin (mTOR) and glycogen synthase kinase 3 beta (GSK3β).
- Apoptosis, including mouse double minute 2 homolog (Mdm2), IκB, caspase 9 and FKHR.
- Transport, including diverse channels and transports.
- Chemotaxis (as described above).

In addition, Akt further activates mTOR [108] which stimulates the uptake of nutrients including iron, amino acids, glucose and cholesterol. Phosphorylation of p70S6K is regulated by mTOR. PDK1 may similarly stimulate p70S6K. mTOR, in turn, further activates eIF4E-binding protein-1 and is therefore involved in protein translation.

mTOR, DNA-dependent protein kinase, integrin-linked kinase or Akt itself via autophosphorylation have been proposed to act as PDK2 [109], [110]. mTOR is part of two diverse complexes, mTOR complex 1 (mTORC1) and mTORC2, which controls different proteins [111]. mTORC2 works upstream and is proposed to phosphorylate Akt, while mTORC1 works downstream of Akt [111]. There are studies proposed that variety in Akt signalling may in part be due to different roles of the three Akt isoforms Akt1/PKBα, Akt2/PKBβ and Akt3/PKBγ [112]. It has been indicated that Akt1 has a critical function in cell survival [113], [114], whereas another studies proposed Akt2 has a central role in the maintenance of glucose homeostasis [114], [115] and Akt3 function has been suggested in brain development [116]. Liu *et al* demonstrated that Akt1 is the dominant isoform expressed in neutrophils. Additionally, bacterial infection and neutrophil activation lead to downregulate this isoform [117], whereas Chen *et al* found Akt2 has the predominant role in modulating neutrophil functions and showed for the first time that Akt1 and Akt2 act differently in controlling main neutrophil functions [118]. Fischer-Posovszky *et al* found proliferation and adipogenic differentiation of human adipocytes is Akt2-dependent in preadipocytes, while Akt1 and Akt2 are equally important for regulating insulin-stimulated metabolic cascades [119].

It has been found that inhibition of PI3K (by Wortmannin and LY294002) stimulated lipopolysaccharide (LPS)-induced coagulation, as well as inflammation which causes decreased survival of endotoxemic mice. Therefore, in endotoxemic mice, the PI3K-Akt cascade may suppress inflammation and coagulation [120]. It is also known that PI3Ks control phagocytosis. PI3Ks class 1 and 3 work consecutively in the production and maturation of phagosomes. Their products, PIP3 and PIP (phosphatidylinositol 3-phosphate), are assembled temporarily at various stages [121].

The activation of PI3K occurs in response to the dissociation of Gα subunit from Gβγ subunits upon the binding of chemoattractants with G protein-coupled receptor (GPCR). PI3K then converts PIP2 to PIP3. PDK1 and Akt by their PH domain are recruited to the plasma membrane through binding to PIP3. PDK1 activates Akt by phosphorylation resulting in the activation of several other proteins responsible for a range of cellular functions (Figure 1.3).

Published data indicated that PI3Kγ controls T cell activation, neutrophil migration, thymocyte development and the oxidative burst [61]. In addition, preceding findings proposed that platelet activating factor (PAF) causes intracellular alkalinisation through PI3K-MAPK activation. This influence in bovine neutrophils is upstream controlled by PAF receptor, pertussis toxin (PTX)-sensitive G protein, tyrosine kinase, PI3K and MEK1/2 [122]. Furthermore, it has been published that PI3Ks and mTOR in the innate immune system integral players in coordinating defence mechanisms. Accordingly, in neutrophils and mast cells PI3K and mTOR positively regulate immune cell activation [123], as already alluded to in 1. 3. 4.

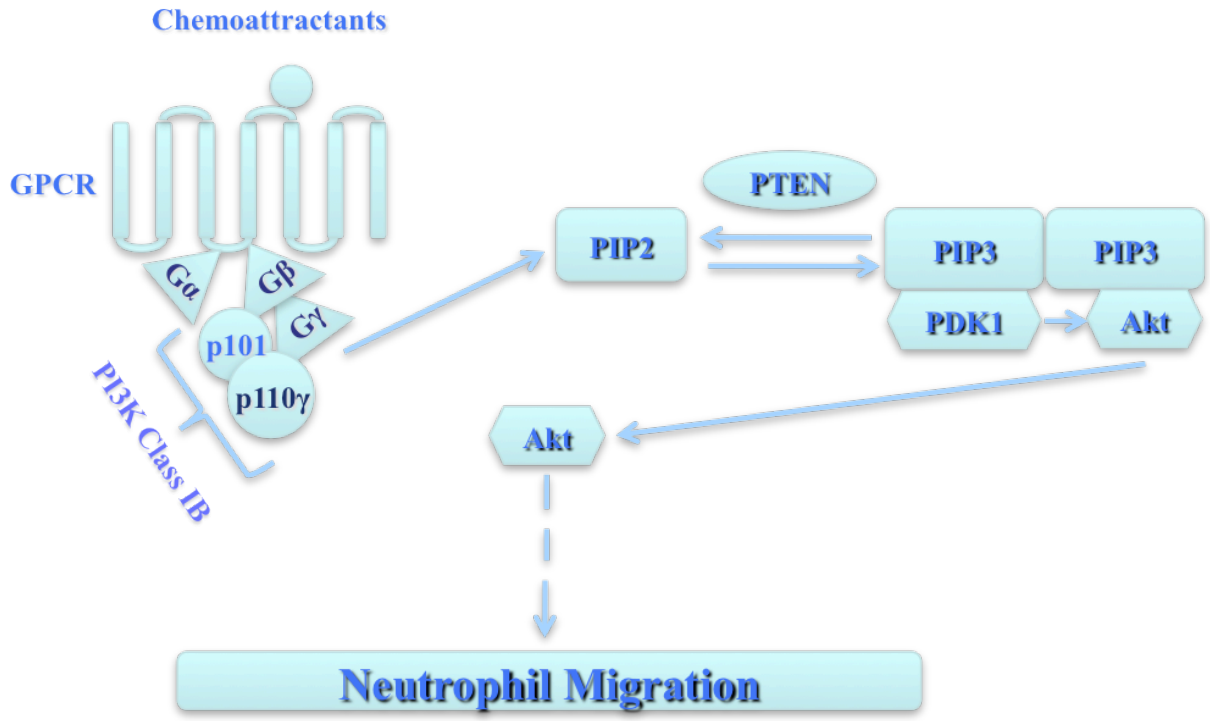

Figure 1. 3: Neutrophil migration by the PI3K/Akt signalling cascade

In response to binding of chemoattractants with G protein-coupled receptor (GPCR) the Gα subunit dissociates from Gβγ subunits causing activation of PI3K. This results in the plasma membrane phosphatidylinositol-3,4,5-trisphosphate (PIP3) being converted from phosphatidylinositol-4,5-bisphosphate (PIP2). Phosphoinositide-dependent kinase 1 (PDK1) and protein serine-threonine kinase (Akt) recruit to the plasma membrane as their plackstrin-homology (PH) domains bind PIP3. PDK1 activates Akt by phosphorylation. The Activated Akt then phosphorylates other proteins to promote neutrophil migration.

1.4.3 Other inflammatory signal transduction pathways

In addition to the signaling pathways introduced above, further signalling systems also play an important role in regulating inflammatory activation of cells. These pathways transduce a large variety of external signals, resulting in a wide range of cellular responses such as differentiation, growth, inflammation and apoptosis. The following pathways are just examples of many other pathways involved, although are not central to the background of this project.

NFκB is a transcription factor possessing essential functions in several signalling cascades [124]. This transcription factor exists in an inactive form in the cytoplasm of the cell [125]. However, in response to various stresses like heat shock, inflammation, and infection [124], NFκB can be activated. Upon activation, this transcription factor translocates to the nucleus and promotes the expression of a number of genes [125], including proinflammatory cytokines and chemokines. NFκB has been associated with tissue repair as well as apoptosis [126]. It has been suggested that modulation of signalling actions which mediate activation of this transcription factor, may have an enormous potential in treating many disorders and also repairing tissue [127]. Furthermore, in case of neutrophil-mediated inflammatory disorders, Miskolci *et al* in 2007 demonstrated that NFκB is continuously activated in stimulated human neutrophils [128].

IFNs are cytokines produced by cells in response to pathogens like viruses, bacteria, parasites and tumors. IFNs are responsible for activating signal transducer and activator of transcription (STAT) complexes, which are transcription factors that control particular immune system genes expression by binding to their receptors. Jones *et al* in 2006 found during *E. coli* pneumonia, IL-6 has key roles in activating STAT1 and STAT3, enhancing recruitment of neutrophils and reducing bacterial burden [129].

1.5 Tribbles (TRIBs)

Recently, a family of signalling regular proteins, known as TRIBs have been identified as regulators of intracellular signalling pathways and a number of physiological processes including development [130]. In addition, TRIBs are thought to be involved in cancer and diabetes mellitus [130]. Through their unique action, TRIBs can co-ordinate activation and suppression of different interacting intracellular signalling processes. Therefore, these proteins seem to be essential in determining cell fate while responding to the challenges of the environment [131]. Eder *et al* in 2008 detected TRIB2 as a novel controller of inflammatory activation of monocytes [132], while Wei *et al* in 2012 demonstrated TRIB2 as a novel controller of TLR5 signaling cascade. Changed expression TRIB2 may have a role in inflammatory bowel disease (IBD) [133].

It has been recorded that there are different mechanisms for regulation of cell function. These include enzymes and regulator proteins that may not have a catalytic role; rather they join other proteins and then alter their function. Kinases, lipases and phosphatases are examples of catalytic signal transducers. The TRIB protein family seems to have an undetermined location in this classification. It is still unclear whether a signal kinase-like domain, which TRIB proteins have, has catalytic activity or not. A review by Dobens and Bouyain 2012 discussed TRIBs and found that they may function in some situations as active kinases and in others as passive adaptor proteins [134]. Furthermore, this protein family does not have the protein-protein interaction domains, such as PDZ, SH2, and SH3 which represent a typical characteristic of adaptor/scaffold proteins, as well as several other kinases. Technically, lack of interaction domains and enzyme activity is very unusual, and very interesting, because there are a considerable number of interactions, positive and negative, between TRIB proteins and various signalling cascades in diverse cellular systems [130].

With regards to the role of TRIBs in adipose tissue, a study by Ostertag *et al* in 2012 showed adipose tissue inflammation was regulated via TRIB1 [135], whereas Sung *et al* in 2012 observed enhanced expression of TRIB1 in macrophage of experimental atherosclerotic mice [136].

Takahashi *et al* (2008) showed TRIB3 down-regulates PPAR-γ (peroxisome proliferator-activated receptor-γ), a master controller of adipocyte differentiation, and regulates adipogenesis [137].

Literature relating to the heart includes that of Ti *et al* (2011) who showed in the diabetic rat model TRIB3 gene silencing alleviates diabetic cardiomyopathy [138]. In addition to this Prudente *et al* in 2012 detected that TRIB3 has a role in mechanisms of metabolic and cardiovascular abnormalities in humans [139].

A review in 2012 by Angyal and Kiss-Toth summarised evidence showing that allelic variants of TRIBs were found associated with the regulation of fatty acid synthesis, insulin resistance, plasma triglyceride (TG) level and HDL cholesterol level. In addition, they discussed the importance of TRIBs in human disease [140].

1.5.1 Identification of TRIBs

TRIBs proteins have been identified by three different methods:

- The first method depended on the genetic features. These genes in diverse physiological circumstances were differentially expressed. It has been shown that in mitogen stimulated thyroids, canine TRIB2 is a differentially expressed gene [141]. In granulosa cells of chorionic gonadotropin, downregulation of bovine TRIB2 stimulated dominant

follicles [142]. During the death of a neuronal cell, rat TRIB3 was induced [143]. In a fatty liver dystrophy mouse, there was an altered expression of mouse TRIB3 [144].

- The second approach necessitated functional screens. This strategy identified human TRIB1 as a modulator of MAPK signalling cascades [145], [146], and Drosophila TRIB as an essential regulator of morphogenesis [147], [148].
- The last strategy depended on interaction screens. Interactions between TRIBs and a wide range of signalling protein molecules, including Akt have been demonstrated [130].

1.5.2 TRIBs function *in vivo*

The interactions between TRIBs and other protein molecules have been focused on in several studies. However, there is also emphasis on the roles of TRIBs *in vivo*. During morphogenesis in Drosophila, TRIBs regulate *string* [147], [149]. During oogenesis, this regulatory function was recognized in a diverse developmental setting as well. A set of highly specialized cell divisions is involved in this process; a number of which are regulated by expression levels of TRIB proteins [149]. Naiki *et al* (2007) found TRIB2 inhibits differentiation of adipocyte by suppressing Akt and CCAAT/enhancer-binding protein β (C/EBPβ) in mice [150]. TRIBs interaction with other proteins has also been demonstrated by Saka *et al* in 2004. They found that mitotic progression and nervous system development required a TRIBs orthologue in Xenopus [151]. Obviously, there are diverse experiments demonstrating an essential regulatory function for TRIBs in cellular regulation and development, although TRIBs' role and molecular mechanism of action in signalling pathways are unclear as of yet [130].

1.5.3 TRIBs interacting proteins

Overexpressed TRIBs activated slbo ubiquitination. It has been observed that, for proper cellular behavior during morphogenesis, accurate regulation of slbo levels is needed. There is a suggestion that a key regulator of this pathway may be TRIB [152]. The interaction between TRIB1 and MAPKKs [145] have been recognized in the literature. There is a molecular association between MAPKKs and TRIB3, when overexpression in Hela cells takes place [145], likewise to TRIB1. However, TRIB3 is linked to MEK1 and MKK7 instead of MKK4. Nevertheless there is a suggestion of some functional specificity for these two members of the TRIBs family. The biological relevance of these results is still poorly understood and requires further studies [145]. It has been identified that TRIB2 proteins interact with overexpressed Akt [153]. The PI3K cascade activates a serine/threonine kinase, Akt, which plays an essential function in the cell, such as in the activation of the cell, cell division and apoptosis. Proteins that interact with an Akt1 mutant (which lacks the N-terminal PH domain) demonstrated in yeast two-hybrid system (Y2H) that TRIB3 is a binding partner [153]. In 239T cells, in a mammalian 2-hybrid assay, the interaction was verified showing that in Akt1, 240-315 aa are necessary for this interaction. In addition, it has been shown that *in vitro* translated TRIB3 interacts with baculovirus expressed Akt1. Co-precipitation assay confirms interaction between endogenous TRIB3 and Akt, using HepG2 cell extracts (Hepatocellular carcinoma, human) [153]. There may also be an interaction between TRIB2 and ras homolog gene family, member B (RhoB) [154]. Koo *et al* in 2004 found TRB3 is a target for PPAR-α in liver as the induction of TRB3 promotes insulin resistance via peroxisome proliferator-activated (PPAR)-γ coactivator-1 (PGC-1) [155].

1.5.4 TRIBs cellular localization

There are many investigations showing different TRIBs intracellular localizations [130]. Interpretation requires caution as these are based on overexpression. Whilst these overexpressed proteins often imitate the localisation of endogenous genes, sometimes overexpression leads to experimental artefacts. Whilst the majority of signalling proteins work as part of multiprotein compounds, exorbitant amounts of individual parts may lead to abnormal intracellular localization.

1.6 TRIBs, MAPK, and PI3K pathways

Control of MAPK pathways is essential for regulating various cellular responses. Human TRIBs homologues (HTRIBs) organize MAPK activity. MAPK binds with TRIBs and controls the levels of their steady state. Moreover, this protein family, TRIBs, coordinates p38 MAPK, JNKs, and ERKs activation with diverse relative activity levels for the three MAPK categories according to TRIB expression level [145].

It has been shown that a canine TRIB-2-like protein was reported as a very labile cytoplasmic phosphoprotein, mitogen stimulated and transiently expressed. However, its biological role is not fully understood [156], [141]. During apoptosis of nerve cells, rat TRIB is rapidly upregulated [143]. In the liver, TRIB3 controls Akt activation by insulin [153], as well as regulating the activity of activating transcription factor 4 (ATF4) [157], [158]. TRIBs bind to MAPKK and control the activation of MAPK. It has been recorded that TRIBs seem to play an important role in the MAPK cascade, but at high concentrations they inhibit this cascade. To explain these results, many mechanisms are hypothesised; for example, TRIBs could act as scaffolds [145]. MAPKKs conjugate TRIBs and stabilize them. TRIBs and TRIB mRNA are

rapidly stimulated by mitogen and have short half-lives [156], [141]. Therefore, these findings suggest that TRIB/MAPK interactions are dynamic and are under the control of extracellular signals. Furthermore, MAPK pathways are proposed to have a nonlinear behaviour due to incorporation of a positive feedback loop [159]. TRIBs might behave either as activators of MAPK activity or as inhibitors, according to the TRIB to MAPKK ratio in the cell. Similarly, TRIB mediated regulation of NFκB [160], [161], and the control systems of the cell cycle have been found [162].

TRIB3 has been implicated in the regulation of metabolic processes, the stress response and cell viability. It also has a role in a number of medical conditions such as cardiovascular disease, diabetes and insulin resistance [163]. It has been identified that Akt activation is negatively regulated by TRIB3 and that insulin stimulates expression of TRIB3. Depending on cell type, TRIB3 expression is stimulated by insulin, for example in the liver and adipocytes, but not in muscle and beta cells. Expression of TRIB3 by the insulin hormone inhibits Akt in Fao hepatoma cells [164]. Furthermore, expression of this type of TRIBs by insulin needs PI3K [164]. On the other hand, inhibition of Akt induces expression of TRIB3, while inactivation of the expression of protein kinase C, zeta (PKCτ) restrains expression of TRIB3 enhanced by insulin. Therefore, as a result, PI3K stimulates signals both positively and negatively to regulate the expression of TRIB3. It has been proposed that TRIB3 expression enhanced by insulin acts as an indicator for how the many signalling processes stimulated by insulin are balanced [164]. In addition, a study by Takahashi demonstrated that TRIB3 containing a kinase domain without enzymatic activity negatively regulates PPARγ transcriptional activities by protein-protein interaction [137].

Further recent studies looked at the role of TRIB3 in metabolism. A study by Avery *et al* in 2010 found that TRIB3 induction is an essential part of the endoplasmic reticulum stress

response in cardiac myocytes, in addition to TRIB3 antagonizes cardiac myocyte survival and cardiac glucose metabolism [165]. Reinforcing importance of TRIB3, Liu *et al* in 2012 points the finger at TRIB3 as a potent physiological controller of insulin sensitivity and nutrient metabolism under conditions lack and excess nutrient [166].

1.7 The role of TRIB3 in vascular inflammation, insulin signalling and lipid homeostasis

Du *et al* proposed in 2003 that TRIB3 regulates insulin signalling through Akt in liver [153]. Contradictory results in rat hepatocytes demonstrate that TRIB3 overexpression has no effect on insulin signaling [167]. Qi *et al* in 2006 proposed the function of TRIB3 in lipid metabolism in the adipocyte, which is the interaction of TRIB3 with acetyl coenzyme A carboxylase (ACC) and with caspase recruitment domain-containing protein 16 (COP1) which results in ACC degradation [168]. A publication in 2008 by Takahashi *et al* reported that TRIB3 inhibits differentiation of adipocyte and accumulation of intracellular TG through suppressing PPARγ transcriptional activity [137]. Okamoto *et al* in 2007 recorded no changes occurring in TRIB3-/- mice compared to wild type (WT) littermates in glucose and lipid homeostasis, and insulin dependent signalling responses [169]. However, Weismann *et al* (2011) observed knockdown rats gained considerable weight, improved insulin sensitivity and increased PPARγ expression. Unexpectedly, Akt activation was not altered remarkably, which suggests TRIB3 may regulate lipid synthesis through PPARγ mediated mechanism [170]. It is possible that TRIB3 controls signalling mechanisms modulating lipid metabolism, and TRIB3 dysfunction can lead to developing disease such as type II diabetes and metabolic syndromes.

Literature looking at vascular inflammation include that of Wang *et al* in 2012 whom recorded that TRIB3 silence in diabetic apolipoprotein E (ApoE)-/-/LDL receptor-/- mice suppresses

atherosclerosis and stabilises plaques [171]. Furthermore, Andreozzi *et al* in 2008 found TRIB3 R84 variant is a more effective Akt inhibitor, thus *in vitro* impairs insulin signaling of human endothelial cells. This finding proposing TRIB3 R84 variant may contribute to genetic susceptibility to endothelial dysfunction and coronary artery disease [172].

A study by Prudente (2005) showed Q84R a human TRIB3 polymorphism reduced insulin-induced Ser473-Akt phosphorylation in human HepG2 hepatoma cell lines. Results suggest that the TRIB3 gene has a function in human insulin resistance and related cardiovascular risk [173]. This proposes a possible link between TRIB3 and a chronic inflammatory disease.

Given the above, it seems plausible despite the discrepancies in the literature to suggest TRIB3 as an essential regulator of signalling mechanisms, controlling leukocyte function, glucose metabolism and lipid hemostasis. Furthermore, it has grown gradually based on laboratory data the dysregulation of TRIB3 function could be involved in human disease such as hyperlipidemia, type 2 diabetes, inflammatory and cardiovascular diseases. However, the mechanism by which TRIB3 contributes to such syndromes remains elusive.

1.8 Hypothesis

I hypothesize that neutrophilic inflammation may play a role in metabolic regulation via TRIB3. TRIB3 plays a key role in signalling pathways such as p38 MAPK and PI3K, which in turn may control neutrophil chemotaxis towards keratinocyte-derived cytokine, the murine homolog of GRO-α (KC) and fMLP. It is also possible TRIB3 may regulate the level of circulating glucose and lipid.

1.9 Aims of the project

I. Determine the role of TRIB3 in neutrophil signalling cascade regulation in response to chemoattractants.

II. Determine the effect of absence of TRIB3 on neutrophil function and chemotaxis.

III. Determine the role of TRIB3 on neutrophilic inflammation.

IV. Determine the role of TRIB3 in development of metabolic disease.

Chapter 2: Materials and methods

2.1 Materials

The study involved the use of different materials including chemicals and other laboratory substances (appendix 1), equipment (appendix 2) and software (appendix 3).

2.2 Methods

2.2.1 Animals

Mostly male C57B6 mice were used in wild-type animal experiments. Mouse supplier: Harlan UK (Bicester), work area: Biological Services Unit, University of Sheffield. TRIB+/- mice [B6;129S5-TRIB3Gt(OST324148)Lex/Ieg obtained from European Mouse Mutant Archive, EMMA; ID: EM-02346, LEXKO-1947] were back crossed with C57B6 for ten generations and were then inter-crossed to generate TRIB3 embryos. This line was developed using the OST324148 OmniBank® ES cell line from a sequence tagged gene trap library [174]. Briefly, the gene trap vector included a two expression cassettes. The first cassette encoded for a splice acceptor site, followed by a fusion protein of beta-galactosidase and neomycin, thereby disrupting transcription of the targeted mRNA. The second cassette encoded for a "diagnostic marker", followed by a splice donor site and was used to determine the site of insertion for the targeting vector by 3' RACE. Using this gene trap vector, the TRIB3 allele was targeted in the first intron. Exons 2-4 encode for the TRIB3 Open Reading Frame; insertion of the gene trap vector prevented the expression of the TRIB3 protein. TRIB3-/- mice were obtained from internal animal facilities. The TRIB3-/- mice are bred within the Barrier area at the Western

Bank site, all staff shower and change clothing to enter the Barrier area. All cages, bedding and diet is either autoclaved or irradiated into the unit and the mice are housed in M3 and RB3 cages and bred in monogamous pairs. Both groups (C57B6 and TRIB3-/- mice) aged 6-18 weeks but HFD experiment aged 18 week upon commencement.

The University of Sheffield Ethics Committee and the Home Office Animals (Scientific Procedures) Act 1986 of the United Kingdom approved the experimental procedures listed below.

2.2.2 Calculation of total leukocytes and neutrophils

To calculate total number of blood leukocytes a 10 µl sample of blood was diluted (1:10) with 3% acetic acid to lyse erythrocytes. In every four corner squares of a haemocytometer, cells were counted using x 10 objective (Labovert FS, Leitz). Therefore, the total numbers of cells was calculated as follows:

Total cells = average cells in every quadrants x total volume x dilution factor x 10^4

The total number of isolated neutrophils was calculated in the same way except that samples were not diluted in acetic acid.

2.2.3 Isolation of murine neutrophils

Mice were anaesthetized, with pentobarbital sodium 20% solution [JM Loveridge plc (Southampton)], 200 mg/ml, 100 µl/mouse, by an i.p. injection. The blood was collected by

cardiac puncture, using 1 ml insulin syringes (25 g x ½); syringes were heparinised before use to prevent clotting.

Anti-coagulated blood was mixed with dextran solution (1.25 % dextran in saline solution) and erythrocytes were sedimented at room temperature for 30 minutes. The leukocyte-rich upper layer (composed of approximately 70% lymphocytes, 4% monocytes and 26% neutrophils) was retained and washed in cold washing buffer [phosphate buffer saline (PBS) mixed with 0.1% bovine serum albumin (BSA), pH 7.4] by centrifugation (300 x g, for 6 minutes) at 4 ˚C. Then the leukocytes were resuspended in 2 ml buffer, and a total number of leukocytes were counted as mentioned in 2.2.2.

Leukocytes were then incubated for 30 minutes at 4 ˚C with a mixture of primary antibodies; anti-CD2 (1.5 µg/10^6 lymphocytes), anti-CD5 (2 µg/10^6 lymphocytes), anti-CD45R (10 µg/10^6 lymphocytes), anti-F4/80 (2 µg/10^6 monocytes), and anti-CD115 (7.5 µg/10^6 monocytes), which bound surface markers of unwanted cells (lymphocytes, immature and mature monocytes). The concentrations of these antibodies were calculated according to the number of unwanted cells.

Cold buffer was then added and excess antibodies washed out by spinning, 300 x g for 6 minutes at 4 ˚C (this step happened twice). The different types of leukocytes were resuspended in 80 µl PBS and goat anti-rat IgG microbeads, 20 µl/10^7 cells, and then incubated for 15 minutes at 4 ˚C, mixing every 5 minutes. While leukocytes are incubated, the separation column was prepared by running cold buffer through column, as illustrated in figure 2.1. Unwanted cells were then eliminated by passing of the cell/bead suspension through a cold column exposed to a Midi MACS magnet (Miltenyi Biotec). Lymphocytes and monocytes marked with the magnetic microbeads were captured in the metallic matrix of the column and neutrophils were collected as eluate, spun (300 x g, for 6 minutes) at 4 ˚C and the supernatant

discarded. Residual erythrocytes were lysed by resuspension in 0.2% NaCl and inverted x 10 (hypotonic lysis), then in 1.6% NaCl mixed with 0.1% glucose and inverted once (hypertonic rescue). Neutrophils were centrifuged (300 x g for 6 minutes) at 4 ˚C, washed and recentrifuged as before. Finally, neutrophils were resuspended in 1 ml buffer and counted.

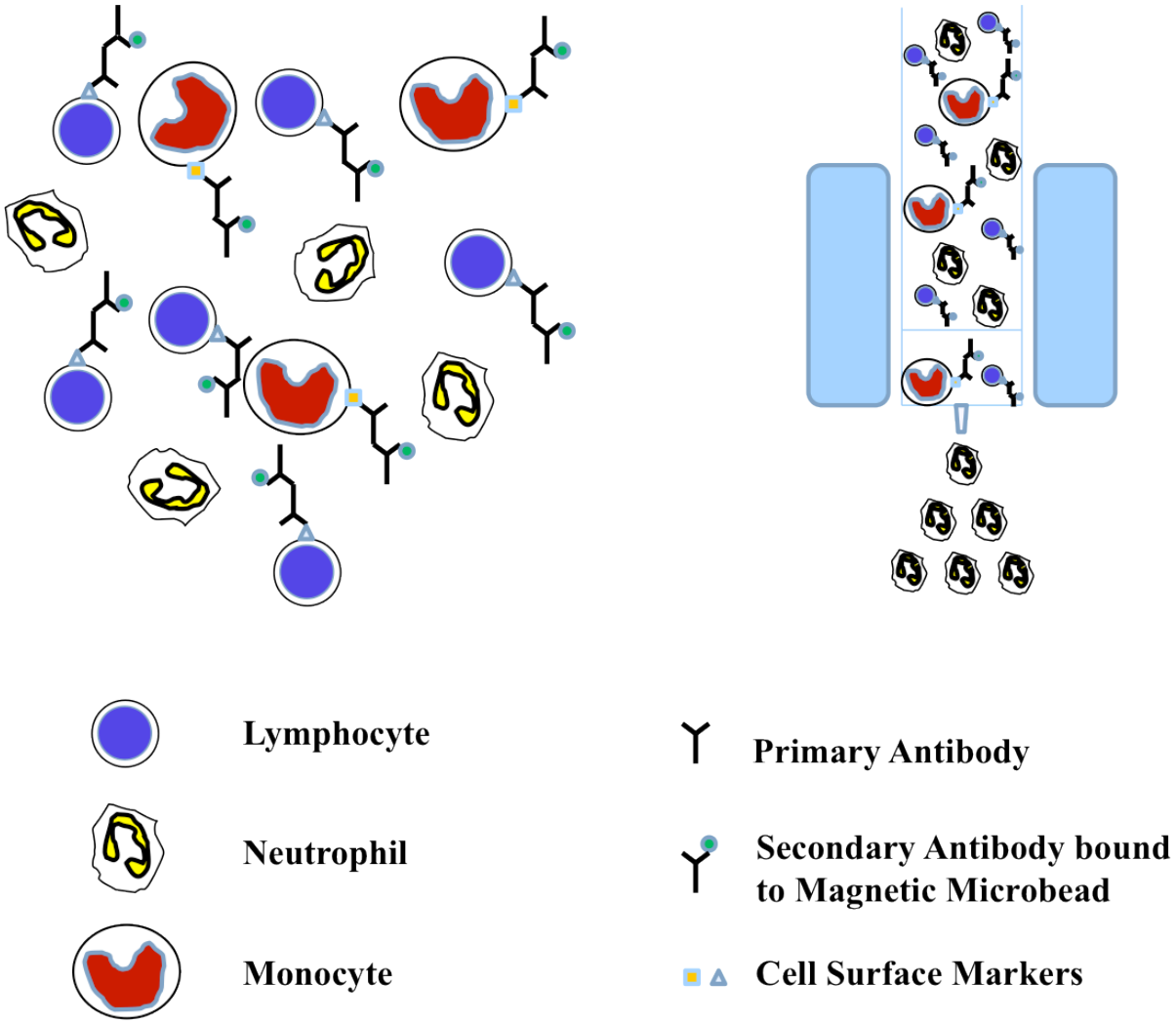

Figure 2. 1: Magnetic separation of murine neutrophils

Neutrophils and unwanted cells (lymphocytes and monocytes) were incubated for 30 minutes at 4˚C with primary antibodies, which bound the cell surface markers of unwanted cells. Secondary antibody coated magnetic microbeads attracted to the primary antibodies were added and the mixture incubated for 15 minutes at 4 ˚C. The unwanted cells were then dislodged by channeling of the cell suspension/bead mixture through a cold metallic matrix into a column attached to a MACS magnet. Lymphocytes and monocytes marked with primary and secondary antibodies coated magnetic microbeads were held in the matrix and neutrophils were collected in the eluate.

2.2.4 Activation of neutrophils by KC, fMLP and LPS

Isolated murine neutrophils were stimulated by diverse stimuli. They were divided into four aliquots for stimulating at different times. Each aliquot was centrifuged and the pellet was resuspended in RPMI (medium). Neutrophils were incubated with a stimulus (10^{-6} M KC, 10^{-6} M fMLP or 1ng/ml LPS) for 0, 15, 30 and 60 minutes at 37 ˚C. Following incubation, the samples were pelleted (300 x g) for 6 minutes and the supernatant discarded.

2.2.5 Lysis of neutrophils

Lysis buffer (1% Triton X-100, 50 Mm 4-(2-hydroxyethyl)-1-piperazineethanesulfonic acid (HEPES), 100 mM sodium fluoride (NaF), 10mM ethylenediaminetetraacetic acid (EDTA), 10 mM Napyrophosphate, 10% glycerol, 0.2 mM phenylmethylsulfonyl fluoride (PMSF), 7% protease inhibitor and 2 mM sodium orthovanadate (Na_3VO_4)) was added to the pellets from the previous procedure. The cells were incubated with lysis buffer on ice for 20 minutes, mixing periodically. The samples were sonicated for 2 minutes then pelleted (at approximately 20,000 x g, for 15 minutes) and the lysates (supernatants) saved for further analysis.

2.2.6 Protein measurement

The protein concentration of the lysates were measured using the Bio-Rad DC protein assay (a colorimetric assay), which is based on protein reaction with copper in an alkaline medium, followed by reduction of folin reagent by the copper-treated protein to produce blue-colored compound with absorbance 405-750 nm^2.

Serial dilutions (2.0 mg/ml, 1.5 mg/ml, 1.0 mg/ml, 0.5 mg/ml, 0.25 mg/ml, 0.125 mg/ml, 0.0625 mg/ml, 0.0315 mg/ml) were prepared from a BSA stock (2.0 mg/ml) using the lysis buffer. Standards (5 µl) were pipetted in triplicate into microwells, while samples only once. Then a cocktail of reagents [reagent A (an alkaline copper tartrate solution), reagent B (a dilute folin reagent), reagent C] was added. The microplate was incubated for 5-10 minutes at room temperature to develop the blue color. The mean values of the triplicate protein standards were calculated and a standard curve was drawn by Revelation Quickline software version 4.25 (Chantilly, VA, USA).

2.2.7 Western blot analysis of p38 MAPK & Akt isolated from murine neutrophils

Active (phosphorylated) forms of p38 MAPK and Akt were evaluated by western blotting. Both protein samples (lysates) and a rainbow molecular weight (MW) marker were prepared by boiling for 5 minutes after adding 5x reducing agent. After preparation they were run in 30% SDS polyacrylamide gel electrophoresis (approximately 1 hour at 170 V), followed by transferring to a nitrocellulose membrane using Towbin transfer buffer (composed of 39 mM glycine, 48 mM Tris, 0.037% SDS and 20% methanol) by semi-dry electro blotting at 5 V for 90 minutes. Subsequently, non-specific binding sites of the membrane were blocked with blocking buffer containing 5% milk/Tris-buffered saline (TBS) 0.1% Tween buffer (washing buffer) by incubating either for 1 hour at room temperature or overnight at 4 ˚C, and washed in the washing buffer several times. The protein was incubated for 2 hours at room temperature or overnight at 4 ˚C with primary antibodies, phospho p38 MAPK antibody and phospho Akt antibody, diluted 1:1000 or 3:1000 with washing buffer. Excess antibody was eliminated by washing the membrane 3 times for 15 minutes by washing buffer on a rotating platform for

5 minutes each. Then the membrane was incubated with a horseradish peroxidase (HRP) bound goat anti-rabbit secondary antibody for 1 hour at room temperature (diluted 1:2000 in blocking buffer). Again excess antibody was removed with washing buffer and the plate was placed on a rotating platform for 5 minutes. This was repeated five to six times to ensure all excess antibody was removed. Conjugated protein was then developed by chemiluminescent detection methods based on substrate luminesce when exposed to the enzyme on the secondary antibody. The light was detected by Amersham Hyperfilm^{TM} ECL (Fisher, Loughborough, UK) or alternatively by CCD cameras (GeneSnap from SynGene software, version 7.04) that take a digital image. Densitometry was performed using GeneTools software (SynGene, version 3.02) that quantifies the relative amount of protein and expresses it as absorbance. Antibodies were stripped for reusing the membrane to detect total p38 MAPK and total Akt, following the same steps except primary antibodies (p38 MAPK antibody and Akt antibody) were diluted 1:1000 in BSA/washing buffer instead of the washing buffer alone.

2.2.8 Neutrophil chemotaxis

Upon completion of isolation, neutrophil chemotaxis was performed (within the least time possible) in a 96-well chemotaxis plate (Neuroprobe ChemoTx system). The plate is composed of small-sized wells, polycarbonate filter membrane with 3 μm pores and lid. These pores are enclosed by hydrophobic rings to hold the cell suspension on the filter (Figure 2.2). Relevant wells were filled with a total volume of 30 μl of buffer (RPMI supplemented with BSA) or chemoattractant at different concentrations (diluted to the required concentration in the buffer), being careful not to let air bubbles form. The membrane was placed over the bottom wells and secured in position with the corner pins. 30 μl of neutrophils at a concentration of 2 x 10^6/ml suspended in buffer were located onto the filters. Chemokinesis controls, to correct for random

movement of neutrophils, were performed by placing 30 µl of neutrophils resuspended in one of chemoattractant concentrations on the filters corresponding to wells containing the same chemoattractant concentration. Therefore, no concentration gradient could occur. The lid was replaced and the chemotaxis plate was incubated at 37 ˚C, 5% CO_2 for 1 or 3 hours. After incubation the lid was removed and the remaining non-migrated neutrophils and buffer on the filter was carefully absorbed using cotton buds and the top surface of the filter was washed several times by 30 µl of buffer each time. The chemotaxis chamber was centrifuged for 10 minutes at 300 x g to remove any adherent neutrophils on the underside of the filter membrane into the wells. The membrane was removed and cells were resuspended in the buffer or chemoattractant already present in the well. The number of migrated neutrophils was counted using a haemocytometer and the percentage of neutrophil migration was calculated. Chemokinesis controls were subtracted from each value.

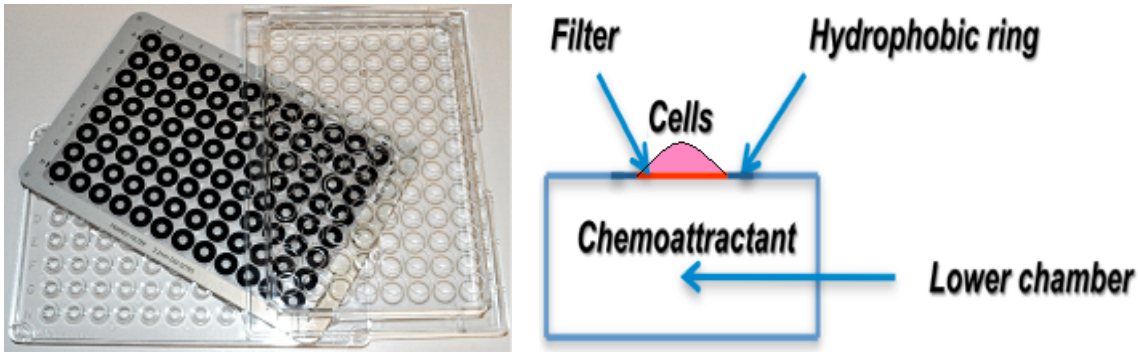

Figure 2. 2: Chemotaxis plate (modified boyden chamber) to investigate neutrophil migration

96 small-sized wells filled with buffer or stimuli with different concentrations. Polycarbonate filter membrane with 3 µm pores is needed for neutrophils. This membrane is positioned over the bottom wells and secured in place with pins in each corner. Neutrophils were placed onto the filter and a lid was covered. The incubation period was at 37 ˚C, 5% CO_2 for 1 or 3 hours (human or murine, respectively). The chemotaxis chamber was then centrifuged for 10 minutes at 300 x g to spin any adherent neutrophils to the underside of the membrane into the wells. Finally, the number of neutrophils migrated towards different stimuli concentrations was counted.

2.2.9 The effect of inhibitors on murine neutrophil migration

The effect of inhibitors on murine neutrophil migration was investigated using the procedure of neutrophil chemotaxis. In addition to this, murine neutrophils were incubated with 10 μM of each of p38 and PI3K inhibitors for 30 minutes at 37 ˚C in 5% CO_2 before being loaded on the filter. The above inhibitors were prepared in dimethyl sulfoxide (DMSO), therefore, DMSO was added to both the control and to the neutrophils (final concentration 0.5%) which were prepared to check chemokinesis.

2.2.10 FACSCalibur flow cytometry procedure

One half of C57B6 and TRIB3-/- murine whole blood were pre-incubated with 10^{-7} M phorbol 12-myristate 13-acetate (PMA) and the other half from each group were left unstimulated (PBS was added instead) for 15 minutes at 37 °C before adding the antibodies. Samples were aliquoted into 100 μl each, keeping a sample of unlabelled cells for reference on ice. Other samples were incubated with either fluorescently conjugated antibodies or their fluorescently conjugated isotypes, non-specific fluorescently conjugated antibodies, in order to check the specificity of each individual antibody. The following antibodies and their isotypes were used: PE anti-mouse PSGL-1 and PE rat IgG1, κ isotype control, PE anti-mouse L-selectin and PE rat IgG2a, κ isotype control and PE anti-mouse CD11b and PE rat IgG2b, κ isotype control. FITC anti-mouse Ly-6G for labelling neutrophils was added to all samples except the sample of unlabelled cells (where neither FITC anti-mouse Ly-6G nor antibodies were used). After mixing well, the samples were incubated for 30 minutes on ice. 2 ml of PGB (PBS containing 20 mM glucose plus 1% BSA) washing buffer was added to the samples and centrifuged at 300 x g for 5 minutes to wash off excess antibodies. Supernatants were discarded and samples, including unlabelled cell samples, were incubated with 2 ml of 1x Erythrolyse for 10 minutes

at room temperature then centrifuged at 300 x g for 5 minutes. Supernatants were discarded and the pellets were washed with a further 2 ml of washing buffer by centrifuging at 300 x g for 5 minutes. Again supernatants were discarded and then the cells resuspended in 200 µl of buffer. The samples were put on ice in the dark to reduce the loss of fluorescent signal, until they were analyzed by flow cytometry.

Results were acquired using a FACSCalibur flow cytometer (BD Bioscience) equipped with CellQuest Pro software BD version 3.01 (Erembodegem, Belgium, Europe). 488 nm argon blue Laser excited the fluorochromes PE (phycoerythrin; emission FL2 BP 575/26 nm) and FITC (fluorescein isothiocyanate; emission FL1 BP 530/30 nm). The variety in granularity, size and fluorescence intensity led to various parameters being applied with murine neutrophils. Size was shown by forward scatter (FSC) and granularity shown by side scatter (SSC). In addition, a gate enclosing the population of study was used to eliminate other cells and any debris. Events captured were 5,000-10,000. Histograms were drawn to illustrate the fluorescence profile depending on the number of cells that displayed particular fluorescence intensity at a specific wavelength. The geometric mean of the cells of interest was measured.

2.2.11 Procedure for the detection of p38 MAPK in RAW 264.7 mouse macrophage cells

The RAW 264.7 cultured cells were provided and plated at a density of 2.0 x 10^5 cells/well by a colleague. The medium, Dulbecco's Modified Eagle Medium 1x (4.5 g/L Glucose and L-glutamine), was removed from each well. Cells were stimulated with either 10^{-6} M of fMLP or 50 ng/ml of LPS, diluted in fresh media, at specific timepoints: 0, 10, 20 and 30 minutes at 37 ˚C in 5% CO_2. Following stimulation the plate was put on ice, medium removed and cells washed using ice cold PBS before adding 150 µl ice-cold 1x lysis buffer plus 3mM PMSF.

Then the cells were scraped off the well and transferred to an eppendorf tube, incubated for 20 minutes on ice before sonicating in an ice-cold water bath one time for 2 minutes. The samples were centrifuged (at approximately 20,000 x g, for 10 minutes at 4 ˚C) and the supernatants (cell lysates) collected for western blotting, which can also be stored at -80 ˚C.

2.2.12 p38 kinase assay

2.2.12.1 Preparing cell lysates

Cell lysates (RAW 264.7 cell and murine neutrophil lysates) were prepared as detailed in section 2.2.5 and 2.2.11.

Selective immunoprecipitation (IP) using immobilized phospho p38 MAPK (Thr180/Tyr182) monoclonal antibody (mAb)

20 µl immobilized mAb bead slurry was added to each 200 µl cell lysates and incubated overnight at 4 ˚C with gentle rocking.

2.2.12.2 Kinase assay

Cell lysates-immobilized Ab were centrifuged at 4 °C (for 30 seconds at 14,000 x g). Then pellets were washed twice with 500 µL 1X cell lysis buffer then twice more with kinase buffer while on ice before suspending in 50 µl 1X kinase buffer, 1 µl 10 mM ATP and 1µl ATF-2 fusion protein (kinase substrate). 10µM p38 inhibitor or vehicle control (DMSO) was added to the samples which will be incubated for different periods of times (0, 30 and 60 minutes) at 30 °C. Reaction was terminated by 25 µl 3x SDS sample buffer, vortexed and then centrifuged.

2.2.12.3 Western immunoblotting

Active (phosphorylated) forms of p38 MAPK were evaluated via detecting phospho ATF-2 with western blotting. Protein samples (lysates) and a rainbow MW marker to verify electrotransfer were prepared by boiling for 5 minutes after adding 5x reducing agent to the marker. After preparation they were run with biotinylated protein marker to detect MWs in 30% SDS polyacrylamide gel electrophoresis (approximately 1 hour at 170 V), followed by transferring to a nitrocellulose membrane using Towbin transfer buffer by semi-dry electro blotting at 5 V for 90 minutes. Subsequently, non-specific binding sites of the membrane were blocked with blocking buffer containing 5% milk/TBS 0.1% Tween buffer (washing buffer) by incubating for 1 hour at room temperature, and washed in the washing buffer three times for 5 minutes each. The protein was incubated with gentle agitation overnight at 4 ˚C with primary antibody, phospho ATF-2 (Thr76) antibody, diluted 1:1000 with washing buffer. Excess antibody was eliminated by washing the membrane 3 times with washing buffer on a rotating platform for 5 minutes each. Then the membrane was incubated with a secondary anti-rabbit IgG, HRP-conjugated antibody and anti-biotin, HRP-conjugated antibody for the detection of the biotinylated protein ladder (diluted 1:2000 and 1:1000 respectively in blocking buffer) for 1 hour at room temperature. Again excess antibody was washed 3 times for 5 minutes each on a rotating platform with washing buffer. Conjugated protein was then developed by chemiluminescent detection methods based on substrate luminescence when exposed to the enzyme on the secondary antibody. The light was detected by Amersham Hyperfilm^{TM} ECL (Fisher, Loughborough, UK).

2.2.13 Role of TRIB3 on murine neutrophil recruitment in thioglycollate-induced peritonitis

C57B6 wild type (control) and TRIB3-/- mice received an intraperitoneal injection of 1ml of 4% thioglycollate broth (4% thioglycollate powder in 0.9% w/v NaCl; autoclaved and aged for > 7 days, used for induction of localised inflammatory response). Five time points were taken for sample collection: at 0 hour triplicate (three samples each group) and at 2, 6, 24 and 48 hours tetra (four samples each group) have been obtained. Blood was collected by cardiac puncture using 1 ml heparinised insulin syringes after anaesthetising mice with isofluorane. In addition, 5 ml of lavaging buffer (PBS, 0.1% BSA, 20 mM D-glucose (required to keep cells intact during cytospin) and 10 U/ml heparin (clumping was avoided) was injected i.p. into mice (using 5ml syringe and 21G needle) after cervical dislocation. Peritoneal lavage fluid was recovered and transferred to 15 ml tubes, using either same syringe or Pasteur pipette and kept on ice once collected.

A capillary tube containing 10µl of blood was transferred to a microfuge tube containing 90 µl of 3% acetic acid (needed for lysis red blood cells). Total leukocytes were counted from both, blood sample in acetic acid and peritoneal lavage fluid, using disposable haemocytometers. Cytospins of lavage samples were performed in duplicate for each sample at 900 rpm for 6 minutes (100 µl lavage fluid/cytospin, maximum 1 x 10^6 cells/ml lavaging buffer), fixed in methanol for 5 seconds (5 dips), air dried, stained using Diff-Quick and flushed with generous amounts of slow running tap water. Differential cell counts from cytospin of lavage microscopy slides were performed. The remaining blood was collected in EDTA blood collection tubes and centrifuged for 20 minutes at 250 x G, supernatant (plasma) then collected for lipid profile (required at least 100 µl). After counting the cell and cytospin preparation, peritoneal lavage fluid was centrifuged at 350 x g for 6 minutes and the supernatant stored at -80 °C for cytokine experiment.

Calculation of neutrophil content in lavage:

Total number of cells in lavage = leukocytes number/ml x total volume lavage x 10^4

(leukocyte numbers have been counted by a haemocytometer).

Total number of neutrophils = total number of cells in lavage x neutrophil percentage.

2.2.14 Blood plasma lipid profile method

Blood plasma lipid profiles (cholesterol, TG and HDL) of both wild-type and TRIB3-/- mice were measured via enzymatic colorimetric test by the department of Clinical Chemistry at the Royal Hallamshire hospital Sheffield, using Cobas 8000 system from Roche.

2.2.14.1 Cholesterol test principle

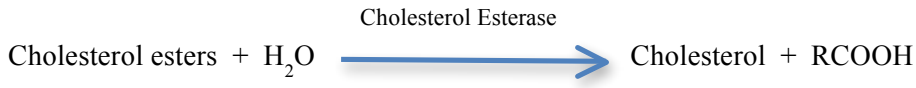

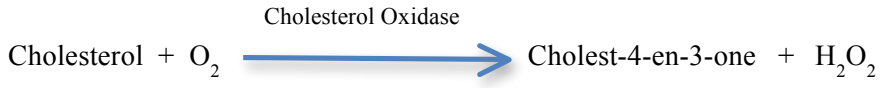

(Roche Assay methodology, cobas c systems, 2010-12, V 3 English)

2.2.14.2 TG test principle

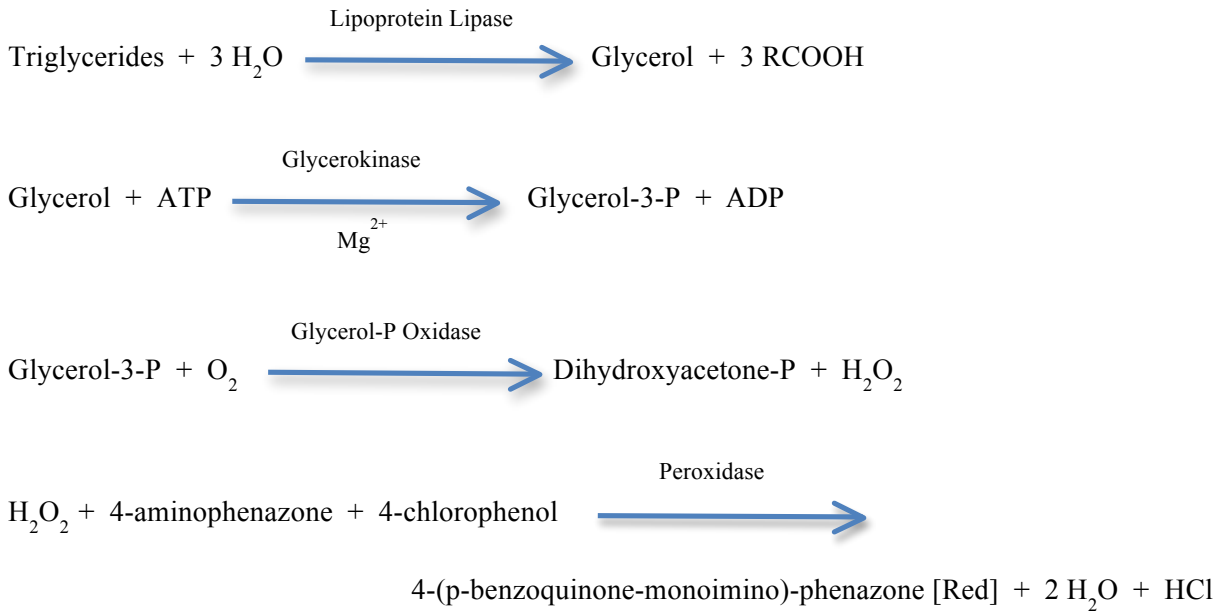

(Roche Assay methodology, cobas c systems, 2009-06, V 1 English)

2.2.14.3 HDL test principle

Water-soluble complexes with LDL, VLDL and chylomicrons are selectively produced by dextran sulfate in the presence of Mg^{2+}. These complexes are resistant to polyethylene glycol (PEG)-modified enzymes.

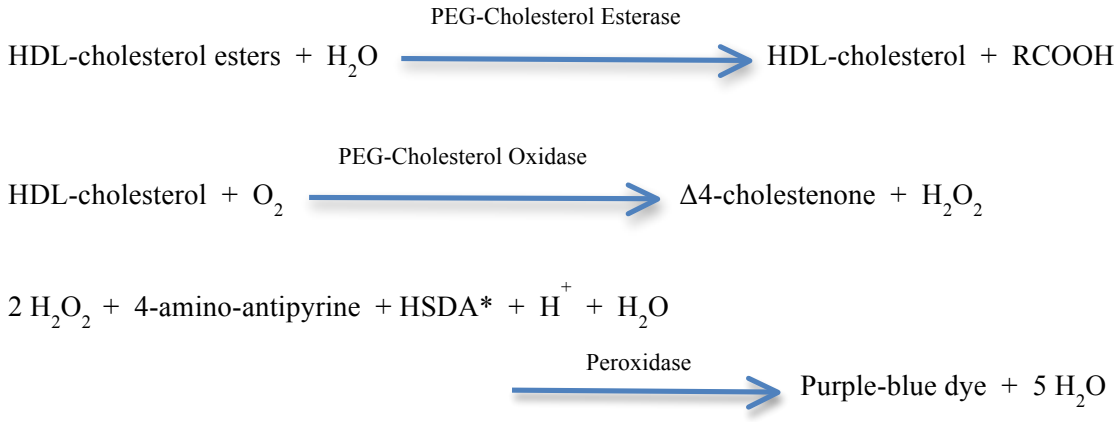

HSDA = Sodium N-(2-Hydroxy-3-Sulfopropyl)-3,5-DimethoxyAniline

(Roche Assay methodology, cobas c systems, 2009-07, V 1 English)

Colour intensities of the specific dyes formed in the tests are directly proportional to the cholesterol, TG or HDL-cholesterol concentrations and are measured photometrically.1

2.2.15 Murine TRIB3 genotyping

2.2.15.1 Ear clip lysis

150 µl lysis buffer (EDTA, Tris-HCl and Tween-20) containing proteinase K (300µg proteinase K/ml lysis buffer) was added to mouse ear clipping samples and then incubated overnight at 55 ^{o}C. Samples were then vortexed briefly and incubated for 12 minutes at 100 ^{o}C to inactivate proteinase K. 600 µl of water was then added to each sample, vortexed briefly and stored at +4 ^{o}C.

2.2.15.2 PCR and sample analysis

The following PCR reaction mix was prepared in 0.5 ml eppendorf tube:

DNA template	3 µl
H2O	9 µl
LTR-2	0.5 µl
LEXKO-1947-3’	0.5 µl
LEXKO-1947-5’	0.5 µl
Biomix	2.5 µl
Total	26µl

The following PCR program was run:

Step 1: 95 ^{o}C for 5 minutes

Step 2: 95 ^{o}C for 30 seconds

Step 3: 65 ^{o}C for 30 seconds } 40 cycles

Step 4: 72 ^{o}C for 30 seconds

Step 5: 72 ^{o}C for 5 minutes

Step 6: 10 ^{o}C hold

A 1% agarose gel was prepared in 1x TAE buffer (Tris, acetic acid and EDTA) containing final ethidium bromide (EtBr) concentration of 1μg/ml. Electrophoresis was then carried out at 90V for approximately 40 minutes. Visualisation of PCR bands was then carried out under UV illumination (Chemi Genius2 Bio Imaging System using GeneSnap version 7.04) (Syngene).

2.2.16 Effect of TRIB3-/- on embryo viability

TRIB3+/- mice were backcrossed onto a C57B6 background for 10 generations. The genotype of the 10th generation (80 mice; 40 from each gender) from heterozygote mating was checked by PCR and produced a ratio of 17:39:24; C57B6, TRIB3+/- and TRIB3-/- mice respectively. This means TRIB3-/- mice represent 30% of the population, which approximately follows Mendel's Law. According to this ratio knocking out TRIB3 from cells has no effect on breeding in this strain of mice.

2.2.17 Cytokine level measurement

The BD cytometric bead array (CBA), a flow cytometric based application was used to measure diverse cytokines (GMCSF, IL-4, IL-13, IL-17A, KC, monocyte chemotactic protein-1 (MCP-1), MIP-1α, MIP-1β and TNF) simultaneously in peritoneal lavage fluid. The set of cytokine specific antibody-coated beads of the kit was applied to capture surface for cytokines of lavage supernatants. Each bead in the array has distinct fluorescence intensity for each cytokine. Therefore, beads were mixed and run together in one tube. The detection reagent delivers a fluorescent signal in proportion to the quantity of bound cytokine. Sandwich complexes (capture bead + standards/unknown samples + detection reagent) were measured, using flow cytometry to detect particles with fluorescence characteristics of the bead and detector. The bead population was resolved in two fluorescence channels of a flow cytometer. This work was carried out by the university Flow Cytometry Core Facility.

2.2.18 Feeding of TRIB3-/- and control mice a high fat diet (HFD)

Diet Name: RM AFE 60%FAT 20%CP 20%CHO (M) 25kGy

Diet	**824054 - '60% AFE Fat'**
Ingredient	**g% (w/w)**
Casein	**29.944**
Choline Bitartrate	**0.334**
L-Cystine	**0.450**
Lard	**29.248**
Rice Starch	**10.079**

Cellulose	**6.964**
Soya Oil	**4.875**
Sucrose	**11.838**
Minuteeral Mix	**4.875**
Vitaminute Mix	**1.393**

Special Diet Services (SDS, Witham, UK).

2.2.18.1 Diet

C57B6 and TRIB3-/- mice were fed 60% HFD (see above table for diet name, ingredients, amounts and company details) 5 g/mouse daily for 11 weeks. Also a further two groups (C57B6 and TRIB3-/- mice) were on chow (Teklad Global 18% Protein Rodent Diet, Harlan, UK).

2.2.19 Weight gain

C57B6 and TRIB3-/- mice were males and aged 18 weeks upon commencement of feeding. The weight was measured once weekly for 11 weeks, initiating with a baseline weight before feeding.

2.2.20 Whole blood differential count (week 5)

The blood was collected from the tail of C57B6 and TRIB3-/- mice at week 5. A cell counting machine (Sysmex KX-21N; Sysmex Corporation) was used to calculate differential blood cell types of both groups.

2.2.21 Glucose tolerance test (GTT)

C57B6 and TRIB3-/- mice were starved overnight at week 9. Next day each mouse was weighed as glucose dose depends on its body weight (BW). Blood was then collected from the tail to determine a baseline glucose reading using glucose meter and strips. The mouse was then injected intraperitoneally with sterile glucose at 10ul/g BW (20% D-glucose in 0.9% sterile saline; a solution that was prepared fresh on the day of use). Readings were taken at different time points (30, 60, 90 and 120 minutes) after injection. Groups on chow (C57B6 and TRIB3-/- mice) were treated the same.

2.2.22 Insulin tolerance test (ITT)

C57B6 and TRIB3-/- mice at week 11 were fasted for 2-3 hours on the morning of the experiment. They were weighed as insulin dose depends on its BW. Blood was then collected from tail to determine a baseline glucose reading, using glucose meter and strips, before injecting the mouse intraperitoneally with sterile insulin at 0.75 U/kg BW (0.25 U/ml in 0.9% sterile saline was freshly made up on the day, which was 3X BW in μl). Readings were taken at different time points (20, 40 and 60 minutes) after injection. Groups on chow (C57B6 and TRIB3-/- mice) were treated the same. In case the mice become hypoglycaemic, 20% D-glucose in 0.9% sterile saline was prepared to be quickly injected.

2.2.23 Whole blood differential count (week 11)

Blood was collected in the final week of the experiment (week 11) from C57B6 and TRIB3-/- mice through cardiac puncture using 1ml heparinised insulin syringes after anaesthetising mice

with isofluorane. A cell counting machine (Sysmex KX-21N; Sysmex Corporation) was used to calculate differential blood cell types for both groups.

2.2.24 Blood plasma lipid profile

Blood was centrifuged for 20 minutes at 250 x G, supernatant (plasma) then collected for lipid profile. Blood plasma lipid profiles (cholesterol, TG and HDL) of both C57B6 and TRIB3-/- mice were measured via enzymatic colorimetric test. Details and the process of measuring were previously described in 2.2.14.

2.2.25 *In vitro* peritoneal cells

Following the collection of blood and after cervical dislocation, 5ml of lavaging buffer was injected interperitoneal into C57B6 and TRIB3-/- mice. Peritoneal lavage fluid was recovered. The cells were cytospinned after counting. Differential cell types were counted from the cytospin of lavage microscopy slides. Neutrophil content in lavage then was calculated as per the formula described previously 2.2.13.

2.2.26 Harvesting the organs

Following the recovery of the peritoneal lavage fluid, organs were removed for further analysis, as required: adipose tissue, liver, heart and aorta:

2.2.26.1 Adipose tissue and liver

A midline incision was made from the abdomen up to the chest using scissors. The long ribs and costodiaphragmatic recess was cut and removed. Adipose tissue was also removed and fixed in FBS (10% Formalin) at 4 °C. Adipose tissue was transferred to PBS after 24 hours in 10% FBS. Liver was also excised and saved in liquid nitrogen.

2.2.26.2 Heart and aorta

1 ml PBS was injected directly into the heart, for flushing, followed by 1 ml FBS for fixation. Then aorta and heart were removed. Fat, vena cava, connective tissue and small branching vessels were detached from aorta. Once the aorta was cleaned it was opened exposing the internal surface. The heart was cut along the line of the atria. Next, all tissues were stored at 4 °C until processing. They were transferred to PBS post 24 hours in 10% FBS.

2.2.27 Preparing Oil Red O stain

1 ml H_2O was added to 99 ml isopropanol (propan-2-ol). Oil Red O powder was added to the solution until saturated, then filtered using Whatman filter paper. The final stain was diluted to 60% v/v by H_2O.

2.2.28 *En Face* Oil Red O staining of aorta

The aorta was stored in 10% FBS at 4 °C. The following day this was changed to PBS. The aorta was then stained using *En Face* Oil Red O staining as follow: aorta was rinsed in ddH_2O

then in 60% isopropanol (2 minutes) followed by dipping in Oil Red O (10-15 minutes). Next, aorta was rinsed again in 60% isopropanol (2 minutes) then ddH_2O before pinning out and photographing.

2.2.29 Pinning out, capturing and analysis

Melted wax was poured into a Petri dish. Once wax was firm, but warm, the aorta was placed on top and labelled (8 aortas per dish should fit). Insect pins were pinned through the aorta (pinning was done quickly as inserting pins are difficult when wax becomes cold). Aorta was dipped in PBS or H_2O during pinning process and then the entire dish was covered with PBS to get clear picture. Photographs at 1.5x magnification were taken for image analysis. Percentage lesion coverage was measured, using NIS-Elements software.

$$\% \text{ Lesion coverage} = \frac{\text{object numbers} \times \text{mean lesion area}}{\text{total aorta area}} \times 100$$

2.2.30 Dehydration and embedding heart, liver and adipose tissues

Heart, liver or adipose tissue was placed into a plastic cassette with a sheet of Whatman Grade 1 filter paper (heart did not require paper) after labelling samples with pencil. The cassettes were then covered with increasing concentrations of alcohol.

Dehydration sequence:

50% Ethanol	1hour
70% Ethanol	1hour
90% Ethanol	1hour
100% Ethanol	1hour
100% Ethanol	1hour (Ethanol was changed)
50:50 Ethanol/Xylene	1hour
100% Xylene	1hour
100% Xylene	1hour (Xylene was changed)

The cassettes were immersed into pots containing melted wax in 60 °C oven over night. After dehydration the tissues were embedded into wax before sectioning them.

2.2.31 Sectioning paraffin embedded murine heart, liver and adipose tissue

Embedded heart, liver and adipose tissues from C57B6 and TRIB3-/- mice on 60% HFD and on chow (no heart samples on chow) were cut to sequential 5 μm thick sections (10 slides/mouse) using a LEICA RM2135 Microtome. Sections were then floated out on a 37 ˚C water bath to smooth out wrinkles. Following this, each section was transferred to labelled microscopic slides before placing in a 37 ˚C incubator overnight to dry.

2.2.32 Re-hydrating in addition to staining heart, liver and adipose tissue slides

For removing wax and re-hydrating tissues, heart, liver and adipose tissue slides were immersed in the following sequentially:

- 100% Xylene 10 minutes
- 100% Ethanol 2 minutes
- 90% Ethanol 2 minutes
- 70% Ethanol 2 minutes
- Water 2 minutes (to rinse alcohol off)

Tissue slides were then stained with haematoxylin for 2 minutes to stain the nucleus of the cells. The slides were rinsed with distilled water (DW) to remove excess haematoxylin; stained with eosin for 30 seconds to stain eosinophilic structures of the cells and then rinsed with DW to remove excess eosin. A drop from DPX mounting medium was added to the slide's centre to mount the glass coverslip gently on the slide. The slides were left overnight before visualising cells under the microscope.

2.2.33 F4/80 immunohistochemistry for macrophages

All test and control slides were de-waxed and re-hydrated via graded alcohols to water at room temperature (RT) as follows:

100% Xylene	10 minutes
100% Ethanol	2 minutes
100% Ethanol	2 minutes

90% Ethanol	2 minutes
70% Ethanol	2 minutes
50% Ethanol	2 minutes
Water	2 minutes

Endogenous peroxidases were blocked by incubation in fresh 3% hydrogen peroxide (H_2O_2) (1:10 ratio of 30% stock solution and PBS) 10 minutes at RT. They were rinsed in tap water at RT. Antigen was retrieved by incubation in hot 10 mM sodium citrate buffer (pH 6) in a 95 ˚C water bath 20 minutes. Then container of citrate buffer with slides inside was removed, left to cool at RT 20 minutes and permeabilised by incubation in 0.5% Triton X-100 (1 ml Triton X-100 in 200 ml PBS) at RT 10 minutes. Non-specific binding of secondary antibody was blocked with 1% milk buffer (2 g milk in 200 ml PBS) at RT 30 minutes, following this, milk buffer was tipped off, but not washed, and the excess blotted. 100µl fresh primary antibody (1:100 ratio of anti-mouse F4/80 antigen and PBS) was added to each slide, covered with a plastic coverslip and incubated at 4 ˚C overnight before washing in 3 changes of PBS at RT 5 minutes each. Then 100 µl fresh secondary antibody (1:200 ratio of biotinylated anti-rat IgG and PBS) was added to each slide, covered with a plastic coverslip and incubated at RT 30 minutes before washing in 3 changes of PBS at RT 5 minutes each. Fresh Vectastain ABC-HRP reagent (actin/biotin complex-HRP; 1 drop reagent A and 1 drop reagent B were added per 2.5 ml PBS, mixed and made up 30 minutes prior to use) was added to each slide, covered with a plastic coverslip, incubated at RT 30 minutes and washed in 3 changes of PBS 5 minutes each at RT. Following this, fresh DAB (1 drop buffer pH 7.5, 2 drops DAB and 1 drop H_2O_2 were added per 2.5 ml ddH2O) was added to each slide, covered with a plastic coverslip, incubated at RT 10 minutes (in case colour development becomes too strong stop reaction early) and rinsed in tap water at RT. Slides were then counterstained using haematoxylin at RT 1 minute, washed in water at RT, dehydrated via graded alcohols to xylene and mounted using

DPX mountant at RT. The primary and secondary antibodies, ABC and DAB incubations were carried out in a Humidifier.

2.2.34 Statistical analysis

Results are displayed as mean ± SEM. Statistical analysis was performed using GraphPad PRISM software version 5.00 (La Jolla, CA, USA). Statistical significance was tested using paired and unpaired student's t tests (parametric tests) to compare two groups, whereas one-way ANOVA (analysis of variance), followed by Dunnett or Bonferroni post tests and two-way ANOVA were used for multiple comparisons. P values less than 0.05 were considered statistically significant.

Chapter 3: The role of p38 and Akt activation in murine neutrophil function *in vitro*

3.1 Introduction

p38 MAPK has a number of roles in inflammation, proliferation, differentiation, development, survival, apoptosis, in addition to stress responses [77]. Interestingly, published data indicated that PI3Kγ controls T cell activation, neutrophil migration, thymocyte development and the oxidative burst [61]. The interactions between TRIBs and other protein molecules have been the focus of many studies. Clearly, there are diverse experiments demonstrating an essential regulatory function for TRIBs in cellular regulation and development, although TRIBs' role and molecular mechanism of action in signalling pathways are unclear as of yet [130]. All the above were discussed earlier in the thesis.

As previously mentioned in the introduction, the control of MAPK cascades is essential for regulating various cellular responses. [145]. TRIBs bind to MAPKK and control the activation of MAPK. It has been documented that TRIBs may play an important role in the MAPK cascade, but at high concentrations they inhibit this cascade [145]. To explain these results, many mechanisms are hypothesised; for example, TRIBs could act as scaffolds [145]. TRIBs may behave either as activators of MAPK activity or as inhibitors, according to the TRIB to MAPKK ratio in the cell. Similarly, TRIB mediated regulation of NFκB [160], [161], and the control systems of the cell cycle have been found [162].

This chapter will build an understanding of TRIB3 action in the context of the effect of fMLP and KC on p38 MAPK and PI3K/Akt activation in murine neutrophils. It will discuss whether

knocking out TRIB3 alters specific signalling pathways, which in turn modulate murine neutrophil function, compared to C57B6 control.

3.2 RESULTS

A) Evidencing existence of TRIB3 in neutrophils

Unpublished data by my group have demonstrated that murine neutrophils express TRIB3 (Table 1). This provides a rational for studying the function of TRIB3 in neutrophils.

	TRIB1	TRIB2	TRIB3
Human neutrophils	+	-	+
HL60 cells	+	-	(+)
Mouse neutrophils	+	-	+
32Dcl3 cells	+	(+)	+

Table 3.1: Proving presence of TRIB3 in murine neutrophils

It has been found by using conventional RT-PCR that TRIB3 mRNA is expressed in human and mouse neutrophils and cell lines. + High expression, (+) low level of expression and - no expression.

B) Effect of chemoattractants (KC and fMLP) and LPS on p38 and Akt activation in mouse neutrophils

This section is to confirm what was shown in previous studies, regarding activation of p38 and Akt in murine neutrophils by KC, fMLP and LPS [175], [176]. The activation of isolated murine neutrophils through p38 or Akt was studied between 0-60 minutes, using diverse physiologically relevant stimuli (10^{-6} M KC, 10^{-6} M fMLP and 1ng/ml LPS). Activated cells were lysed and activation of p38 and Akt was detected by western blotting (Figure 3.1). The results show that exposure of isolated murine neutrophils to KC, fMLP and LPS activated the p38 MAPK signalling pathway at 15 and 30 minutes but this decreased at 60 minutes. It also shows insignificant inhibition on Akt signalling pathway by these stimuli. However, whilst there was an apparent trend to a transient activation of p38 and an inhibition trend on Akt in response to stimulation, statistical analysis (one-way ANOVA, Dunnett post test) did not show any significant difference.

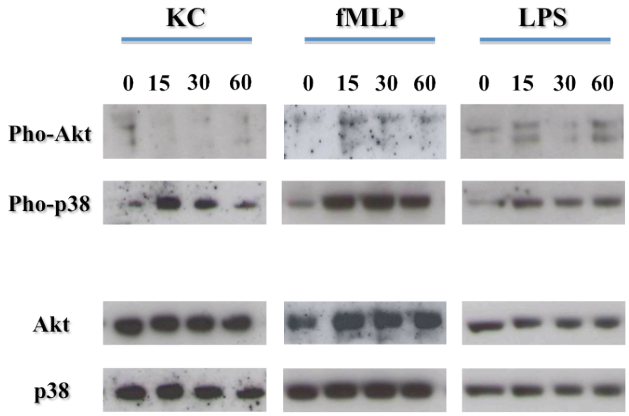

Figure 3. 1: Activation of p38 and Akt signalling by KC, fMLP and LPS in neutrophils

Isolated murine neutrophils were stimulated for different periods of times (0, 15, 30 and 60 minutes) using various stimuli (10^{-6} M KC, 10^{-6} M fMLP or 1ng/ml LPS). The cells were then lysed with lysis buffer for 20 minutes on ice. Protein from neutrophil lysates was measured by the Bio-Red DC protein assay. Subsequently, protein was electrophoresed on a 30% SDS acrylamide gel, transferred to nitrocellulose membrane and identified with phospho p38 MAPK antibody and phospho Akt (ser 473) antibody, or p38 MAPK antibody and Akt antibody as primary antibodies. A secondary anti-rabbit IgG, HRP-conjugated antibody was added, and detected by enhanced chemiluminescence. Results are displayed as western blot images, using 0 minute as a control. KC and fMLP pictures are representative of 3 experiments, while 5 for LPS.

A

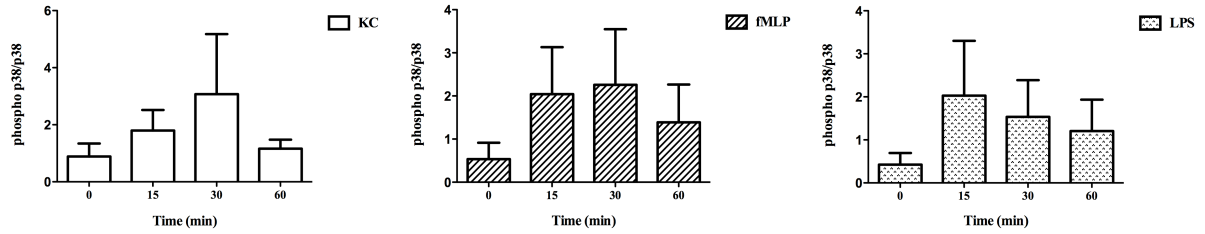

B

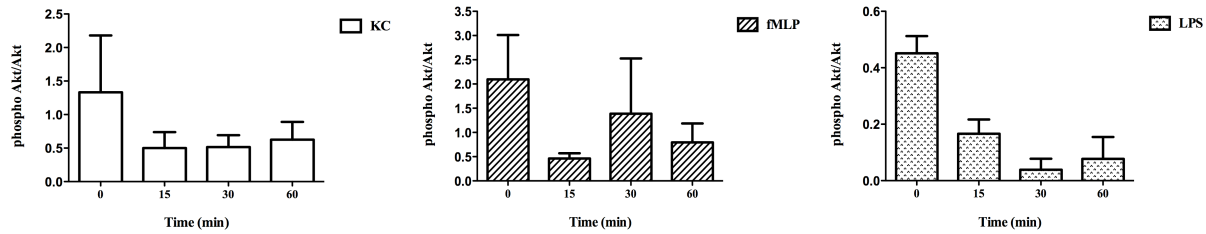

Figure 3. 2: Quantification activation of p38 and Akt signalling by KC, fMLP and LPS in neutrophils

Isolated murine neutrophils were stimulated for different periods of times (0, 15, 30 and 60 minutes) using various stimuli (10^{-6} M KC, 10^{-6} M fMLP or 1ng/ml LPS). Results are displayed as a ratio of the phospho p38 MAPK/p38 MAPK (A) and phospho Akt/Akt (B) by densitometry. Data shows mean ± SEM, n = 4 for KC and fMLP and n = 5 for LPS. Statistical analysis (one-way ANOVA, Dunnett post test) was carried out using 0 minute as a control. No significant differences are observed.

C) Effect of chemoattractants (KC and fMLP) on p38 activation in murine neutrophils of C57B6 versus TRIB3-/-

It has been found that p38 is activated by KC and fMLP in neutrophils [177]. This study is to clarify the importance of TRIB3 on this signalling pathway. Activation of isolated murine neutrophils through p38 MAPK was studied between 0-60 minutes, using diverse physiologically relevant stimuli (10^{-6} M KC, 10^{-6} M fMLP). Activated cells were lysed and activation of p38 MAPK was detected by western blotting (Figure 3.3). The results display that exposure of isolated murine neutrophils to KC and fMLP activated p38 MAPK signalling pathway at 15 and 30 minutes time points, with the signal then decreasing by 60 minutes in C57B6 and TRIB3-/-. Thus, no difference was observed between both groups for either chemoattractants.

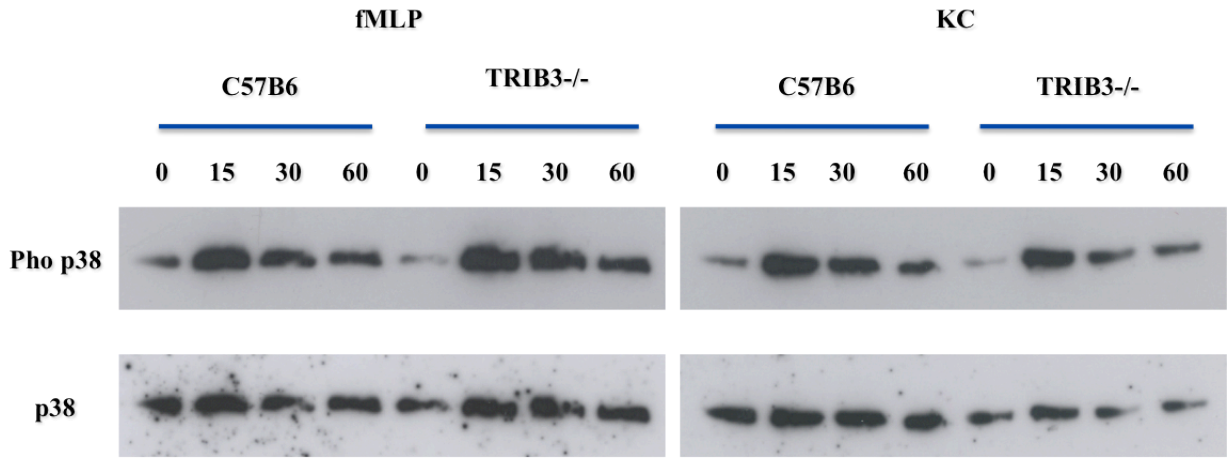

Figure 3. 3: Activation of p38 MAPK signalling by KC and fMLP in murine neutrophils of C57B6 versus TRIB3-/-

Isolated murine neutrophils were stimulated for different periods of times (0, 15, 30 and 60 minutes) using various stimuli (10^{-6} M KC or 10^{-6} M fMLP). The cells were then lysed with lysis buffer for 20 minutes on ice. Subsequently, protein from neutrophil lysates were electrophoresed on a 30% SDS acrylamide gel, transferred to nitrocellulose membrane and identified with phospho p38 MAPK antibody or p38 MAPK antibody as primary antibodies. A secondary anti-rabbit IgG, HRP-conjugated antibody was added, and detected by enhanced chemiluminescence. Results are displayed as western blot images. Each picture is representative of 3 experiments.

D) Effect of fMLP and LPS on p38 MAPK activation in RAW 264.7 cells

p38 inhibitor (SB 203580) has previously been used in neutrophil migration assay successfully [49], [178], [179]. In this study human neutrophils were used to validate the function of p38 inhibitor to investigate later whether migration of murine neutrophils in response to fMLP and KC occurred through the p38 MAPK pathway or other signaling pathways. The cells were pre-incubated with 10 μM of p38 inhibitor for 30 minutes at 37˚C. Following this the cells were stimulated using 10^{-7} M fMLP between 0-30 minutes and compared to control cells without the p38 inhibitor pre-incubation. Whole cell lysates were made and phosphorylation of p38 was detected by western blotting. The results demonstrate that the neutrophils were already activated at 0 minute which made it difficult to differentiate the effect of 10^{-7} M fMLP as a stimulator for different periods of times (0, 10, 20 and 30 minutes) thus verifying the impact of p38 inhibitor. Therefore, activation of p38 MAPK in RAW 264.7 cells was studied between 0-30 minutes using physiologically relevant stimuli (10^{-6} M fMLP or 50 ng/ml LPS). Activated cells were lysed and phosphorylation of p38 was detected by western blotting (Figure 3.4).

The results show fMLP and LPS individually activated p38 MAPK signalling pathway in RAW 264.7 cells at 10^{-6} M and 50 ng/ml respectively compared to the untreated control. The effect of fMLP was more transient in comparison to LPS (i.e. there was an increase in p38 phosphorylation at 10 minutes). This was not sustained for a long period of time as shown by the gradual decrease in the signal at 20 and 30 minutes. By contrast, LPS activation was longer lasting with a gradual increase in the signal for phosphorylated p38 with a greater activation at 20 and 30 minutes when compared to fMLP.

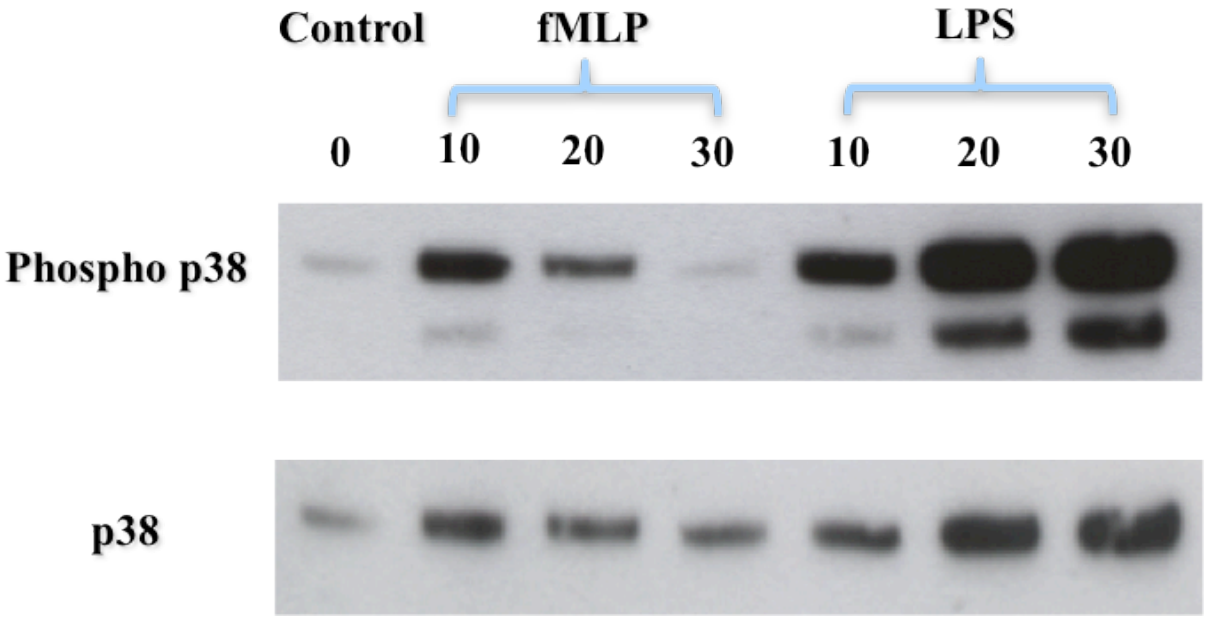

Figure 3. 4: Activation of p38 MAPK signalling by fMLP and LPS in RAW 264.7 cells

p38 MAPK in RAW 264.7 cells were stimulated for different periods of times (0, 10, 20 and 30 minutes) using various stimuli (10^{-6} M fMLP or 50 ng/ml LPS). The cells were then lysed with lysis buffer for 20 minutes on ice. Subsequently, protein (p38 MAPK) from RAW 264.7 cells lysates was electrophoresed on a 30% SDS acrylamide gel, transferred to nitrocellulose membrane and identified with phospho p38 MAPK antibody or p38 MAPK antibody as primary antibodies. A secondary anti-rabbit IgG, HRP-conjugated antibody was added, and detected by enhanced chemiluminescence. Results are displayed as western blot images, using 0 minute as a control. n = 1.

E) Verifying the impact of p38 inhibitor on kinase activity in RAW 264.7 cells

As it was impossible to determine whether the p38 inhibitor was functioning in the human neutrophils, the inhibitor was next tested on RAW 264.7 cells in order to validate the activity of p38 inhibitor and eventually study its effect on murine neutrophil migration towards fMLP and KC. The impact of p38 inhibitor on p38 MAPK signalling activity in RAW 264.7 cells post incubation for different periods of times (0, 30 and 60 minutes) at 30˚C was studied and compared to the control, using physiologically relevant stimulus 50 ng/ml LPS for 10 minutes. Treated cells were lysed and phosphorylation of p38 was detected through phospho ATF-2 by western blotting (Figure 3.5).

The results show LPS activated at 10 minutes p38 MAPK signalling pathway, detected through phosphorylation ATF-2, in RAW 264.7 cells compared to the untreated control. The effect of phospho p38 on phosphorylation ATF-2 was longer lasting with a gradual increase in the signal for phosphorylated ATF-2 with a much greater activation at 30 and 60 minutes when compared to control. By contrast, adding 10 μM p38 inhibitor suppressed ATF-2 phosphorylation shown by the marked reduction in the signal in control cells and after LPS at 30 and 60 minutes.

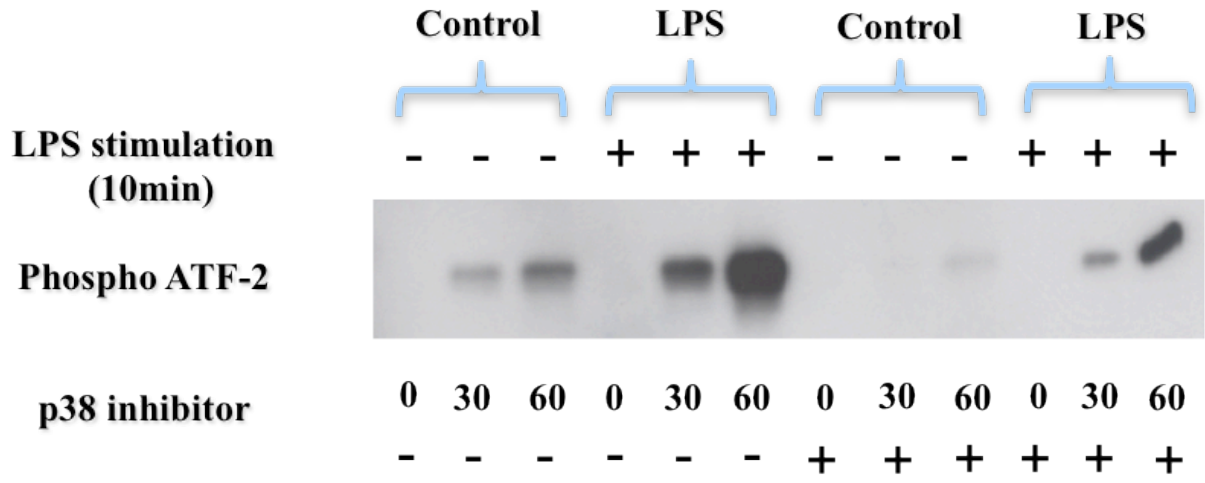

Figure 3. 5: Verifying the impact of p38 inhibitor on p38 MAPK activity in RAW 264.7 cells

p38 MAPK in RAW 264.7 cells was stimulated for 10 minutes using 50 ng/ml LPS. The cells were then lysed with lysis buffer for 20 minutes on ice. Phospho p38 MAPK from RAW 264.7 cells lysates was immobilised by adding mAb bead slurry and incubated overnight at 4˚C. Cell lysates-immobilised Ab was centrifuged. The pellets were then suspended in kinase buffer, ATP and ATF-2 fusion protein (kinase substrate) before 10μM p38 inhibitor or vehicle control (DMSO) being added and incubated for different periods of times (0, 30 and 60 minutes) at 30°C. Reaction was terminated by SDS sample buffer. Subsequently, phospho p38 MAPK was evaluated through detecting phospho ATF-2 by western blotting; protein samples (lysates) was electrophoresed on a 30% SDS acrylamide gel, transferred to nitrocellulose membrane and identified with primary antibody, phospho ATF-2 antibody. A secondary anti-rabbit IgG, HRP-conjugated antibody was added, and detected by enhanced chemiluminescence. Unstimulated cells were used as a control. n = 1.

F) Verifying the impact of p38 inhibitor on kinase activity in murine neutrophils

The impact of p38 inhibitor on p38 MAPK signalling activity in murine neutrophils after incubation for 60 minutes at 30˚C was tested and compared to the control to verify its effect and study it later on neutrophil migration towards KC and fMLP, using physiologically relevant stimulus 10^{-6} M fMLP for 30 minutes. Treated cells were lysed and phosphorylation of p38 was detected through phospho ATF-2 by western blotting (Figure 3.6).

The results show fMLP activated at 30 minutes p38 MAPK signalling pathway, detected through phosphorylation ATF-2, in murine neutrophils at 10^{-6} M compared to the untreated control. The effect of phospho p38 on phosphorylation ATF-2 was greater, lasting 60 minutes when compared to control. By contrast, adding 10 μM p38 inhibitor inhibited ATF-2 phosphorylation shown by a decrease in the signal at 60 minutes. This validated the function of p38 inhibitor. There is no similar commercially available kinase assay exists for PI3K inhibitor (LY 294002). Therefore, the activity of this inhibitor was not tested in my work. However, this molecule has previously been used in neutrophil migration assay [49].

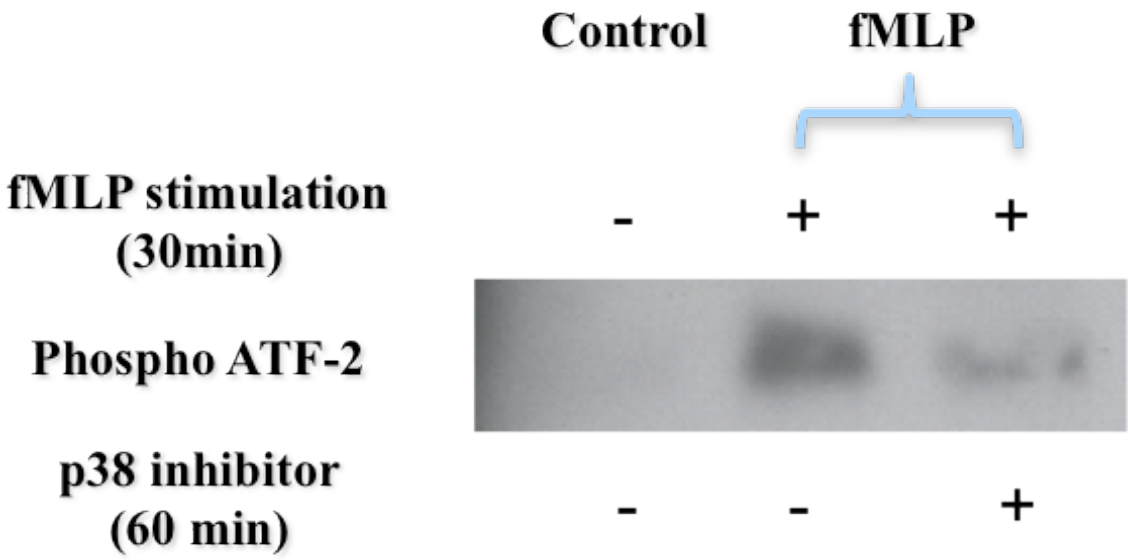

Figure 3. 6: Verifying the impact of p38 inhibitor on p38 MAPK activity in murine neutrophils

Murine neutrophils wild-type isolated from C57B6 were stimulated for 30 minutes using 10^{-6} M fMLP. The cells were then lysed with lysis buffer for 20 minutes on ice. Phospho p38 MAPK from lysates was immobilised by adding mAb bead slurry and incubated overnight at 4 °C. Cell lysates-immobilised Ab was centrifuged. The pellets were then suspended in kinase buffer, ATP and ATF-2 fusion protein (kinase substrate) before 10μM p38 inhibitor or vehicle control (DMSO) being added and incubated for 60 minutes at 30°C. Reaction was terminated by SDS sample buffer. Subsequently, phospho p38 MAPK was evaluated through detecting phospho ATF-2 by western blotting; protein samples (lysates) was electrophoresed on a 30% SDS acrylamide gel, transferred to nitrocellulose membrane and identified with primary antibody, phospho ATF-2 antibody. A secondary anti-rabbit IgG, HRP-conjugated antibody was added, and detected by enhanced chemiluminescence. Unstimulated cells were used as a control. n = 1.

G) Effect of p38 MAPK and PI3K inhibitors on wild-type murine neutrophil migration in response to KC and fMLP

Many studies showed opposing effects of p38 MAPK and PI3K inhibitors on mouse neutrophil chemotaxis towards KC and fMLP [49], [180], [179]. Therefore, this section will try to reconcile these results and firmly establish the impact of these inhibitors on chemotactic migration of purified murine neutrophils. Migration of murine neutrophils with and without 10 μM of each p38 and PI3K inhibitors towards 10^{-5} M fMLP and 10^{-7} M KC were investigated by pre-incubating these cells with either p38 or PI3K inhibitors or their relevant vehicle control for 30 minutes at 37 °C. They were then incubated for 1 hour at 37 °C on filter membrane and the chemoattractant in the lower chamber of chemotaxis plate (Figures 3.7 and 3.8).

Figures 3.7B and 3.8A show p38 and PI3K inhibitors significantly increased murine neutrophil chemotaxis towards 10^{-7} M KC and 10^{-5} M fMLP respectively compared to their controls (neutrophils without p38 or PI3K inhibitors). The p38 inhibitor decreased murine neutrophil migration towards fMLP at 10^{-5} M, whereas PI3K inhibitor increased cell migration to KC at 10^{-7} M compared to their controls, although the results for both were not statistically significant (Figures 3.7A and 3.8B).

A

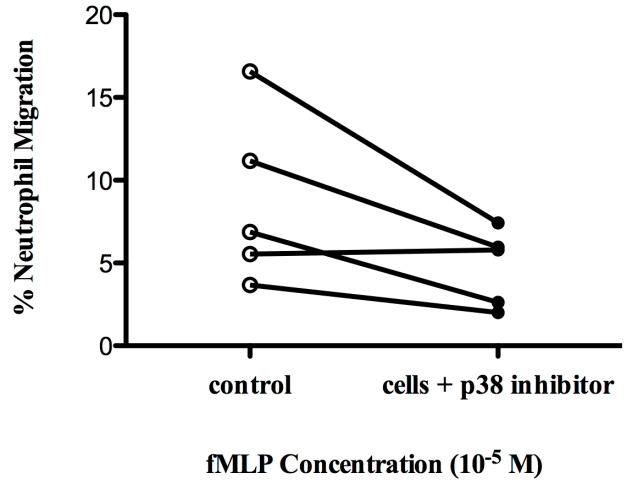

B

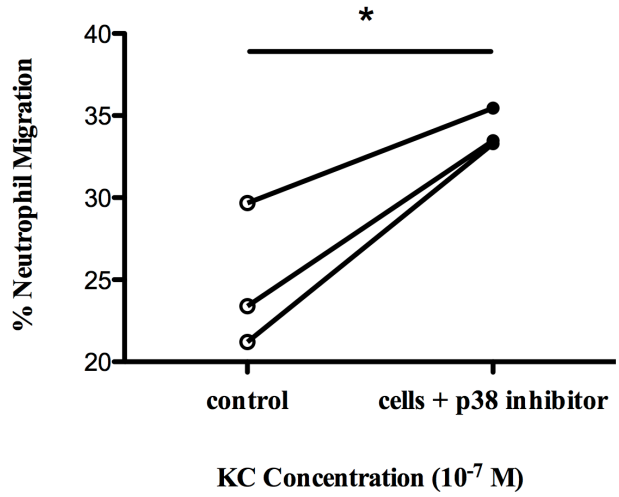

Figure 3. 7: Verifying the impact of p38 inhibitor on migration of murine neutrophils towards fMLP and KC

Neutrophils of wild type mice were re-suspended in a buffer (RPMI supplemented with BSA), and pre-incubated with p38 inhibitor (SB 239063) or vehicle control for 30 minutes at 37 °C. They were then incubated for 1 hour at 37 °C, 5% CO_2. The number of migrated neutrophils with and without 10 µM of p38 inhibitor responding to 10^{-5} M fMLP or 10^{-7} M KC was counted. Findings were corrected for chemokinesis (random migration) of neutrophils by subtracting the chemokinesis control. Data shows mean ± SEM, n = 3-5. Statistical analysis (paired t test) was carried out using neutrophils without inhibitor as a control. (* $p < 0.05$). The figure displays the migration as a percentage of the total number of neutrophils added to the filter (6×10^4).

A

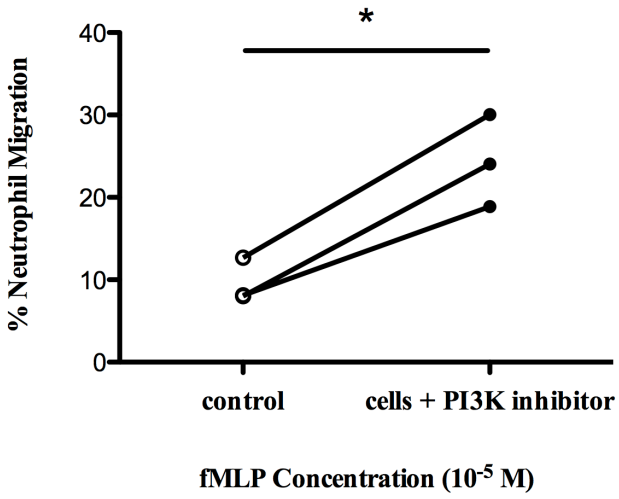

B

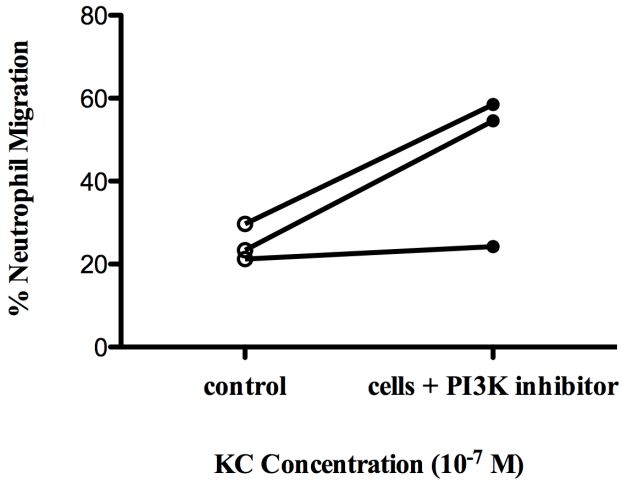

Figure 3. 8: Verifying the impact of PI3K inhibitor on migration of murine neutrophils towards fMLP and KC

Neutrophils of wild type mice were re-suspended in a buffer (RPMI supplemented with BSA), and pre-incubated with PI3K inhibitor (LY 294002) or vehicle control for 30 minutes at 37 °C. They were then incubated for 1 hour at 37 °C, 5% CO_2. The number of migrated neutrophils with and without 10 μM of PI3K inhibitor responding to 10^{-5} M fMLP or 10^{-7} M KC was counted. Findings were corrected for chemokinesis (random migration) of neutrophils by subtracting the chemokinesis control. Data shows mean ± SEM, n = 3. Statistical analysis (paired t test) was carried out using neutrophils without inhibitor as a control. (* $p < 0.05$). The figure displays the migration as a percentage of the total number of neutrophils added to the filter (6×10^4).

3.3 Discussion

Neutrophils play an essential role in the inflammatory response. They represent the first line of defence against infection. Neutrophils respond to infection and/or tissue damage following chemoattractants (endogenous and bacterial signals) out of the blood vessels, via the interstitium to the place of infection [49]. Studies have confirmed that exposure of human neutrophils to fMLP [177] and LPS [181] activates p38 MAPK. The results of this experiment suggest that p38 MAPK signalling in neutrophils isolated from mice is stimulated by KC, fMLP and LPS for 15–30 minutes as seen in the western blot images (Figure 3.1). Although on initial inspection, the lack of statistical significance is evident; it is actually due to the different development timings of western blot processing that led to the varied results seen on densitometry (Figure 3.2A). At later time points, a reduction in the stimulation was recorded; this may be due to phosphatase action which dephopshorylates active p38. In contrast, the data in figures 3.1 and 3.2B show that KC, fMLP and LPS had no significant inhibitory effect on Akt signalling in neutrophils.

It has been published by Nick *et al* in 2000 that there is greater dependence on p38 pathway in the neutrophil compared to other WBC [182]. Separate data by Zu *et al* show in human neutrophils, activation of p38 MAPK is essential for the TNF-α- or fMLP-mediated cellular functions. This study proposed p38 MAPK may have a different function in response to distinct stimulation [177].

A further investigation on p38 phosphorlation has been conducted however, this time on two different groups (C57B6 and TRIB3-/- mice). Again neutrophils isolated from mice are stimulated by KC and fMLP for 15–30 minutes, through phosphorlation p38 MAPK, as illustrated in the western blot images (Figure 3.3), and then at a later time point (60 minutes) decreased. Surprisingly, this result shows no difference between C57B6, as a control, and

TRIB3 -/- mice. Therefore, our observations strongly suggest that TRIB3 does not control activation of neutrophils via p38 MAPK, as its deficiency does not alter p38 phosphorlation compared to C57B6, or it may be that its effect is minute to the extent it is undetectable by western blotting technique.

Based on published observations in human neutrophils, neutrophils migrate towards the end target (fMLP) through activating p38 MAPK while they migrate towards intermediary chemoattractants such as IL-8 via PI3K/Akt [49]. Although the molecular mechanisms of neutrophil navigation remain unclear, it is known that leukocytes migrate in a step-by-step pathway via multiple different chemoattractants, responding to one agonist source after another [53]. A study by Heit *et al* suggested that PI3K is dispensable for neutrophil migration towards fMLP, though PI3K may enhance early responses to the fMLP. In contrast, p38 MAPK-inhibited cells could not polarize in response to fMLP [180].

Activation of murine neutrophils with chemoattractants such as fMLP and KC leads to various functional responses for example neutrophil migration, which we are interested in. This study assessed whether fMLP or KC stimulates murine neutrophil chemotaxis through p38 MAPK or PI3K in C57B6. Therefore, in the current study the impact of p38 inhibitor on kinase activity in RAW 264.7 cells was verified to assess the function of p38 inhibitor. This was successful (Figure 3.5), post testing the effect of fMLP and LPS on p38 MAPK activation in RAW 264.7 cells and the results show fMLP and LPS individually activated p38 MAPK signalling pathway in RAW 264.7 cells compared to the untreated control (Figure 3.4). Finally, the impact of p38 inhibitor on kinase activity in murine neutrophils was confirmed (Figure 3.6). Hence, the effect of p38 inhibitor on wild-type murine neutrophil migration in response to KC and fMLP was studied.

A study by Nick *et al* in 1997 demonstrated that fMLP activated MKK3 (the activator of p38 MAPK). The p38 inhibitor decreased human neutrophil adhesion and chemotaxis in response to fMLP [59]. Cara *et al* in 2001 proposed that p38 has no effect on rolling or adhesion; however it is involved in neutrophil migration via tissue in response to KC in vivo. This study suggested KC stimulates p38 MAPK, which in turn phosphorylates downstream proteins such as LSP-1, to allow neutrophil chemotaxis [60]. A study by Knall *et al* demonstrated that neutrophil migration to IL8 is PI3K-dependent [183], [184]. In vivo PI3Kγ and PI3Kδ appear to have an indispensable function for the early and later phases of leukocyte recruitment respectively, in response to macrophage inflammatory proteins 2 (MIP-2) and KC significantly [185]. Research by Heit *et al* in 2008 showed PI3Kγ had a similar function in mediating neutrophil recruitment in response to fMLP [180].

The mechanisms that regulate neutrophil migration through various signalling pathways (p38 MAPK and PI3K) in response to different chemoattractants, fMLP or KC, is illustrated in figures 3.7 and 3.8. These show p38 inhibitor significantly increased murine neutrophil chemotaxis towards 10^{-7} M KC compared to its control, neutrophils without p38 MAPK inhibitor, (Figure 3.7B), whereas p38 MAPK inhibitor appeared to reduce murine neutrophil migration towards fMLP at 10^{-5} M, although the result was not statistically significant (Figure 3.7A). On the other hand, PI3K inhibitor significantly increased murine neutrophil chemotaxis towards 10^{-5} M fMLP compared to its control, neutrophils without PI3K inhibitor (Figure 3.8A). PI3K inhibitor also increased cell migration to KC at 10^{-7} M compared to its control, but again the result was not statistically significant (Figure 3.8B). This data clearly indicates that different signalling pathways for various stimuli control neutrophil migration, i.e. selective stimulation of signalling pathways may cause various neutrophil responses. An example of that is the varying effects of fMLP and KC stimuli on migration of neutrophils through p38 or PI3K pathways as demonstrated above.

In summary, my results suggest that TRIB3 may not control activation of neutrophils through p38 MAPK. Furthermore, evident data propose that neutrophil migration towards some chemoattractants, KC and fMLP, is dependent upon on various signalling pathways such as p38 MAPK and PI3K, which could be regulated by TRIB3 (see chapter 4). Given that there are discrepancies in the literature, in addition to observations in this project, further *in vitro* studies on the impact of TRIB3 on neutrophil function through various intracellular signalling pathways in response to various chemoattractants would be recommended.

Chapter 4: The role of TRIB3 in neutrophil function *in vitro*

4.1 Introduction

Neutrophil function relies on expression of adhesion molecules. They enable neutrophils to interact with endothelium. For example tethering and rolling of neutrophil on endothelial cells occurs via L-selectin, while firm adhesion and arresting happens through CD11b [186]. In 1995 Phillips *et al* found that L-selectin is indispensable for circulating neutrophils [187]. In response to inflammation, stimulated neutrophils adhere to endothelium and aggregate with one another. Research by Guyer *et al* (1996) proposed that L-selectin and PSGL-1 support a collisional cell-cell interaction, which represents the initial stage of neutrophil aggregation [188].

It has been published by Cavanagh in 1998, increasing expression CD11b is a neutrophil activation marker. This adhesion complex permits neutrophil migration from the blood stream to the target [189]. Chen *et al* (2003) suggested neutrophil CD11b expression and reactive oxygen species (ROS) production could help to predict the stage of murine AIDS [190].

Neutrophils migrate to sites of inflammation by a process known as chemotaxis [191]. Neutrophils are exposed to many different chemoattractants and evidence indicates a hierarchical status of these. End target chemoattractants (from infected sites) are prioritised by activating the p38 MAPK pathway. In comparison, the intermediate chemoattractants (which occur along the path) even at high level activate the PI3K/Akt cascade [49], [51], [52], [53], [54].

The PI3K cascade is one of the most important signalling pathways of neutrophil chemotaxis [58]. On the other hand, in humans and mice the p38 MAPK has an essential function in neutrophil chemotaxis [59], [60]. However, various aspects related to these pathways are still vague, such as the p38 MAPK and PI3K/Akt cascades are overlapping, opposing or complementary to each other [49].

This chapter will verify whether TRIB3 controls the expression of adhesion molecules (PSGL-1, L-selectin and CD11b) on murine neutrophils with and without PMA stimulation by FACSCalibur flow cytometry. It will also discuss the impact of TRIB3 on neutrophil migration in response to KC and fMLP.

4.2 Results

A) Effect of TRIB3 on PSGL-1, L-selectin and CD11b expression on PMA stimulated and un-stimulated murine neutrophils

Expression of adhesion molecules (PSGL-1, L-selectin and CD11b) on murine neutrophils by various stimuli including PMA was already demonstrated in various studies, giving diverse findings [192], [193], [194]. This section will see the effect of PMA on expression of above adhesion molecules on neutrophils, in addition to testing the impact of TRIB3 on them. Expression of PSGL-1, L-selectin and CD11b on C57B6 and TRIB3-/- murine neutrophils was investigated by pre-incubating murine whole blood with or without 10^{-7} M PMA at 37 °C before adding the fluorescently conjugated antibodies. Absence of TRIB3 from murine neutrophils had no significant effect on expression of the above studied adhesion molecules on the cells. Stimulating both C57B6 and TRIB3-/- murine neutrophils with PMA significantly up regulated CD11b (Figure 4.3), but neither stimulating C57B6 nor TRIB3-/- murine neutrophils showed significant differences on expression of PSGL-1 compared to the un-stimulated cells (Figure 4.1). However, stimulating TRIB3-/- murine neutrophils with 10^{-7} M PMA demonstrated statistically significant shedding of L-selectin. In contrast, no significant shedding of L-selectin was observed in the wild type cells after stimulation (Figure 4.2).

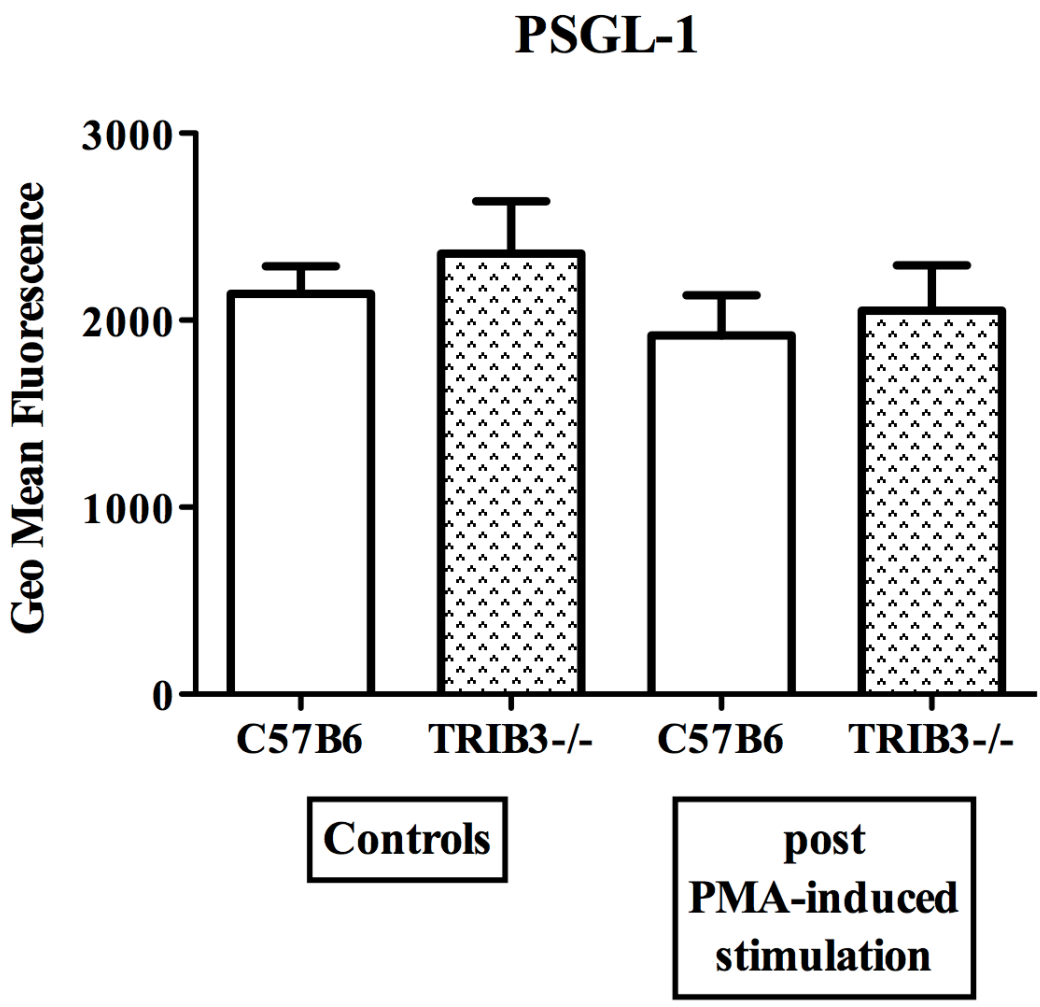

Figure 4. 1: FACS determines adhesion molecule, PSGL-1, expressed on C57B6 and TRIB3-/- PMA stimulated and un-stimulated murine neutrophils

C57B6 and TRIB3-/- murine whole blood samples were pre-incubated with/without 10^{-7} M PMA for 15 minutes at 37 °C, 5% CO_2. Samples were incubated with fluorescently conjugated antibody (PE anti-mouse PSGL-1) and FITC anti-mouse Ly-6G (for labeling neutrophils). They were then incubated for 30 minutes on ice. Further incubation with 1% erythrolyse for 10 minutes at RT occurred prior to washing. Surface expression was determined by FACS. Data showed mean ± SEM, n = 3-4. Statistical analysis (one-way ANOVA, Bonferroni) was carried out.

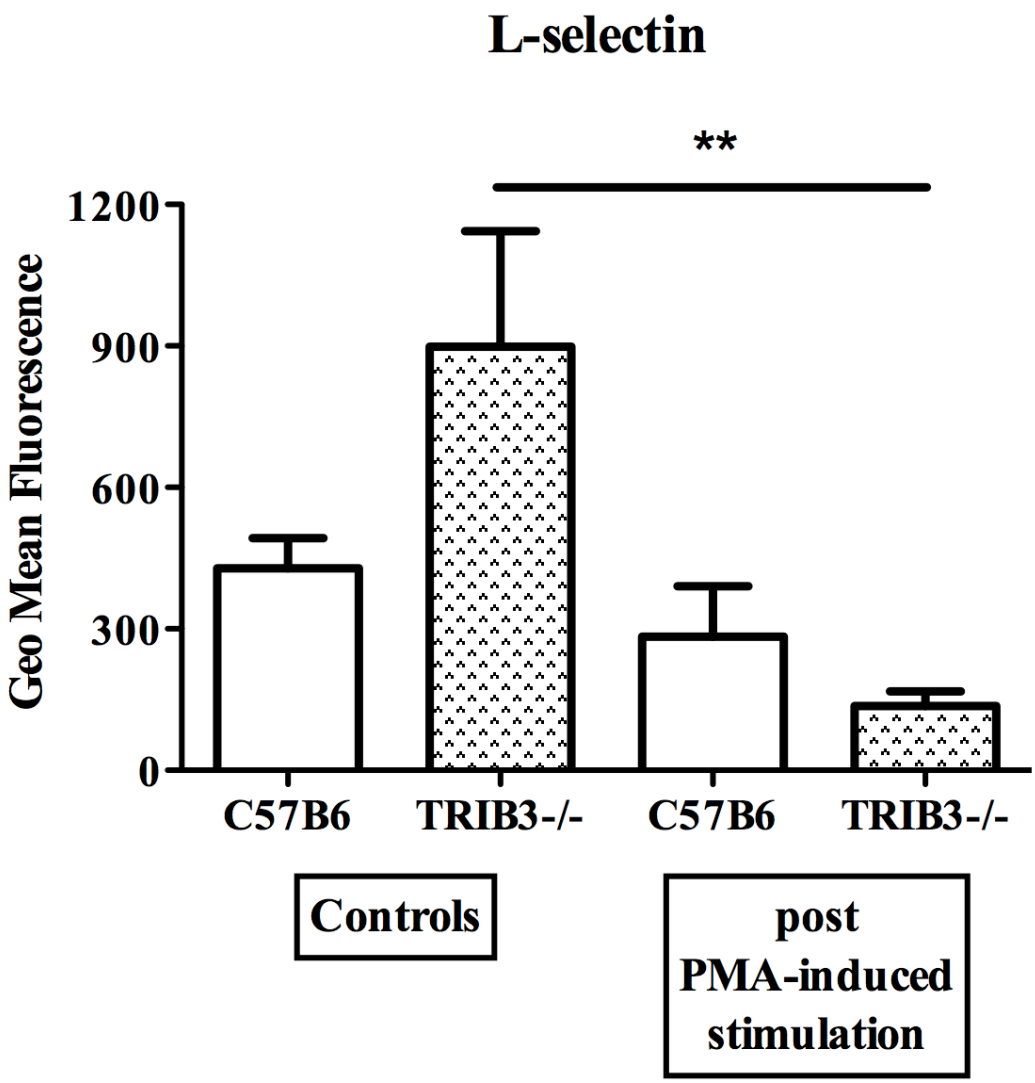

Figure 4. 2: FACS determines adhesion molecule, L-selectin, expressed on C57B6 and TRIB3-/- PMA stimulated and un-stimulated murine neutrophils

C57B6 and TRIB3-/- murine whole blood samples were pre-incubated with/without 10^{-7} M PMA for 15 minutes at 37 °C, 5% CO_2. Samples were incubated with fluorescently conjugated antibody (PE anti-mouse L-selectin) and FITC anti-mouse Ly-6G (for labeling neutrophils). They were then incubated for 30 minutes on ice. Further incubation with 1% erythrolyse for 10 minutes at RT occurred prior to washing. Surface expression was determined by FACS. Data showed mean ± SEM, n = 6-8. Statistical analysis (one-way ANOVA, Bonferroni) was carried out. (** $p < 0.01$).

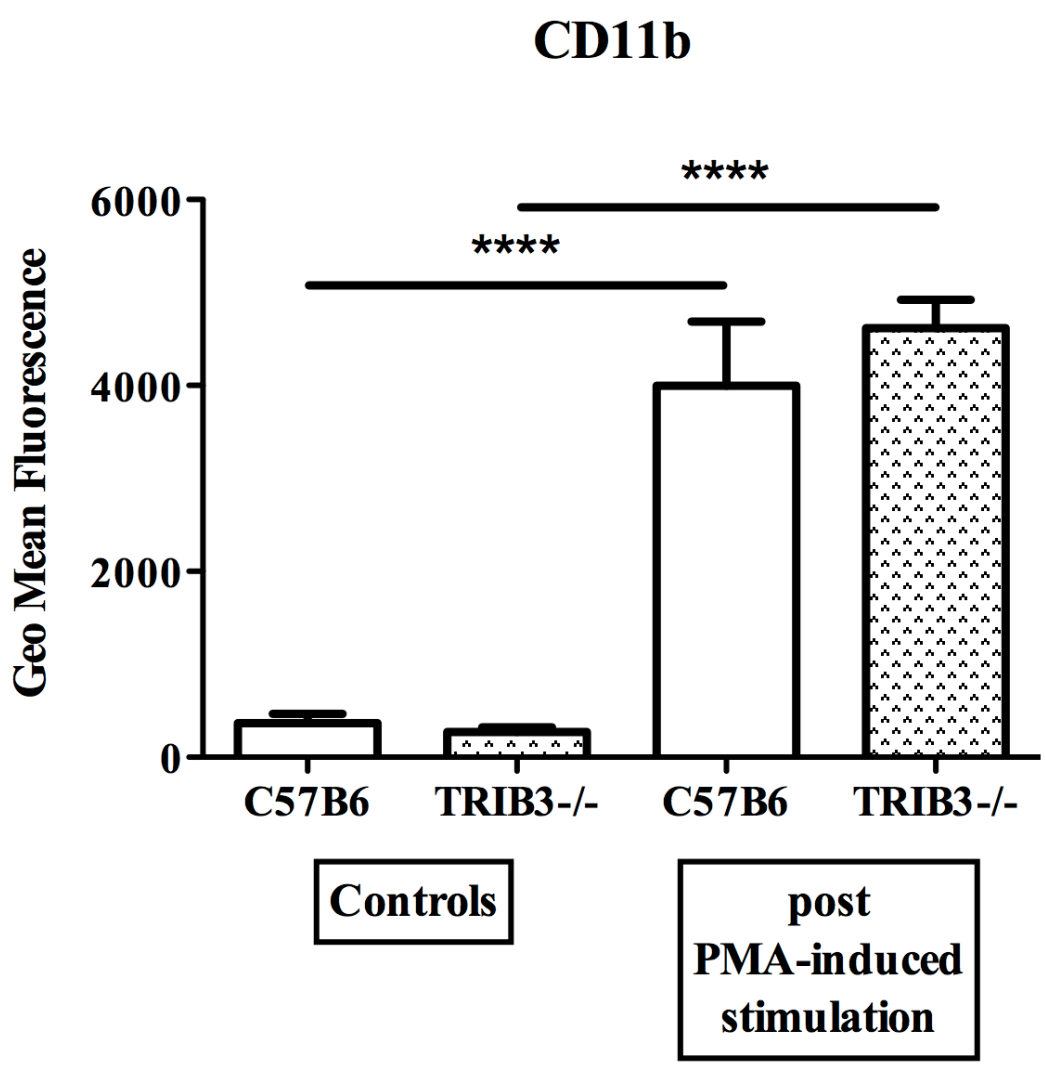

Figure 4. 3: FACS determines adhesion molecule, CD11b, expressed on C57B6 and TRIB3-/- PMA stimulated and un-stimulated murine neutrophils

C57B6 and TRIB3-/- murine whole blood samples were pre-incubated with/without 10^{-7} M PMA for 15 minutes at 37 °C, 5% CO_2. Samples were incubated with fluorescently conjugated antibody (PE Rat anti-mouse CD11b and FITC anti-mouse Ly-6G (for labeling neutrophils). They were then incubated for 30 minutes on ice. Further incubation with 1% erythrolyse for 10 minutes at RT occurred prior to washing. Surface expression was determined by FACS. Data showed mean ± SEM, n = 4-5. Statistical analysis (one-way ANOVA, Bonferroni) was carried out. (**** $p < 0.0001$).

B) Optimisation of chemoattractant concentrations on neutrophil migration

KC, fMLP and LPS optimal concentrations on neutrophil migration were optimised in previous studies [195]. This section is to confirm these data and in the next section to apply it on TRIB3-/- and study the impact of TRIB3 on neutrophil migration in response to different chemoattractants. Migration of isolated murine neutrophils to various stimuli (KC, fMLP and LPS) was demonstrated by incubating these cells for 3 hours at 37 ˚C on filter membrane and the chemoattractant in the lower chamber of chemotaxis plate (Boyden chamber). In addition, increasing concentrations of these chemoattractants was used to check their optimal concentration for neutrophil migration. The following figures show the migration of murine neutrophils towards KC, fMLP and LPS.

KC significantly enhanced murine neutrophil chemotaxis compared to the control (buffer) at 10^{-5}–10^{-7} M (Figure 4.4). The maximum response was at 10^{-7} M. It can be seen from the figure that a lower concentration (10^{-8} M) reduced the functional response to the chemotactic factor in a dose-dependent manner, whilst at this level it still remained above the control level. On the other hand, fMLP enhanced murine neutrophil chemotaxis compared to the control at 10^{-5} M and 10^{-6} M (Figure 4.5). There was a significant increase in migration at 10^{-5} M, whilst there was a trend to an increased response at 10^{-6} M. It can be seen from the figure that the lower concentrations (10^{-6}–10^{-8} M) reduced the functional response to the chemotactic factor. In contrast, LPS had no significant effect on murine neutrophil chemotaxis compared to the control at any of the concentrations used (Figure 4.6). Moreover, it can be seen from the graph that there were no trends observed.

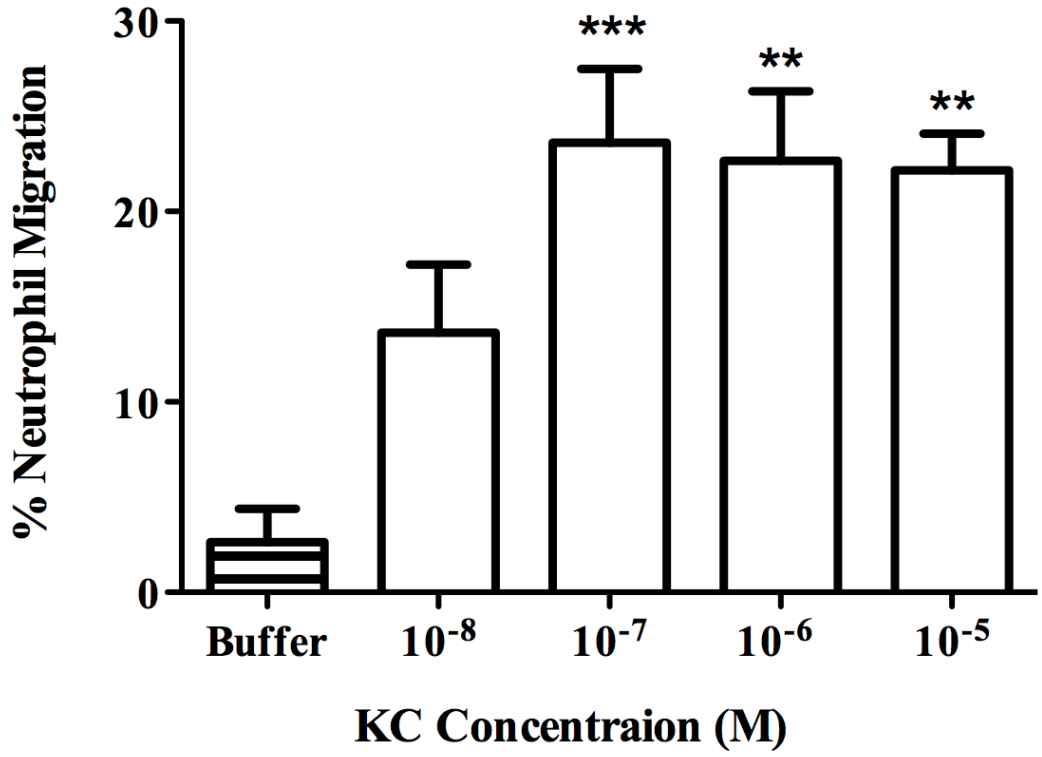

Figure 4. 4: Migration of murine neutrophils towards KC

Murine neutrophils isolated from C57B6 were re-suspended in buffer (RPMI supplemented with BSA) and incubated for 3 hours at 37 ˚C, 5% CO_2 on filter membrane and the buffer or KC (10^{-5}–10^{-8} M) in the lower chamber of chemotaxis plate. The number of migrated neutrophils responding to the buffer or KC was counted. Findings were corrected for chemokinesis (random migration) of neutrophils by subtracting the chemokinesis control from every value including the cells migrated to the buffer. Data shows mean ± SEM, n = 4. Statistical analysis (one-way ANOVA, Dunnett post test) was carried out using buffer as a control. (** $p < 0.01$ and *** $p < 0.001$). Figure displays the migration as a percentage of the total number of neutrophils added to the filter (6×10^4).

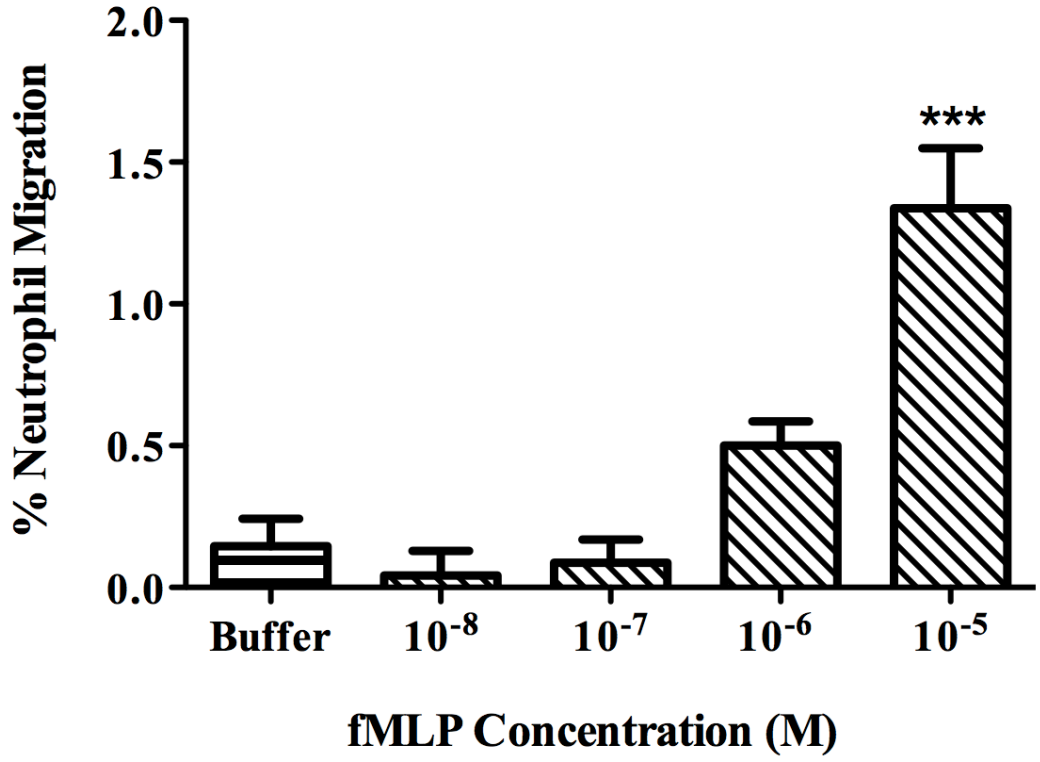

Figure 4. 5: Migration of murine neutrophils towards fMLP

Murine neutrophils isolated from C57B6 were re-suspended in a buffer (RPMI supplemented with BSA) and incubated for 3 hours at 37 ˚C, 5% CO_2 on filter membrane and the buffer or fMLP (10^{-5}–10^{-8} M) in the lower chamber of chemotaxis plate. The number of migrated neutrophils responding to the buffer or fMLP was counted. Findings were corrected for chemokinesis (random migration) of neutrophils by subtracting the chemokinesis control from every value including the cells migrated to the buffer. Data shows mean ± SEM, n = 4. Statistical analysis (one-way ANOVA, Dunnett post- test) was carried out using buffer as a control. (*** $p < 0.001$). Figure displays the migration as a percentage of the total number of neutrophils added to the filter (6×10^4).

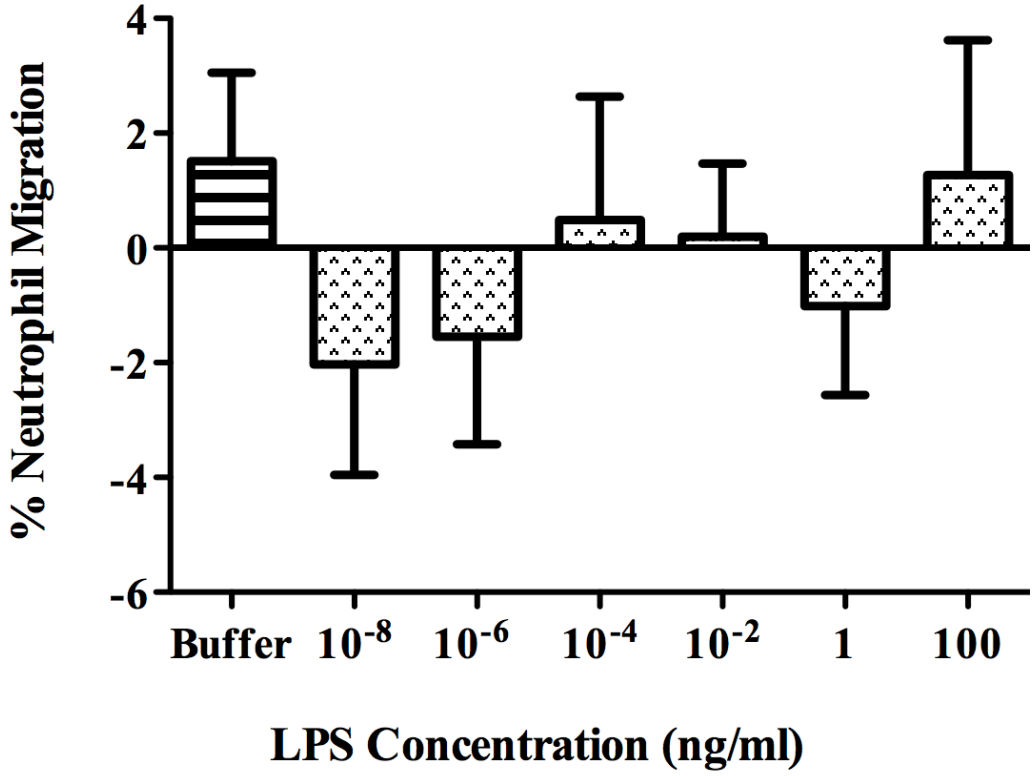

Figure 4. 6: Migration of murine neutrophils towards LPS

Murine neutrophils isolated from C57B6 were re-suspended in a buffer (RPMI supplemented with BSA) and incubated for 3 hours at 37 ˚C, 5% CO_2 on filter membrane and the buffer or LPS (10^{-8}–100 ng/ml) in the lower chamber of chemotaxis plate. The number of migrated neutrophils responding to the buffer or LPS was counted. Findings were corrected for chemokinesis (random migration) of neutrophils by subtracting the chemokinesis control from every value including the cells migrated to the buffer. Data shows mean ± SEM, n = 5. Statistical analysis (one-way ANOVA, Dunnett post-test) was carried out using buffer as a control. There were no significant differences. Figure displays the migration as a percentage of the total number of neutrophils added to the filter (6×10^4).

C) Effect of TRIB3 on murine neutrophil chemotaxis in response to KC and fMLP

Neutrophil migration towards KC and fMLP was already detected in different studies [49], [179]. However, the effect of TRIB3 on regulating that migration needs to be investigated. Therefore, the role of TRIB3 on murine neutrophil migration in response to KC and fMLP was studied by incubating C57B6 and TRIB3-/- neutrophil groups for 1 hour at 37 ˚C on filter membrane and the chemoattractant in the lower chamber of chemotaxis plate at increasing concentrations. The figures 4.7 and 4.8 below show the migration of murine neutrophils towards KC and fMLP.

It can be seen from the graphs that absence of TRIB3 had no significant effect on neutrophil migration whether cells enhanced by KC or fMLP.

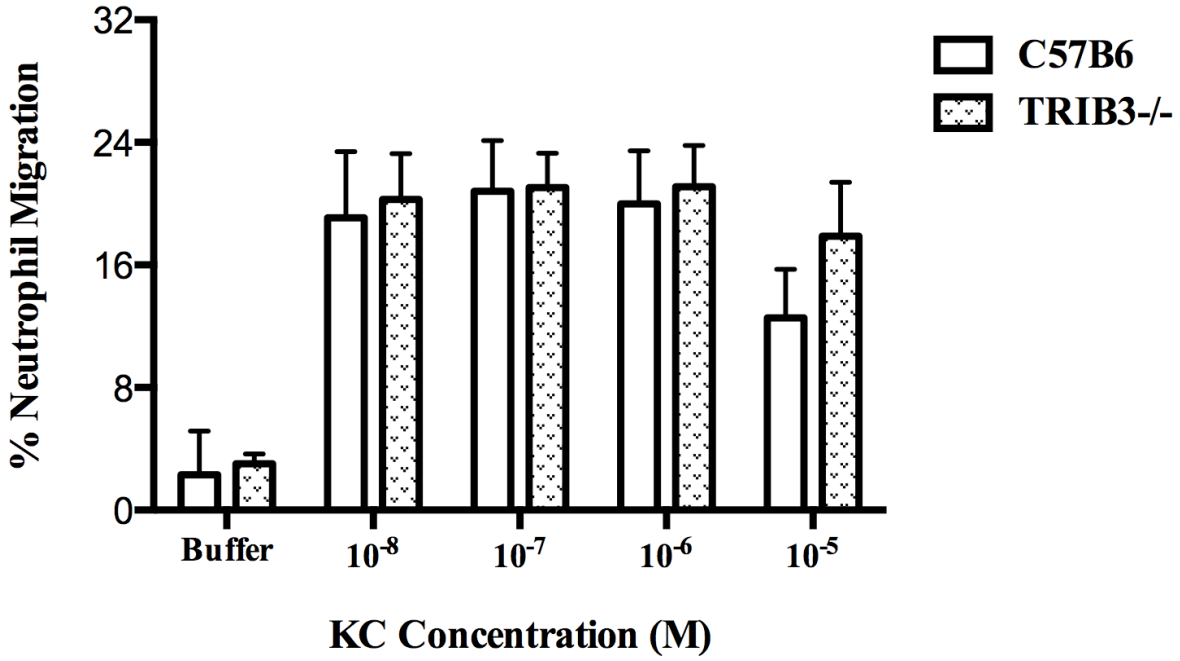

Figure 4. 7: Role of TRIB3 on murine neutrophil migration in response to KC

Neutrophils isolated from C57B6 and TRIB3-/- mice were re-suspended in buffer (RPMI supplemented with BSA) and incubated for 1 hour at 37 ˚C, 5% CO_2 on filter membrane and the buffer or KC (10^{-8}–10^{-5} M) in the lower chamber of chemotaxis plate. The number of migrated neutrophils responding to the buffer or KC was counted. Findings were corrected for chemokinesis (random migration) of neutrophils by subtracting the chemokinesis control from each value including the cells migrated to the buffer. Data shows mean ± SEM, n = 4. Statistical analysis (one-way ANOVA, Bonferroni post-test) was carried out. There was no significant difference. Figure displays the migration as a percentage of the total number of neutrophils added to the filter (6×10^4).

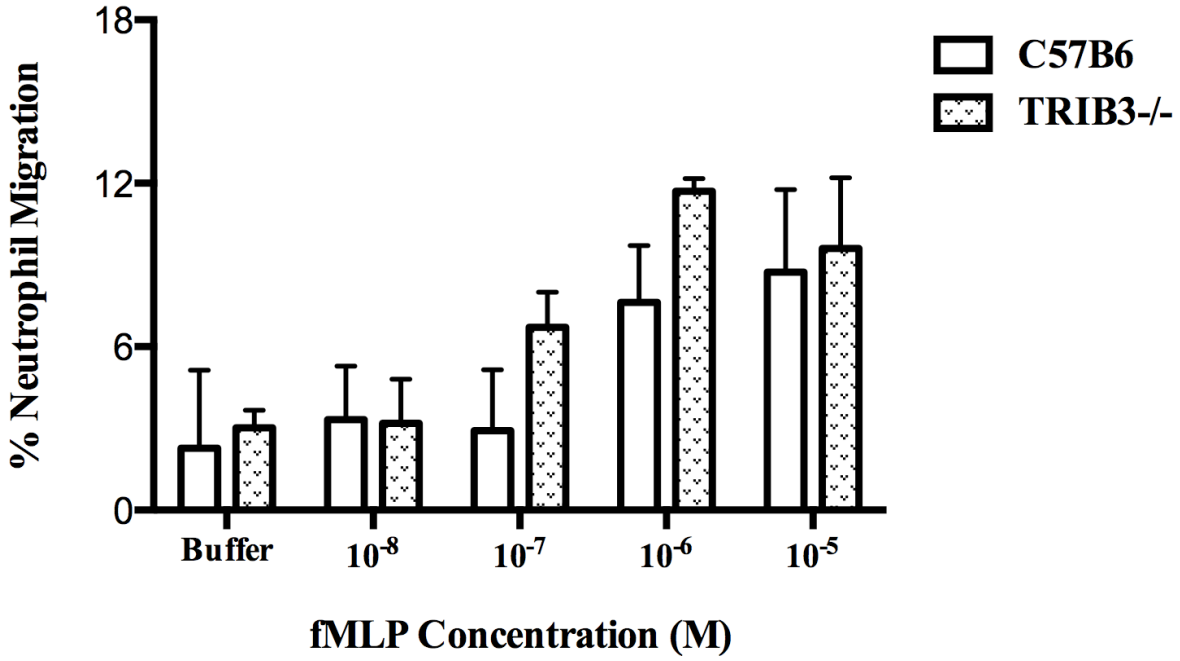

Figure 4. 8: Role of TRIB3 on murine neutrophil migration in response to fMLP

Neutrophils isolated from C57B6 and TRIB3-/- mice were re-suspended in buffer (RPMI supplemented with BSA) and incubated for 1 hour at 37 ˚C, 5% CO_2 on filter membrane and the buffer or fMLP (10^{-8}–10^{-5} M) in the lower chamber of chemotaxis plate. The number of migrated neutrophils responding to the buffer or fMLP was counted. Findings were corrected for chemokinesis (random migration) of neutrophils by subtracting the chemokinesis control from each value including the cells migrated to the buffer. Data shows mean ± SEM, n = 4. Statistical analysis (one-way ANOVA, Bonferroni post-test) was carried out. There was no significant difference. Figure displays the migration as a percentage of the total number of neutrophils added to the filter (6×10^4).

4.3 Discussion

Neutrophil migration is essential to physiological and pathological processes. Preceding investigations have recorded a relationship between fMLP [49], [180], [53] and IL-8, an intermediary chemoattractant that is equivalent to KC in mice and migration of neutrophils [49], [53]. It has been observed that chemokines in a concentration gradient can bind with leukocytes through GPCRs which result in leukocyte directional migration [53]. Furthermore, each class of leukocyte is able to respond to a variety of chemokines [53], and since this study is about neutrophils, attention has been focused on this class.

Given the above, positive results were recorded in these experiments, the murine neutrophils migrated to KC and fMLP (intermediary and end target [49] chemoattractants respectively) as displayed in figures 4.4 and 4.5. However, there was no migration to LPS (Figure 4.6), although p38 MAPK signalling in neutrophils is stimulated by LPS, suggesting LPS is capable of activating neutrophils but does not act as a chemoattractant. Furthermore, a study by Aomatsu *et al* found that human neutrophils displayed increased random motility but not directed migration after stimulation with LPS within 10 minutes which lasted for more than 90 minutes, leading to activation of ERK and p38 MAPK [181]. This observation is also seen in the data shown in figure 4.6.

In this project, I have investigated the response of freshly isolated neutrophils to intermediate (KC) and end target (fMLP) chemokines from wild type mouse and found that the optimal concentration for KC was 10^{-7} M whereas, 10^{-5} M for fMLP.

It also assesses whether knockout TRIB3 affects neutrophil chemotaxis differently. The results (Figures 4.7 and 4.8) clearly highlight no profound differences between TRIB3-/- mice and the control in neutrophil migration towards KC or fMLP. The concentrations of KC used were

similar to that used for the control. In the controls this proved optimal in maximizing neutrophil migration. There were hardly any differences between C57B6 and TRIB3-/- mice. These findings may indicate that TRIB3 has no effect on neutrophil migration towards KC. The other explanation for this could be that optimum KC concentration for the wild type is too high for TRIB3-/- mice, which may have resulted in excess KC binding with other receptors. This in turn inhibits neutrophil migration. Hence, if lower concentrations were used, differences may have been observed. However, a limitation on the number of mice available prevented further experiments.

Interestingly, there was a trend to an increased response to KC at 10^{-5} M in TRIB3-/- mice compared to C57B6. There was also a trend to an increased response to fMLP at 10^{-7} M and 10^{-6} M. This possibly increased the sensitivity of neutrophil migration towards chemoattractant due to the knockout of TRIB3. This was confirmed by the data in chapter 5 whilst studying the effect of TRIB3 on neutrophil recruitment in thioglycollate-induced peritonitis. The neutrophil influx of TRIB3-/- mice towards the peritoneum was greater than the neurophil influx of C57B6 at 2 hours, but it was not found to be significant. Therefore, TRIB3 may control neutrophil chemotaxis in response to different chemoattractants (KC and fMLP). However, to find a significant effect the number of experiments conducted should be increased.

A study by Davenpeck *et al* (2000) verified that exposure of neutrophils to PAF or PMA results in activated cells, which in turn reduced surface expression of PSGL-1 within minutes [192]. Neeley *et al* published with his group the expression of L-selectin on purified human neutrophils caused by varied activators. The results show PAF and fMLP reduced L-selectin expression in neutrophils, but IL-5 had no effect on the expression of L-selectin in the cells [193]. Siddiqi *et al* in 2001 found CD11b expression is clearly increased in PMA-stimulated neutrophils [194].

Figures 4.1–4.3 compared murine neutrophils from both wild type and TRIB3-/- mice. This illustrated that no significant difference was seen in the expression of adhesion molecules (PSGL-1, L-selectin and CD11b) on neutrophils for both types, whether the cells were stimulated with 10^{-7} M PMA or not. This excludes the effect of TRIB3 on the expression of these adhesion molecules on murine neutrophils, although there was a trend towards higher L-selectin expression in TRIB3-/- mice before stimulation. However, stimulation of neutrophils with PMA showed significant differences in the expression of adhesion molecules in both groups (C57B6 and TRIB3-/- mice). Some shedding of L-selectin in PMA post-stimulated C57B6 neutrophils was noted but this was not as significant as quoted in other studies in the literature. In contrast, TRIB3-/- post-stimulated neutrophils demonstrated shedding of L-selectin, giving statistically significant result (Figure 4.2). On the other hand, stimulating both C57B6 and TRIB3-/- murine neutrophils with PMA significantly up regulated CD11b (Figure 4.3), but neither stimulating C57B6 nor TRIB3-/- neutrophils showed significant differences on expression of PSGL-1 compared to the un-stimulated cells (Figure 4.1). Thus, this result would suggest that removing TRIB3 and stimulating the neutraphils has a significant effect on the shedding of L-selectin from the cell surface. It is thought that the key in increasing CD11b expression is the stimulation of the cells not TRIB3 effect, as in both PMA post-stimulated neutrophil groups CD11b was up regulated significantly, while with PSGL-1 neither removing TRIB3 nor stimulation the cells has an impact on PSGL-1 expression. The discrepancies in the literature and the *in vitro* observations of this project may be a consequence of certain variables such as the possibility of infection in mice and technical differences (selection of samples, substances, concentration and the process of eliminating the erythrocytes).

In summary, this study clearly excludes the significant effect of TRIB3 on the expression of adhesion molecules on murine neutrophils. However, it does show stimulation of the cells with

PMA may regulate expression significantly, some up and others down-regulation in C57B6 and TRIB3-/- mice. Furthermore, clear data propose that neutrophil migration towards some chemoattractants, KC and fMLP, is dependent upon on various signalling pathways such as p38 MAPK and PI3K (seen in chapter 3), which could be regulated by TRIB3. Again, due to inconsistencies in research and observations in this study, additional *in vitro* studies on the impact of TRIB3 on neutrophil migration and adhesion molecules would be suggested.

Chapter 5: The role of TRIB3 on neutrophilic inflammation *in vivo*

5.1 Introduction

Cytokines act as chemical messengers binding to specific receptors, regulating the behaviour of other cells. They affect differentiation, development, growth, blood clotting and repair of the target cells. Furthermore, cytokines have an essential role in defending the immune system against disease.

This chapter will review whether TRIB3 regulates cytokine levels in lavage fluid derived from mice with thioglycollate-induced peritonitis using BD CBA. We also studied whether neutrophil migration across the microvasculature and invasion are influenced by the TRIB3 altered cytokine level. In addition, the effect of knocking out TRIB3 on WBC recruitment in blood and on the type of WBC recruited in murine peritoneal lavage fluid was investigated in both groups. These were collected at different time points after injecting 4% thioglycollate intraperitoneally.

5.2 Results

A) Function of TRIB3 on murine cytokine levels in thioglycollate-induced peritonitis

Diverse studies have revealed that cytokines are required for neutrophil recruitment [196], [197]. However, the impact of TRIB3 on controlling their levels has not previously been investigated. Therefore, the effect of knocking out TRIB3 on different murine cytokine levels in thioglycollate-induced peritonitis of lavage fluid was demonstrated by injecting wild type and TRIB3-/- mice intraperitoneally with 4% thioglycollate prior to collecting peritoneal lavage fluid from each group at different time points. Levels of cytokines in lavage fluid were quantified using CBA. TRIB3 deficiency increased murine IL-13 level in thioglycollate-induced peritonitis significantly compared to the control (Figure 5.1). Table 5.1 below illustrates the levels of each cytokine (GMCSF, IL-4, IL-13, IL-17A, KC, MCP-1, MIP-1α, MIP-1β and TNF) individually for lavage fluid.

	0 h		2 h		6 h	
	C57B6	TRIB3-/-	C57B6	TRIB3-/-	C57B6	TRIB3-/-
GMCSF	ND	ND	ND	42.99 ± 3.93	398.25 ± 21.80	347.67 ± 30.82
IL4	ND	ND	ND	ND	329.00 ± 8.44	363.67 ± 38.65
IL13	ND	ND	ND	ND	235.25 ± 8.23	273.67 ± 12.88**
IL17A	ND	ND	24.73 ± 4.90	221.02 ± 43.20	6331.00 ± 1438.11	7730.33 ± 4129.74
KC	ND	ND	28.26 ± 17.07	42.42 ± 12.36	59637.00 ± 1816.09	55618.33 ± 27426.97
MCP-1	23.33 ± 3.80	22.57 ± 3.90	851.34 ± 116.44	2979.14 ± 904.74	78182.00 ± 1923.31	63830.67 ± 31022.49
MIP-1 alpha	ND	ND	558.56 ± 99.72	833.22 ± 52.80	47103.75 ± 1522.35	40400.33 ± 20007.93
MIP-1 beta	ND	ND	130.34 ± 42.04	225.79 ± 41.37	3382.25 ± 101.60	2799.67 ± 927.13
TNF	ND	ND	451.26 ± 51.74	629.41 ± 37.74	3258.25 ± 425.52	2659.33 ± 1218.54

Table 5.1: Effect of TRIB3 on murine cytokine levels in thioglycollate-induced peritonitis of lavage fluid

The table shows levels of cytokines in thioglycollate-induced peritonitis of lavage fluid of wild type versus TRIB3-/- mice, using BD CBA. Cytokine levels were measured in lavage fluid, taken at different time points (0, 2, 6 and 24 hours) after injecting 4% thioglycollate intraperitoneally. Data show mean ± SEM in pg/ml. Each group is represented by 3-4 mice at each time point (n). Statistical significance was tested using one-way ANOVA, followed by Bonferroni post test (** $p < 0.01$). C57B6 served as a control. ND: below the detection limit of the kit (<10 pg/ml).

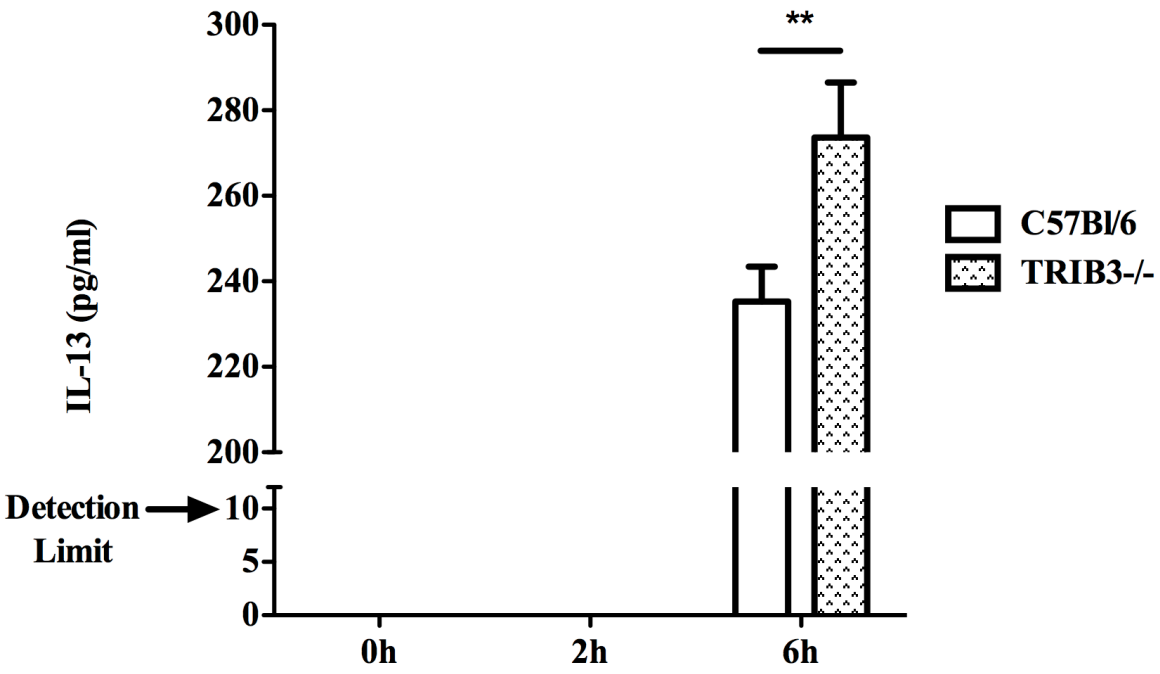

Figure 5. 1: Effect of TRIB3 on murine IL-13 level in thioglycollate-induced peritonitis of lavage fluid

The graph illustrates IL-13 concentrations in thioglycollate-induced peritonitis of lavage fluid of wild type versus TRIB3-/- mice, using BD CBA. IL-13 level was measured in lavage fluid, taken at different time points (0, 2, 6 and 24 hours) after injecting 4% thioglycollate intraperitoneally. Data show mean ± SEM in pg/ml. Each group is represented by 3-4 mice at each time point (n). Statistical significance was tested using one-way ANOVA, followed by Bonferroni post test (** $p < 0.01$). C57B6 served as a control. Values below the detection limit (10 pg/ml) of the kit are undetectable by this experiment.

B) Function of TRIB3 on WBC recruitment in thioglycollate-induced peritonitis

Leukocyte chemotaxis in response to various chemoattractants was studied extensively [198]. The current study will see the role of TRIB3 on their migration. The effect of absence of TRIB3 on murine leukocyte recruitment in thioglycollate-induced peritonitis were investigated by injecting C57B6 and TRIB3-/- mice intraperitoneally with 4% thioglycollate before collecting blood and peritoneal lavage fluid from each group at different time points. The level of circulating leukocytes was significantly less in TRIB3 deficient animals compared to the control (Figure 5.2). Figures 5.3A–C demonstrate the total leukocyte cell count versus neutrophils (including the percentage) between 2 to 48 hours in peritoneal lavage specimens. The graphs highlight that at 2 hours mononuclear cells predominated, but at 6 hours this was reversed, demonstrating a predominance of neutrophils in both groups. In addition, there was a trend towards an increased neutrophil migration in the peritoneum at 2 hours and persisted at 24 hours in the TRIB3-/- mice compared to the control.

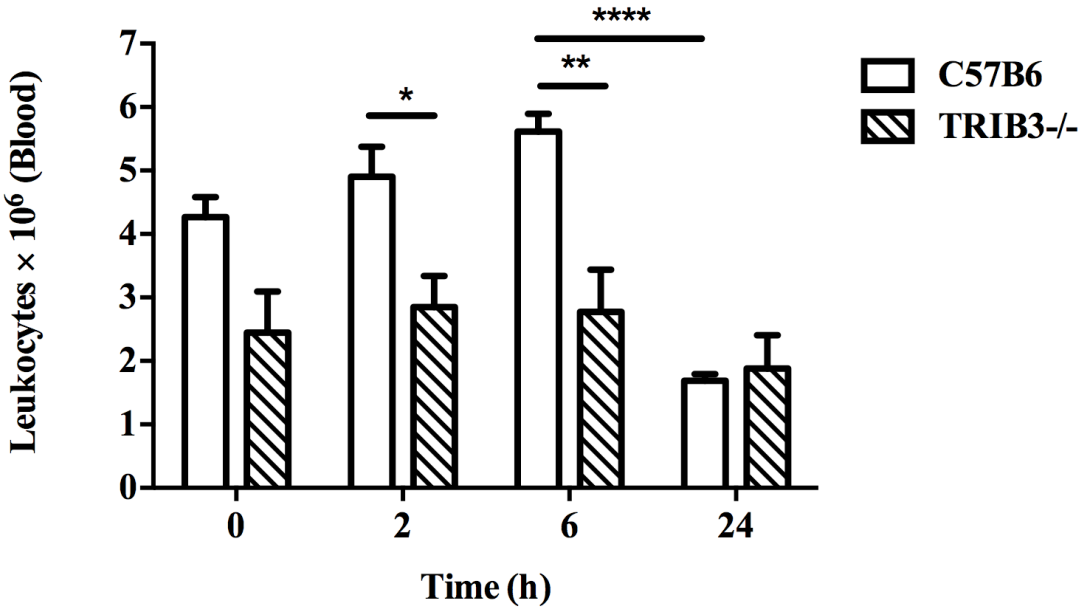

Figure 5. 2: Effect of TRIB3 on blood leukocyte recruitment in thioglycollate-induced peritonitis

The number of migrated leukocytes in blood of thioglycollate-induced peritonitis in C57B6 versus TRIB3-/- mice were counted. Samples were collected at different time points (0, 2, 6 and 24 hours) after injecting 4% thioglycollate intraperitoneally. Data show mean ± SEM. Each group is represented by 3-6 mice at each time point. Statistical significance was tested using one-way ANOVA, followed by Bonferroni post test (* $p < 0.05$, ** $p < 0.01$ and **** $p < 0.0001$). C57B6 served as a control.

A

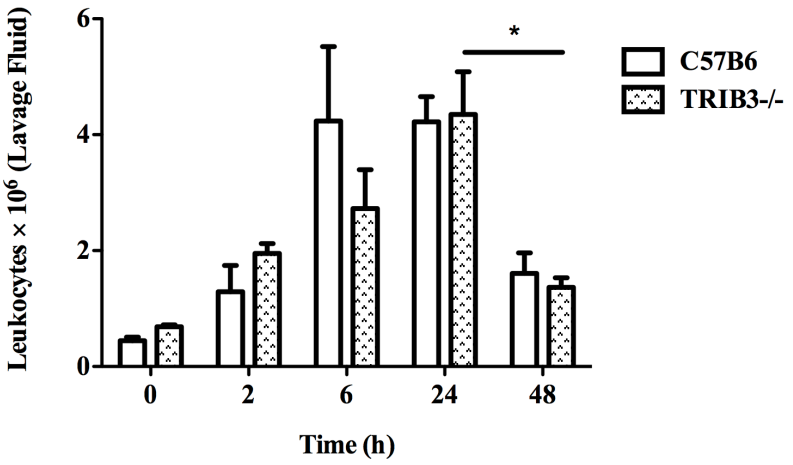
Leukocytes × 10⁶ (Lavage Fluid)
6
4
2
0
*
C57B6
TRIB3-/-
0
2
6
24
48
Time (h)

B

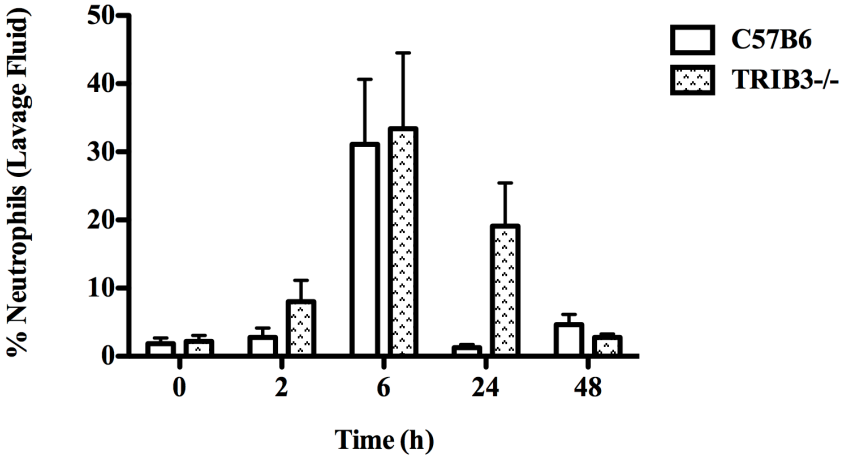
% Neutrophils (Lavage Fluid)
50
40
30
20
10
0
C57B6
TRIB3-/-
0
2
6
24
48
Time (h)

C

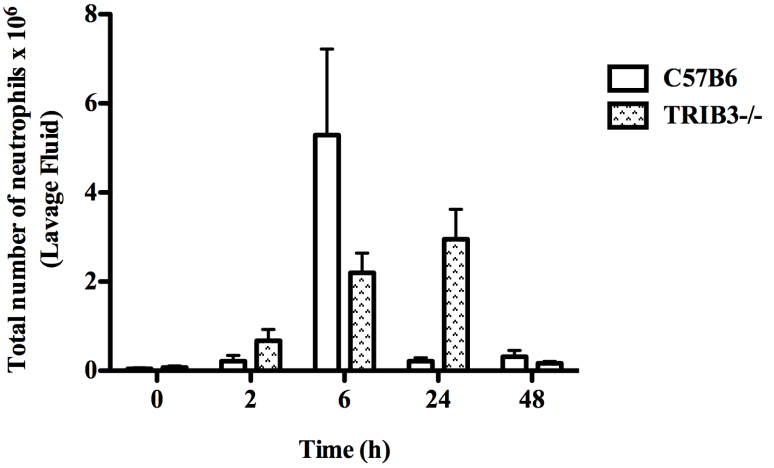
Total number of neutrophils x 10⁶ (Lavage Fluid)
8
6
4
2
0
C57B6
TRIB3-/-
0
2
6
24
48
Time (h)

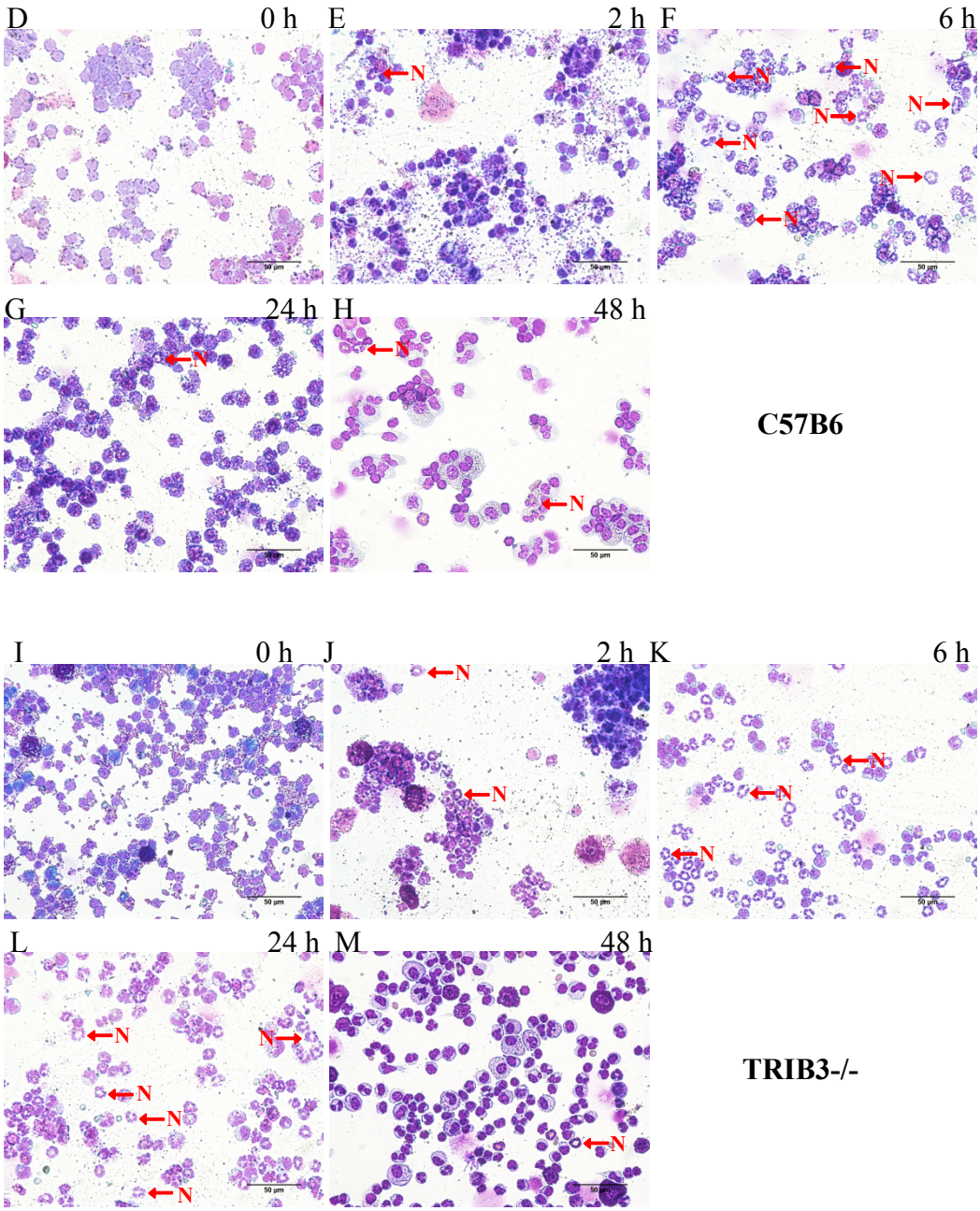

Figure 5. 3: Effect of TRIB3 on peritoneal lavage fluid leukocyte recruitment in thioglycollate-induced peritonitis

The number of migrated leukocytes in peritoneal lavage fluid of thioglycollate-induced peritonitis in C57B6 versus TRIB3-/- mice were counted (A). Samples were collected at different time points (0, 2, 6, 24 and 48 hours) after injecting 4% thioglycollate intraperitoneally. Following counting the cells in peritoneal lavage fluid, the cells were cytospined to obtain the percentage of neutrophils (B) and then the total number of neutrophils was calculated (C). D-H show pictures of neutrophils recruited in lavage fluid in thioglycollate-induced peritonitis of C57B6 after 0, 2, 6, 24 and 48 hours respectively, whereas I-M belong to TRIB3-/- mice. Data show mean ± SEM. Each group is represented by 3-6 mice at each time point. Statistical significance was tested using one-way ANOVA, followed by Bonferroni post test (* $p < 0.05$). C57B6 served as a control. Neutrophil (N).

5.3 Discussion

It is well known that upon infection leukocytes would migrate to the site of infection as a protective attempt to eliminate the injurious stimuli. The previous view held that the greatest number of neutrophils from murine peritoneal cavities was harvested when mice were sacrificed 5 hours post intraperitoneal injection of thioglycolate medium [199].

We investigated the effect of thioglycollate-induced peritonitis at different time points post injecting thioglycollate intraperitoneally, and then studied whether knocking out TRIB3 modulates leukocyte migration to the blood and peritoneum. Graphs 5.2 and 5.3 demonstrate leukocyte numbers in blood and that migrated to the peritoneum respectively in response to thioglycollate. Interestingly, Graph 5.2 demonstrates that blood leukocyte level in the TRIB3-/- mice is less than that of the control and this is noted to be significant at 2 and 6 hours. However, a marked fall in the leukocyte count is recorded in the control at 24 hours, probably resulting in they are went through apoptosis. It appears that knocking out TRIB3 prevents the increase in circulating leukocyte levels seen in the wild type after thioglycollate injection. With regards to leukocyte migration to peritoneum there is no recorded difference in either category (Figure 5.3A). Therefore, neutrophils that have migrated to the peritoneum were tested. As a result, it is very clear from figure 5.3C compared to figure 5.3A that the number of neutraphils at 6 hours, for both groups (C57B6 and TRIB3-/- mice), predominated. Figure 5.3C also illustrates knockout of TRIB3 may increase sensitivity of neutrophil migration. A trend of increase neutrophil migration of TRIB3-/- mice towards peritoneum at 2 hours compared to C57B6. This result was confirmed by the data in chapter 4 when studying the effect of TRIB3 on murine neutrophil migration in response to KC and fMLP; as neutrophil influx of TRIB3-/- mice towards KC at 10^{-5} M and fMLP at 10^{-7} M and 10^{-6} M was greater than C57B6, but was not found to be significant. Figure 5.3C also shows neutrophil numbers in lavage fluid increase with time for both thioglycollate-induced peritonitis groups up to 6 and 24 hours respectively.

At later time points, a reduction in the neutrophil numbers was recorded, as they are thought to undergo apoptosis. It is clear that knocking out TRIB3 from murine cells had no significant effect on neutrophil migration. Furthermore, neutrophil migration in TRIB3-/- mice persisted and continued to increase at 24 hours compared to the control which decreased after 6 hours until a minimal number migrated at 24 hours (again there was no significance), which possibly due to TRIB3 deficiency leading to delay in neutrophil apoptosis. The percentage of migrated neutrophils in thioglycollate-induced peritonitis mice was measured and it showed no significant difference between both groups at any time point (Figure 5.3B). Taking into account the results of the effect of TRIB3-/- on murine multi-cytokine levels in thioglycollate-induced peritonitis of lavage fluid, it is clear that cytokine levels increase with time for both thioglycollate-induced peritonitis groups (Table 5.1 and Figure 5.1). This indicates that the initial process occurring after introducing thioglycollate is increasing levels of neutrophil-attracting chemokines at the site of infection. This could explain the increase in recruiting neutrophils at the peritoneum as an inflammatory response by either a direct or indirect mechanism as a chemoattractant. Considerable volume of research has looked at direct mechanism as a chemoattractant. An article published in the Journal of Leukocyte Biology in 2011 demonstrated that GMCSF is a chemoattractant for murine neutrophil as verified *in vivo* [196]. Further studies have revealed that IL-17A and IFN-γ are produced by neutrophils, which in turn may up-regulate neutrophil transmigration in mouse kidney ischemia-reperfusion injury [200].

An *in vivo* study in 2008 demonstrated that murine tissue macrophage TLR signaling directly induces neutrophil-attracting chemokines (KC and MIP-2) synthesis. These chemokines constitute the key for neutrophil migration, which represents the earliest immune cells to recruit into infected tissue [197]. Furthermore, a study published in 2004 concluded that neutrophils migrating into inflammatory tissues from intravascular space are induced by the

basement membrane to secrete the chemokine MIP-1 β, this in turn caused dendritic cells to migrate in the same way [201].

When looking at literature for indirect mechanisms Ratthé *et al* 2009 found that IL-4 significantly increased the number of leukocytes (neutrophils and monocytes) *in vivo* murine air pouch model by an indirect mechanism. This mechanism involved the up regulation of the chemoattractant MCP-1 [202]. Further research has showed that IL-13 activates human neutrophils to modulate the synthesis of many neutrophil proteins (e.g. IL-8, IL-1R antagonist and IL-1 decoy receptor), which involve increases in tyrosine phosphorylation by tyrosine kinases [203]. A study in 2005 revealed that neutrophil accumulation occurred in an experimental model of allergen-induced immune inflammation in the murine peritoneum is mediated by macrophage-inflammatory protein (MIP)-1α that induces sequential release of TNF-α and LTB_4 through C-C chemokine receptor type 1 (CCR1) [204].

In contrast with the increase in cytokine levels with time for both thioglycollate-induced peritonitis groups, knocking out TRIB3 from murine cells had an effect on several cytokines and it is time dependent, GMCSF, IL-17A and MCP-1 at 2 hours and IL-13 at 6 hours compared to the control, although the findings were not statistically significant except for IL-13 (Table 5.1 and Figure 5.1). As a result of this, it may be that TRIB3 down regulates these cytokines at a certain point in time, although this regulation has no considerable effect on neutrophil migration (Figures 4.7 and 4.8 illustrated in chapter 4). Nevertheless, there has been a general agreement on the chemoattractants involved in neutrophil recruitment, the mechanisms by which neutrophils recruit between endothelia and migrate into the inflammatory site remains unclear.

Overall these observations suggest that some cytokines are involved in increasing neutrophil migration across the microvasculature and invasion of the affected tissue by different

mechanisms. In addition to this, TRIB3 controls cytokine levels. TRIB3 deficiency was also found to inhibit the increase in circulating leukocyte number significantly; may increase neutrophil migration towards peritoneum (inflammation site) and may extend their existence when compared to the control in thioglycollate-induced peritonitis, due to possible effect of TRIB3 deficiency on neutrophil appoptosis. The control was found to be transient as their neutrophils migrated and left the peritoneum rapidly. Interpretation of the *in vivo* cytokine and TRIB3 results is hindered by the fact that the mechanisms are still to be discovered, as cytokines are a prerequisite for neutrophil emigration with TRIB3 regulating several of these.

Chapter 6: The role of TRIB3 in insulin resistance, control of lipid homeostasis and in the development of atherosclerosis

6.1 Introduction

TRIBs coordinate the activation and suppression of various cascades. They have an essential function in determining cell fate during response to environmental challenges [131]. Specifically, TRIB3 has been published by most [153], [155] but not all [167] studies to dysregulate insulin action via interacting with Akt in murine models of diabetes. Increasing levels of TRIB3 may lead to insulin resistance in mice [153], [155]. Data by Weismann *et al* observed TRIB3 knockdown rats gained considerable weight, improved insulin sensitivity and increased expression of PPAR-γ. Interestingly, there was no remarkable variation in Akt activation, which suggest TRIB3 may regulate lipid synthesis through a PI3K-independent but PPAR-γ-mediated mechanism [170].

Publication by Koo *et al* suggested TRIB3 an important regulator of glucose and lipid metabolism, as its expression was induced by fasting through induction of PPARα [155]. Despite the discrepancies in the literature, it seems logical to propose that TRIB3 may be a critical modulator of signalling mechanisms regulating lipid homeostasis. Impairment in TRIB3 function may lead to the development of serious disease such as type 2 diabetes. Given the prevalence of cardiovascular disease, studying genes, for instance TRIB3, contributing to the impaired lipid homeostasis and insulin resistance was taken the priority of this study.

This chapter attempts to synthesise knowledge obtained on TRIB3 action in the context of lipid homeostasis, insulin resistance as well as discussing the importance of TRIB3 in developing atherosclerosis. It will study whether knocking out TRIB3 modulates growth rate of mice on chow and 60% HFD compared to C57B6 control mice and review its effect on the quantity and type of WBC in mouse blood and peritoneal lavage fluid of both groups. Furthermore, it will show the effect of TRIB3 on insulin resistance in glucose- or insulin-injected mice again on normal and HFD, taking the glucose readings at different time points, in addition to the baseline glucose reading before intraperitoneal injection. In addition to this we will look at the role of TRIB3 in lipid homeostasis and development of atherosclerosis. Aortas were stained by Oil Red O to distinguish the plaque regions post feeding the mice 60% HFD for 11 weeks.

6.2 Results

A) Role of TRIB3 on weight gain of mice on 60% HFD and gender effect on TRIB3-/- mice weight fed chow

Murine weight gain has been recorded formerly, but the impact of TRIB3 deficiency and feeding the mice HFD on it requires investigation. The role of TRIB3 on male murine weight gain was studied on C57B6 and TRIB3-/- groups fed 60% HFD for 11 weeks. Both groups were weighed every week and matched with their ages (Figure 6.1A). The percentage weight gain was then measured (Figure 6.1B). Data demonstrates that TRIB3 deficiency and HFD in combination alter murine weight gain. The data also shows that the effect of TRIB3 deficiency on weight was gender specific, as TRIB3-/- males weighed more than the C57B6 males significantly but not females (Figures 6.2A and 6.2B).

A

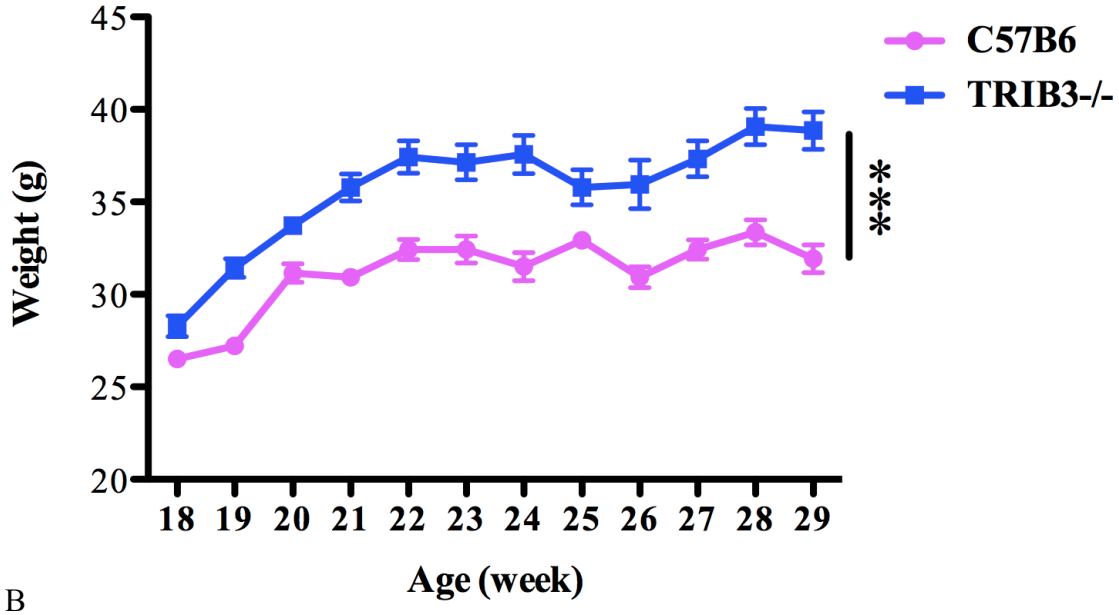

B

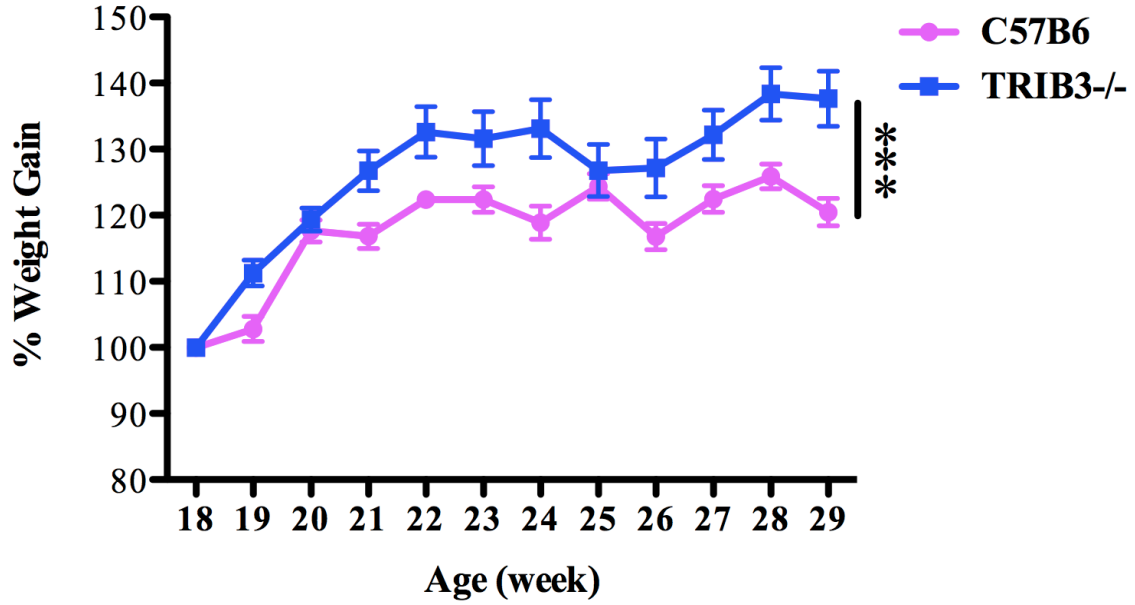

Figure 6. 1: Effect of TRIB3 on weight gain of male mice on 60% HFD

(A) C57B6 versus TRIB3-/- mice were fed 60% HFD for 11 weeks. Weight was taken every week for both groups. They were males and aged 18 week upon commencement of fat feeding. The readings were taken for 11 weeks, initiating with a baseline weight before fat feeding begins. (B) Represents the percentage of weight gain. Data show mean ± SEM. Every group is represented by 7 mice at each condition. Statistical significance was tested using two-way ANOVA. C57B6 served as a control (*** $p < 0.001$).

A

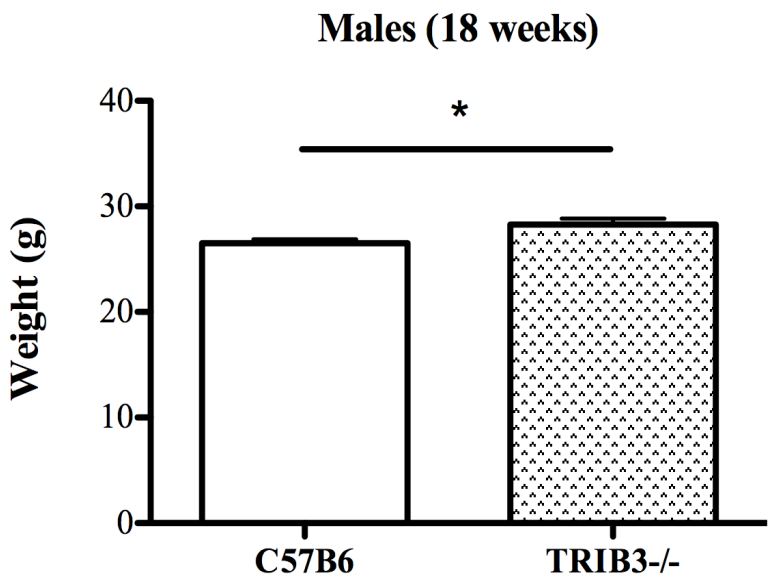

B

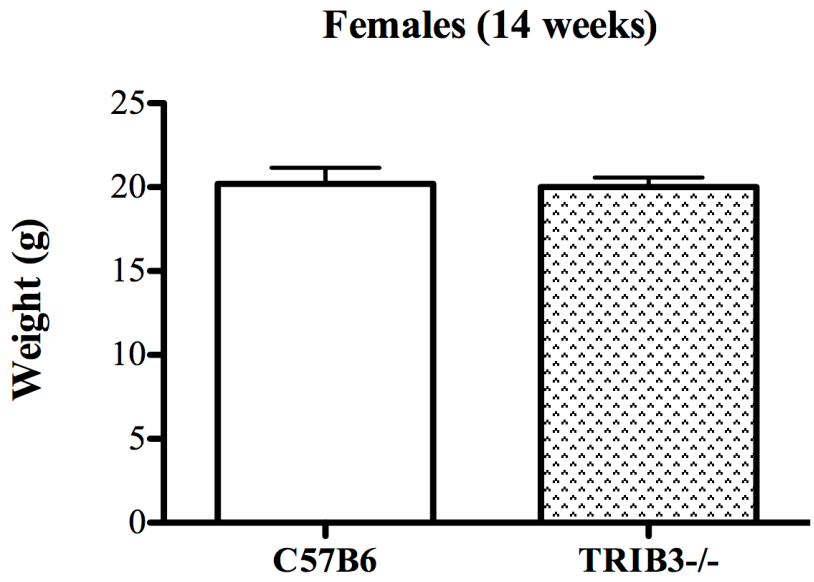

Figure 6. 2: Gender specific effect of TRIB3 on weight for chow fed mice

18 week aged males (A) and 14 week aged females (B) C57B6 versus TRIB3-/- mice respectively were fed chow. Data show mean ± SEM. The male groups consist of 7 of each C57B6 and TRIB3-/- mice. The female groups consist of 5 C57B6 and 3 TRIB3 mice. Statistical significance was tested using unpaired t test. C57B6 served as a control (* $p < 0.05$).

B) Role of TRIB3 on WBC quantity in the peritoneal lavage fluid in mice fed 60% HFD

Leukocyte numbers in peritoneum during an inflammatory response have previously been reported [205]. This study will highlight the possible influence of TRIB3 on peritoneal leukocyte quantity. The function of TRIB3 on WBC quantity in the peritoneal lavage fluid was investigated after feeding C57B6 and TRIB3-/- groups 60% HFD for 11 weeks. Knocking out TRIB3 significantly increased leukocyte numbers in peritoneum compared to C57B6 (Figure 6.3A) but this was not observed specifically to neutrophils in either group (Figures 6.3B and C).

A

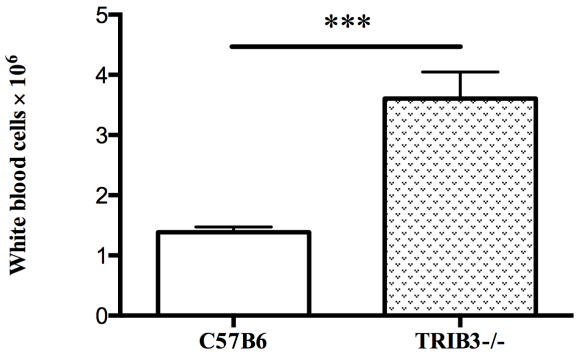

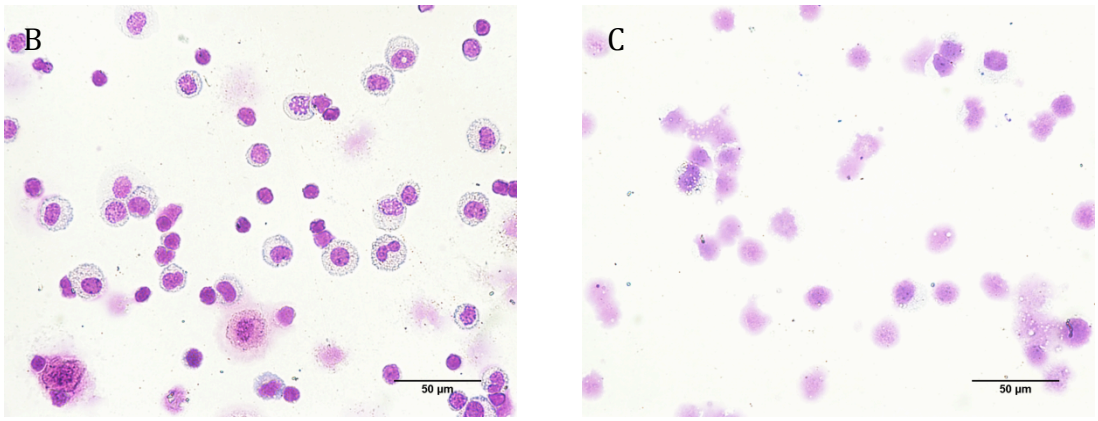

Figure 6. 3: Effect of TRIB3 on WBC quantity in the peritoneal lavage fluid in mice fed 60% HFD

The number of leukocytes from peritoneal lavage fluid of C57B6 versus TRIB3-/- mice was counted (A). Samples were collected after feeding mice for 11 weeks 60% HFD. Following counting the cells, a cytospin was performed on peritoneal lavage fluid of C57B6 (B) and TRIB3-/- (C) mice. Data show mean ± SEM. Each group is represented by 7 mice. Statistical significance was tested using unpaired t test (*** $p < 0.001$). C57B6 served as a control.

C) Role of TRIB3 on WBC types in mouse blood fed chow and 60% HFD

Circulating leukocyte subsets that are involved in inflammation have been studied widely [205]. Yet, the importance of TRIB3 on the quantity of these cells needs to be investigated. The role of TRIB3 on leukocyte types circulating in mouse blood was studied after feeding mice normal and 60% HFD for 5 and 11 weeks. Graph 6.4A illustrates no significant difference in the number of leukocytes in TRIB3-/- blood compared to the control regardless of whether the mice were on normal or HFD. However, post long period of time (11 weeks) feeding both groups 60% HFD resulted in significantly lower leukocyte numbers than feeding them for 5 weeks. Considering the leukocyte types, lymphocytes were shown to predominate in both groups whether on chow or HFD, except C57B6 mice on a normal diet as the majority was shared between lymphocytes and neutrophils. Furthermore, knocking out TRIB3 down-regulated only neutrophils significantly in mice fed normal food. On the other hand, feeding the mice 60% HFD reduced neutrophil and monocyte numbers significantly in both blood groups, while the significant reduction in lymphocytes was just restricted to C57B6 group on diet for 11 weeks compared to 5 weeks feeding of the same group (Graphs 6.4B–D).

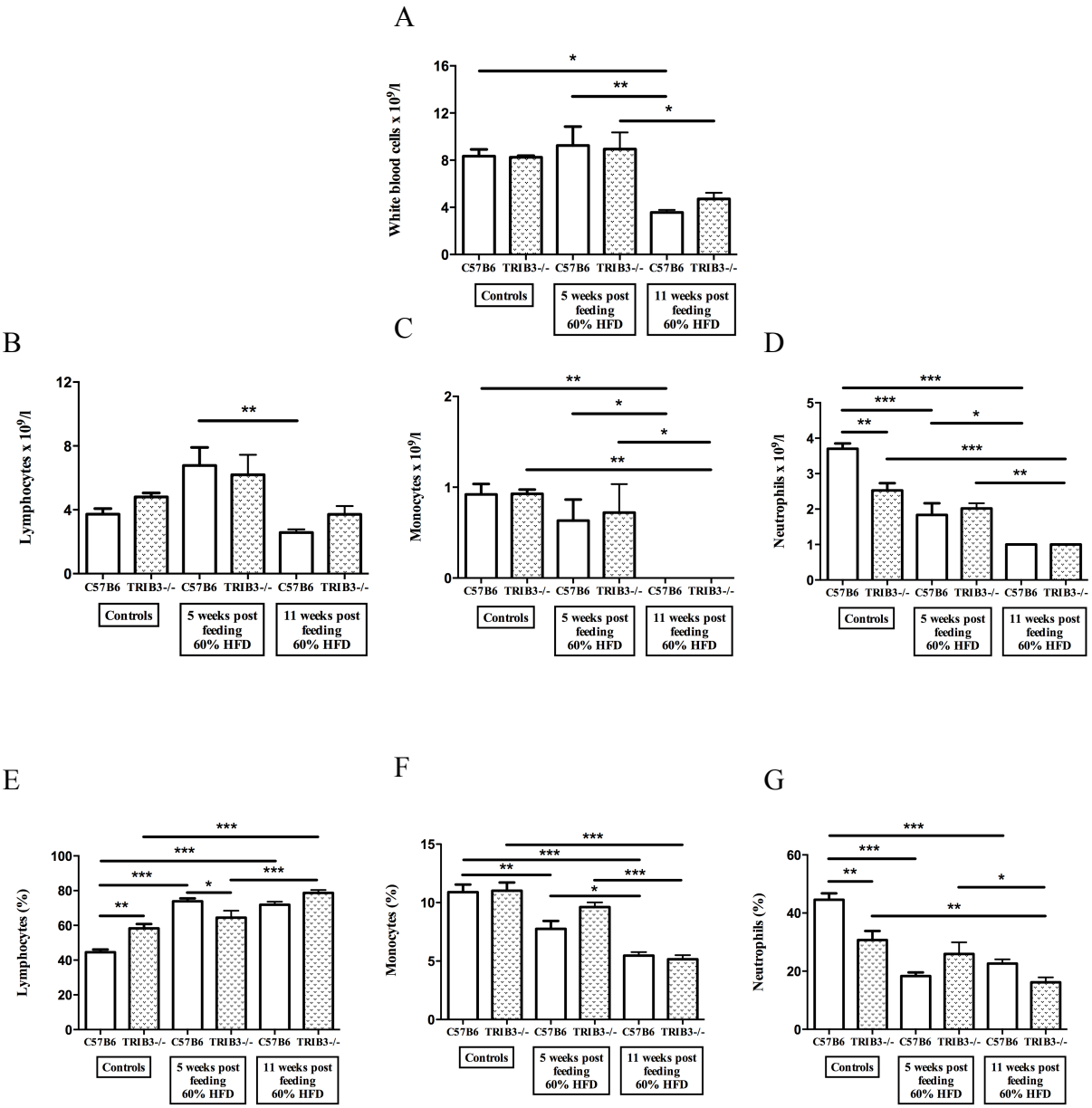

Figure 6. 4: Role of TRIB3 on WBC types in mouse blood fed chow and 60% HFD

The number of leukocyte in blood of C57B6 versus TRIB3-/- mice was counted (A). Samples were collected at different time points; 0, 5 and 11 weeks after feeding the two groups 60% HFD. B-D represent the number of lymphocytes, monocytes and neutrophils in blood/l respectively, while E-G are the percentage of these cells (same order). Data show mean ± SEM. Each group is represented by 4-7 mice at each time point. Statistical significance was tested using one-way ANOVA, followed by Bonferroni post test (* $p < 0.05$, ** $p < 0.01$ and *** $p < 0.001$).

D) Role of TRIB3 in insulin sensitivity in mouse blood fed chow and 60% HFD

Whilst there are wide range studies in terms of impact of TRIB3 on insulin sensitivity [170], its molecular mechanism remains incomplete and its physiological function controversial. This study will confirm/contradict what have already been published. The effect of TRIB3 deficiency on glucose concentration at different time points was investigated in mice injected with glucose or insulin that were fed with normal and 60% HFD food. Figure 6.5 demonstrated that no matter if the mice in both groups were fed with chow or HFD, their glucose concentration have increased trend after 30 minutes from injecting of glucose. The trend of glucose level remained elevated significantly in TRIB3-/- mice on HFD, while it returned to the base line after 2 hours from injection in other groups (both C57B6 groups on chow and HFD, and TRIB3-/- group on chow). In contrast, figure 6.6 showed a significantly decreased blood glucose concentration in C57B6 mice fed HFD compared to their control on chow after 60 minutes from insulin injection, whereas TRIB3-/- mice on chow and both groups on HFD had a significantly lower blood glucose concentration at 60 minutes post insulin injection compared to the start time point.

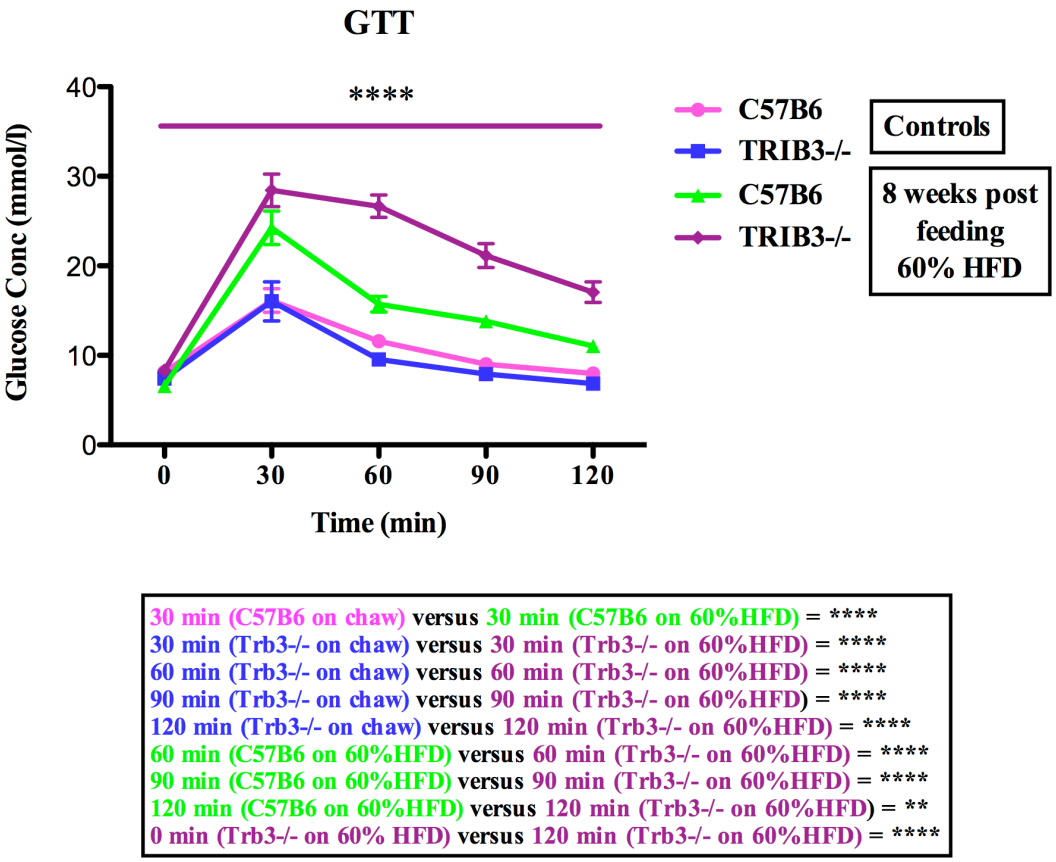

Figure 6. 5: Effect of TRIB3 on blood glucose in glucose-injected mice fed chow and 60% HFD (GTT)

C57B6 and TRIB3-/- mice were fed chow or 60% HFD for 8 weeks and then starved overnight. Blood was collected from tail to take a baseline glucose reading before intraperitoneal injection of the mouse with sterile glucose at 10 ul/g BW (20% D-glucose). Readings were taken at different time points (0, 30, 60, 90 and 120 minutes). Data show mean ± SEM in mmol/l. Each group is represented by 5 or 7 mice at each time point. Statistical significance was tested using one-way ANOVA, followed by Bonferroni Post Test (** $p < 0.01$ and **** $p < 0.0001$).

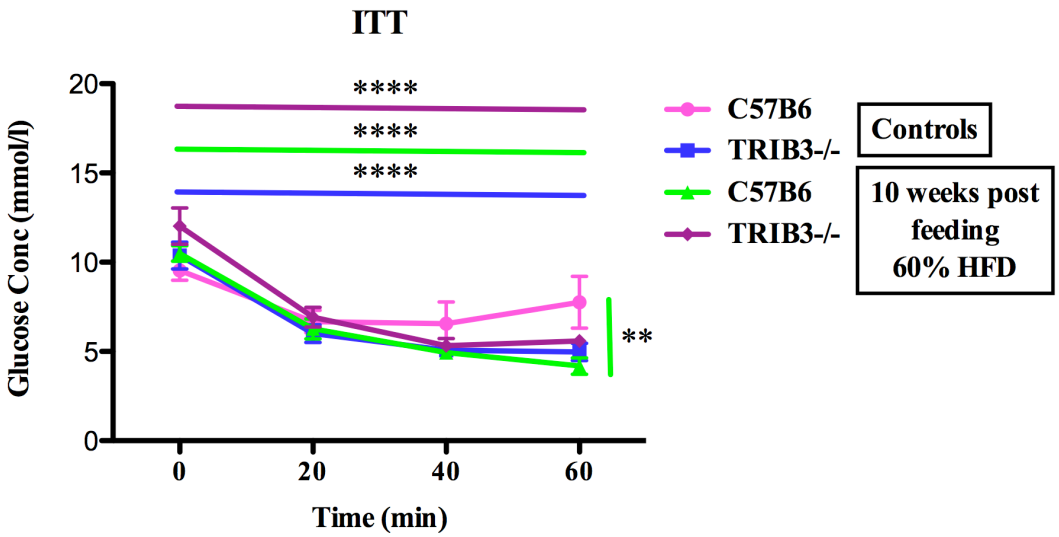

Figure 6. 6: Effect of TRIB3 on blood glucose in insulin-injected mice fed chow and 60% HFD (ITT)

C57B6 and TRIB3-/- mice were fed chow or 60% HFD for 11 weeks and then fasted for 2-3 h. Blood was collected from tail to take a baseline glucose reading before intraperitoneal injection of the mouse with sterile insulin at 0.75 U/kg BW (0.25 U/ml). Readings were taken at different time points (0, 20, 40 and 60 minutes). Data show mean ± SEM in mmol/l. Each group is represented by 5 or 7 mice at each time point. Statistical significance was tested using one-way ANOVA, followed by Bonferroni post test (** $p < 0.01$ and **** $p < 0.0001$). C57B6 served as a control.

E) Role of TRIB3 in control lipid homeostasis in mouse blood fed chow and 60% HFD

TRB3 has been linked to insulin resistance [153] and metabolic syndrome [206]. Part of these disease processes is dysregulated plasma lipid levels. Therefore, I investigated the consequences of TRIB3 deficiency on plasma lipid profile. The function of TRIB3 on lipid homeostasis was investigated in mouse blood after feeding mice normal and 60% HFD for 11 weeks. The following graphs show knocking out TRIB3 decreased cholesterol and HDL concentrations in the blood significantly compared to the control in mice fed 60% HFD, but not in mice on normal diet. In contrast, the diet itself had an effect as feeding mice 11 weeks HFD increased cholesterol and HDL concentrations significantly of both groups (Figures 6.7A and 6.7B).

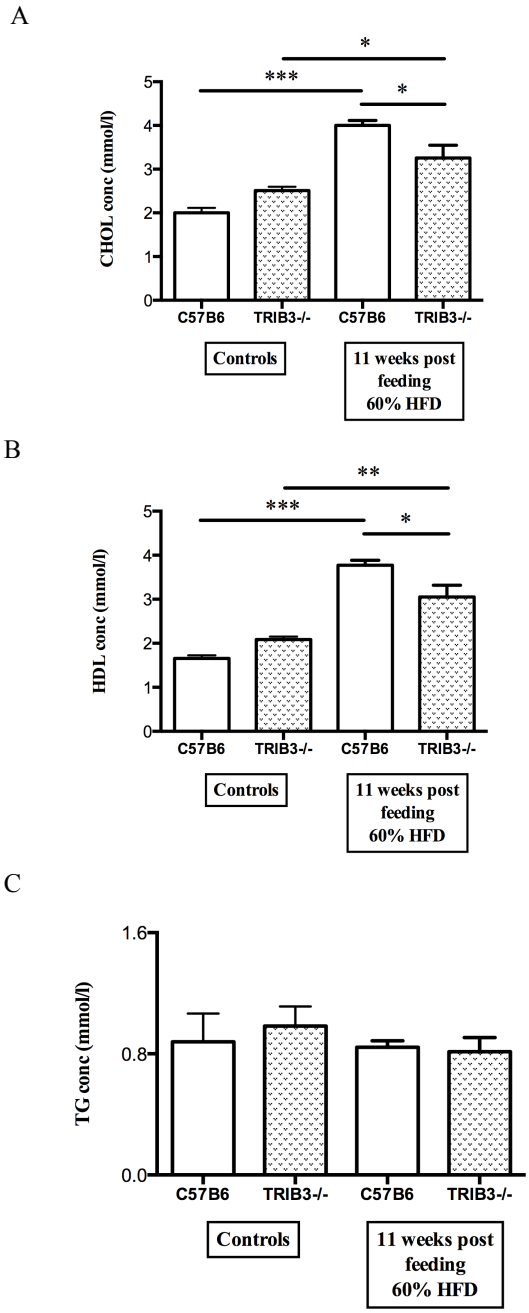

Figure 6. 7: Effect of TRIB3 on lipid homeostasis in mouse blood fed chow and 60% HFD

Blood plasma was collected from C57B6 versus TRIB3-/- mice post chow and 60% HFD feeding for 11 weeks. A-C represent cholesterol, HDL and TG levels respectively for both groups, which were measured via enzymatic colorimetric test by the department of Clinical Chemistry, using Cobas 8000 system. Data shows mean ± SEM in mmol/l. Each group is represented by 5 or 7 mice at each condition. Statistical significance was tested using one-way ANOVA, followed by Bonferroni post test(* $p < 0.05$, ** $p < 0.01$ and *** $p < 0.001$).

F) Role of TRIB3 in the development of atherosclerosis in mouse fed 60% HFD

It has been demonstrated that TRIB3 is involved in atherosclerosis disease [171]. The present study aims to investigate further whether TRIB3 is implicated in this disease. The function of TRIB3 in metabolic processes which contribute to atherosclerosis development was investigated in mice fed 60% HFD for 11 weeks. Aortas were stained by Oil Red O, while each heart sinus by H&E. As a result, graphs show that neither diet nor knocking out TRIB3 had an effect on developing lesions on aorta or heart sinus. This is illustrated in figures 6.8A-D.

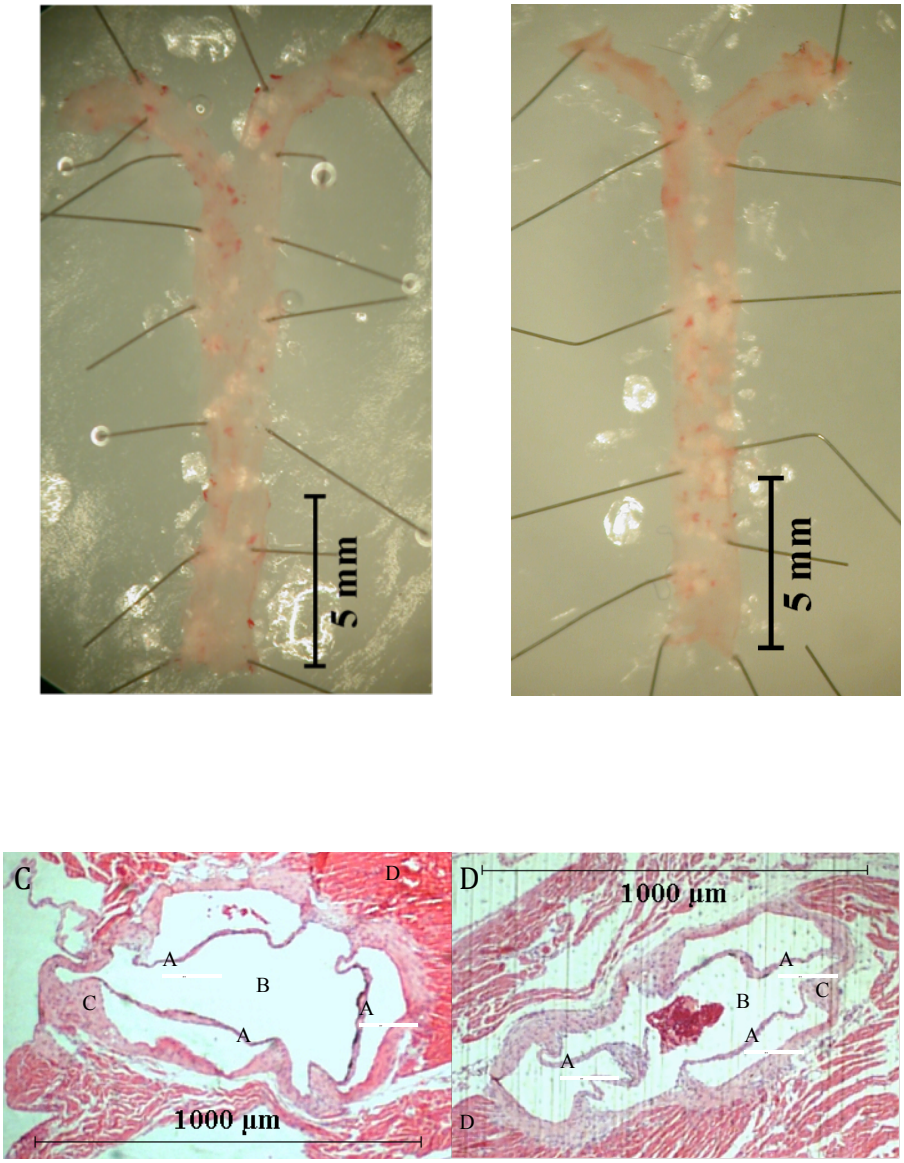

Figure 6. 8: Effect of TRIB3 on developing plaque in mice fed 60% HFD

Histological analysis of aortas and heart sinuses of C57B6 and TRIB3-/- mice on 60% HFD for 11 weeks. Seven aortas were obtained from each group stained with Oil Red O. Images A and B are representatives of each group. Two to three heart sections were obtained from each group stained with H&E, images C and D are representatives of each microscopic heart sinus of C57B6 and TRIB3-/-. Valve leaflet (A), lumen (B), aortic sinus (C) and surrounding heart muscle (D).

G) Role of TRIB3 in heart sinus cells architecture in mouse fed 60% HFD

The current study also aims to investigate whether TRIB3 has an effect on heart sinus cells architecture. The function of TRIB3 in these cells was investigated in mice fed 60% HFD for 11 weeks. Heart sinuses were stained by H&E. As shown in the graphs 6.9A and 6.9B TRIB3 deficiency had no effect on heart sinus cells architecture, given no differences found between C57B6 and TRIB3-/- groups.

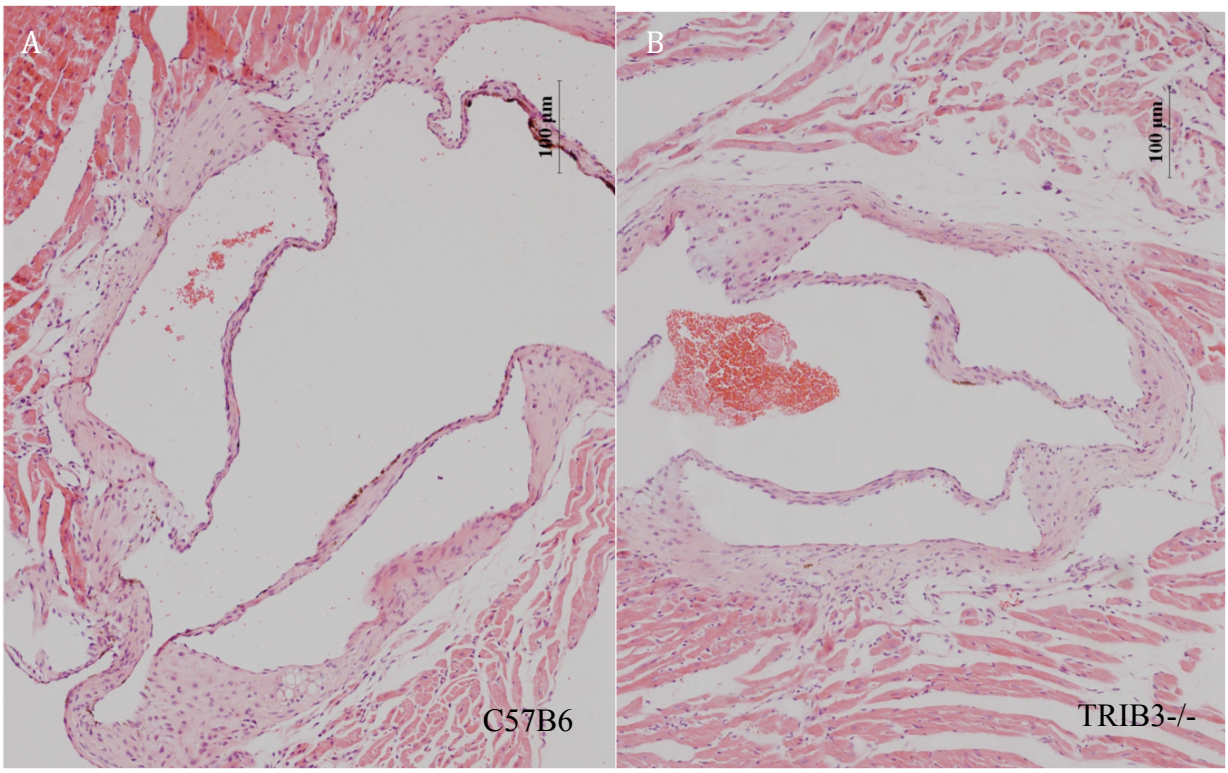

Figure 6. 9: Effect of TRIB3 on heart sinus cells architecture in mouse fed 60% HFD

Histological analysis of heart sinus of C57B6 and TRIB3-/- mice on 60% HFD for 11 weeks. Two to three heart sinus sections were obtained from each group stained with H&E. Images A and B are representatives of each microscopic heart sinus cells architecture of C57B6 and TRIB3-/-.

H) Liver and adipose tissue histology of C57B6 and TRIB3-/- mice fed chow and 60% HFD

Previous studies have shown that TRB3 is expressed in liver and adipose tissue [169]. This experiment aims to investigate whether TRB3 modulates the phenotype of these tissues. Histological analysis of tissues was investigated in C57B6 and TRIB3-/- mice on chow and 60% HFD for 11 weeks. Sections were stained with H&E. Figures 6.10A-D show no difference in liver cells of all 4 group. Figures 6.11A-D illustrate no difference in adipose cells between C57B6 and TRIB3-/- mice on chow, while an increase in cell size of both groups fed HFD and even TRIB3-/- was larger when compared to C57B6 on the same diet.

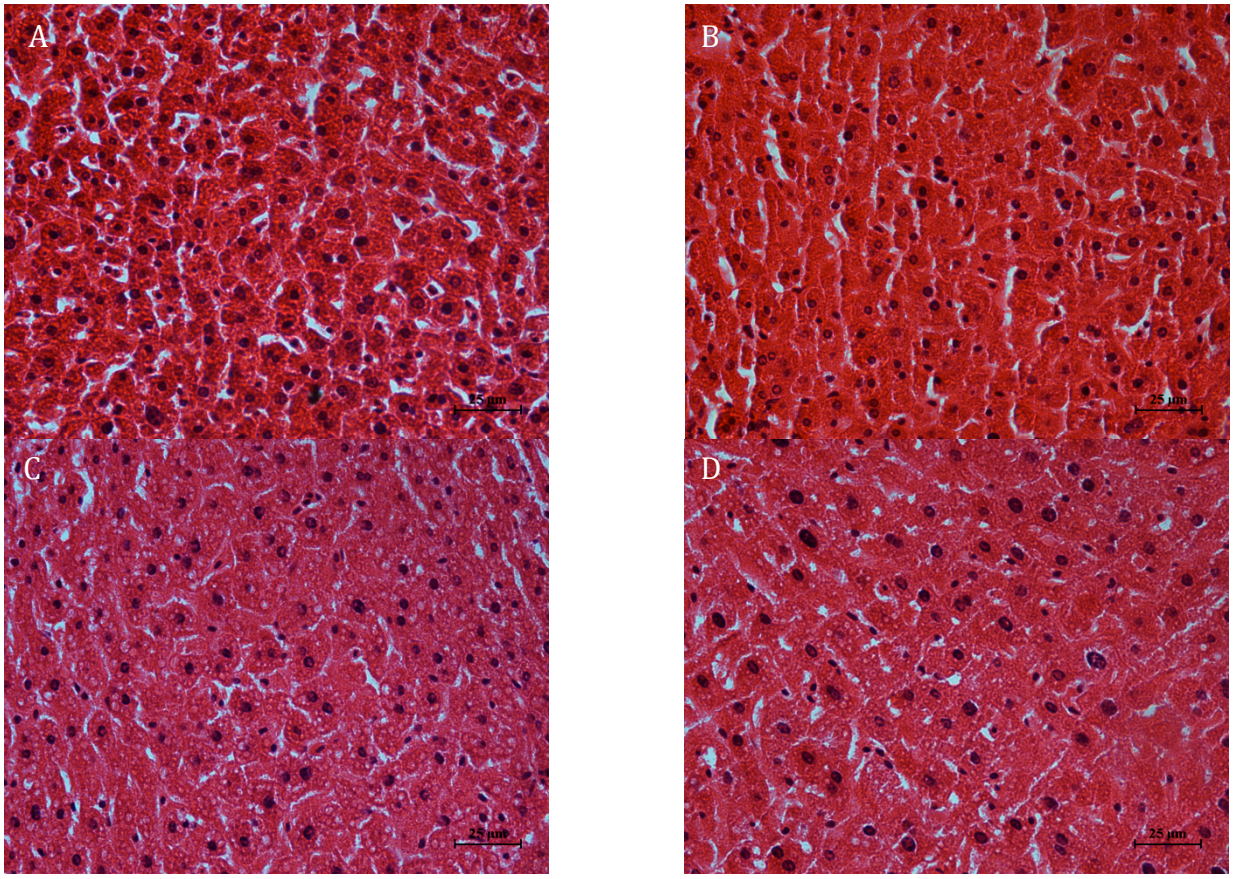

Figure 6. 10: Liver histology of C57B6 and TRIB3-/- mice fed chow and 60% HFD

Histological analysis of liver of C57B6 and TRIB3-/- mice on chow or 60% HFD for 11 weeks. Sections were obtained from 3 mice from each group chow and HFD fed stained with H&E. Images A and B are representatives of microscopic liver cells of C57B6 and TRIB3-/- mice on chow, while images C and D on HFD.

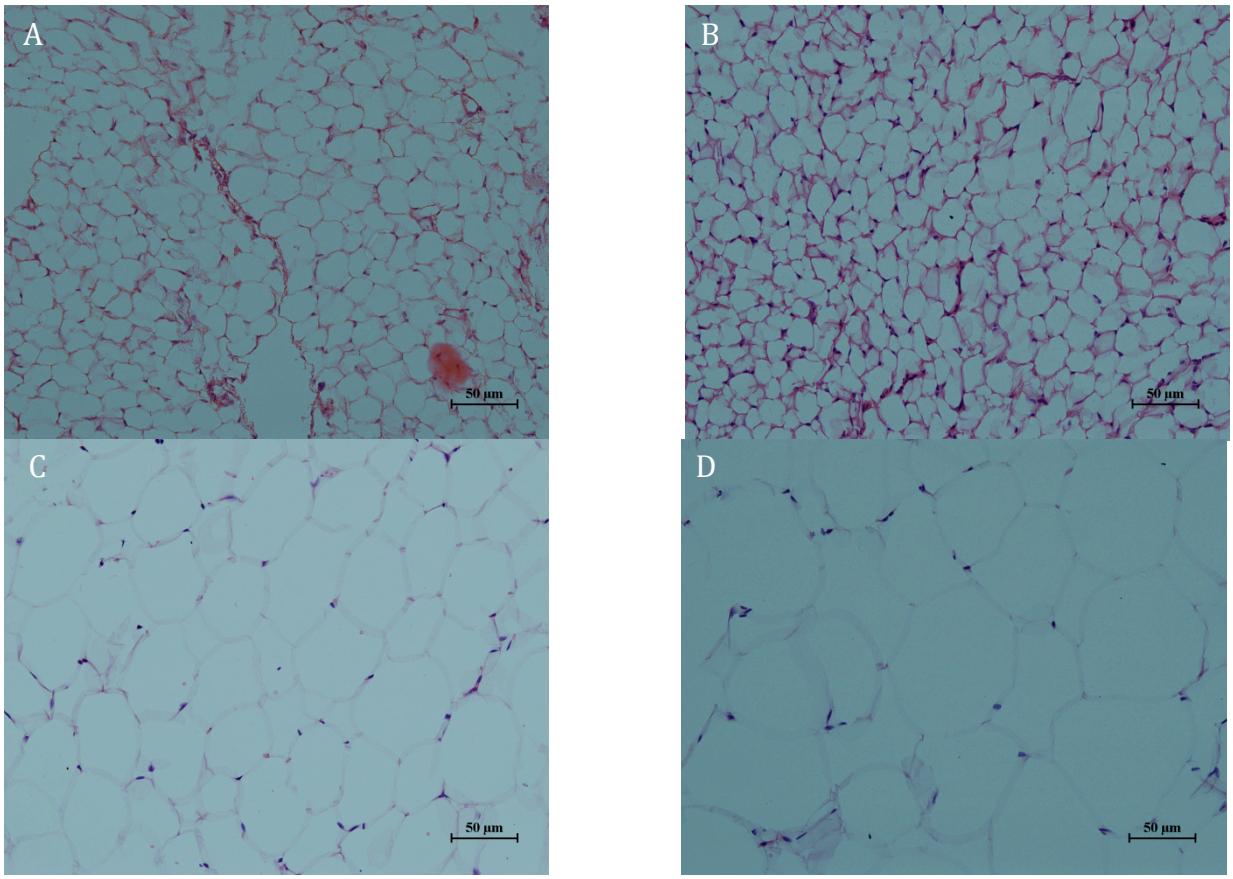

Figure 6. 11: Adipose tissue histology of C57B6 and TRIB3-/- mice fed chow and 60% HFD

Histological analysis of adipose tissue of C57B6 and TRIB3-/- mice on chow or 60% HFD for 11 weeks. Sections were obtained from 3-5 mice from each group chow and HFD fed stained with H&E. Images A and B are representatives of microscopic adipose cells of C57B6 and TRIB3-/- mice on chow, while images C and D on HFD.

I) The effect of TRIB3 deficiency in determining macrophage numbers in heart, liver and adipose tissue

Infiltration of macrophages in the development of atherosclerosis and metabolic syndrome has been demonstrated. These cells are believed to be important local drivers of tissue inflammation [9], [207]. The importance of TRIB3 in determining macrophage numbers in heart, liver and adipose tissue was studied in mice fed 60% HFD for 11 weeks. This was also shown in adipose tissue for chow fed mice. Heart sinus, liver and adipose tissue were incubated with F4/80 antibody (the marker of macrophages; primary antibody), biotinylated anti-rat IgG (secondary antibody), Vectastain ABC-HRP reagent and DAB before counterstaining by haematoxylin. Macrophages in these tissues were then counted. As a result, graphs 6.12A-D and 6.13A-F show neither heart nor liver had macrophages in C57B6 and TRIB3 mice fed HFD. With respect to adipose tissue of mice on chow graphs 6.14A-F illustrate no macrophages in either group. However, feeding mice HFD led to an insignificant increase macrophage number in adipose tissue, whereas TRIB3 deficiency had no effect on macrophages, as no differences were found between C57B6 and TRIB3-/- mice graphs 6.14G-L.

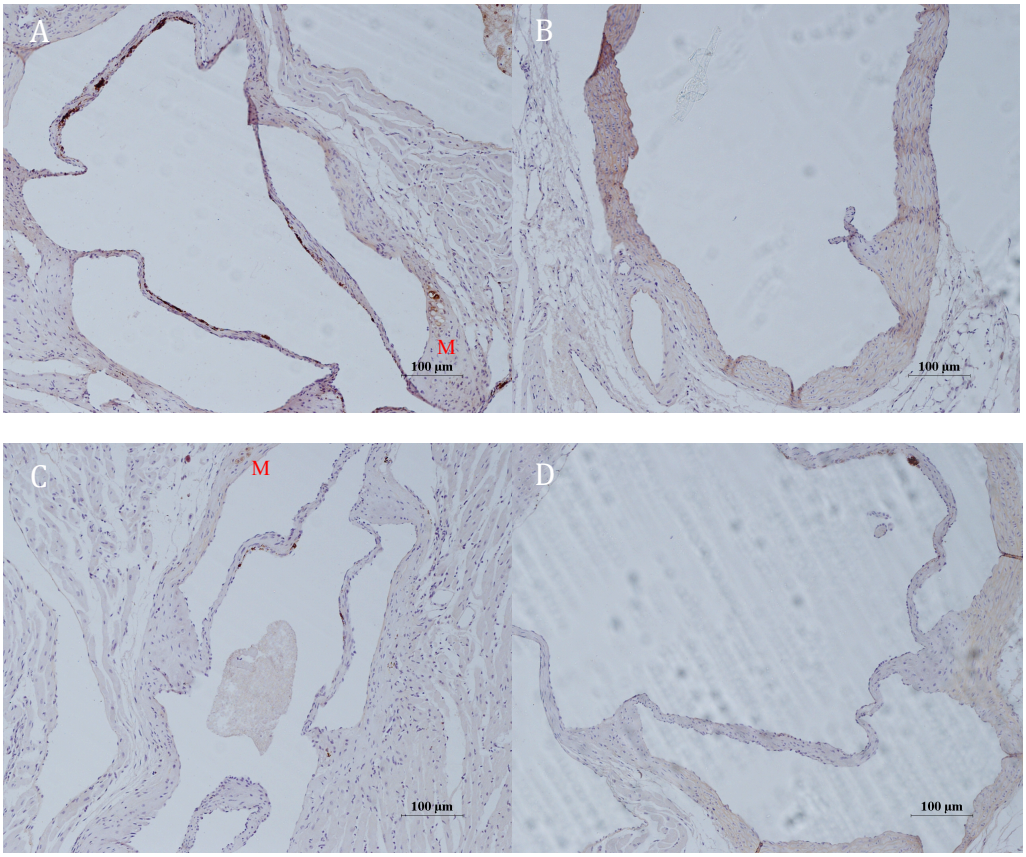

Figure 6. 12: The importance of TRIB3 in determining macrophage number in heart of mouse fed 60% HFD

Histological analysis of heart sinus of C57B6 and TRIB3-/- mice on 60% HFD for 11 weeks. Two to three heart sinus sections were obtained from each group incubated with F4/80 antibody (the marker of macrophages; primary antibody), biotinylated anti-rat IgG (secondary antibody), Vectastain ABC-HRP reagent and DAB before staining by haematoxylin. Images A and B are representatives of microscopic heart sinus of C57B6, while C and D are representatives of TRIB3-/-. Macrophage (M).

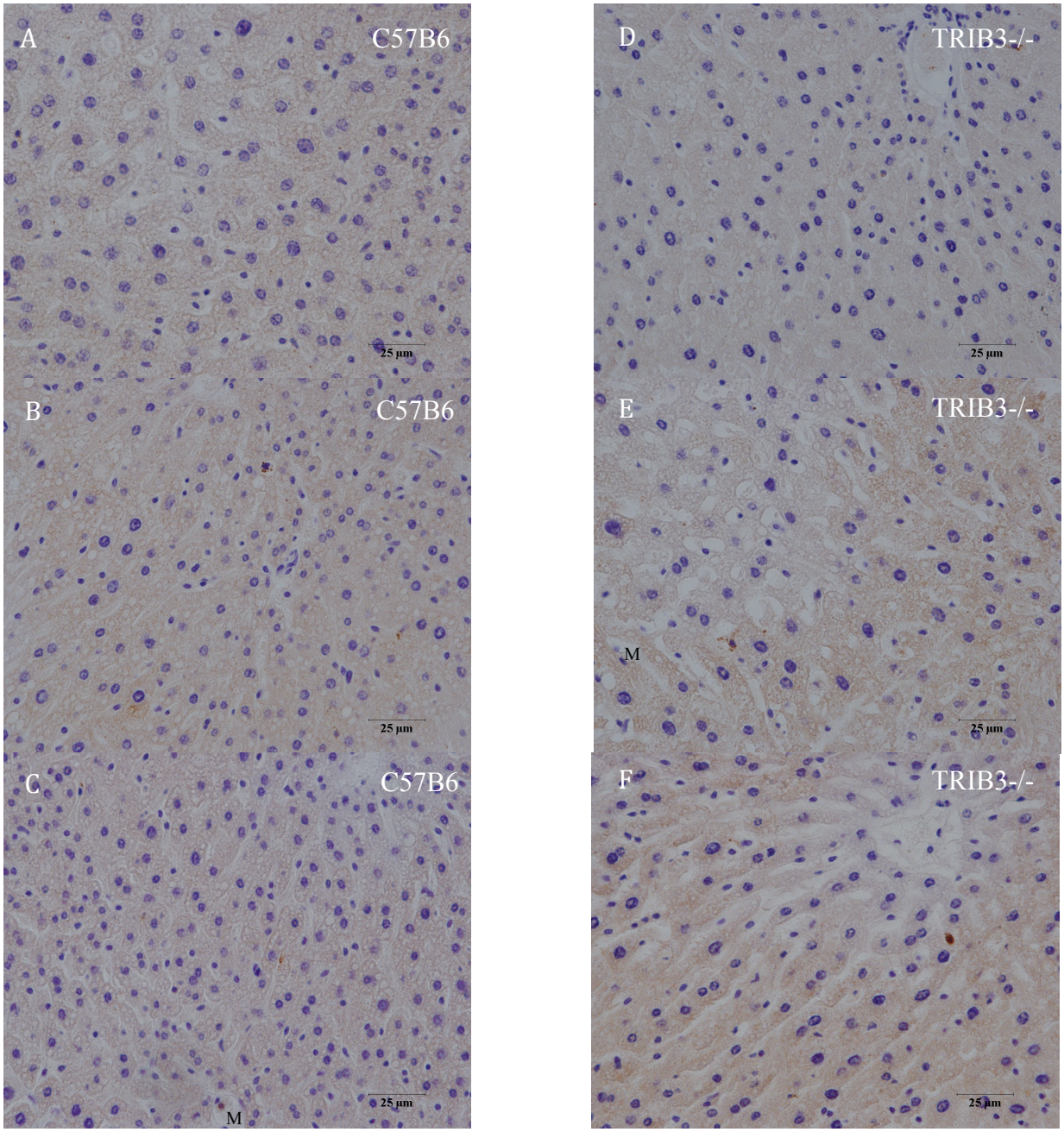

Figure 6. 13: The importance of TRIB3 in determining macrophage number in liver of mouse fed 60% HFD

Histological analysis of liver of C57B6 and TRIB3-/- mice on 60% HFD for 11 weeks. Three liver sections were obtained from each group incubated with F4/80 antibody (the marker of macrophages; primary antibody), biotinylated anti-rat IgG (secondary antibody), Vectastain ABC-HRP reagent and DAB before staining by haematoxylin. Images A-C are representatives of microscopic liver of C57B6, while D-F are representatives of TRIB3-/-. Macrophage (M).

Chow

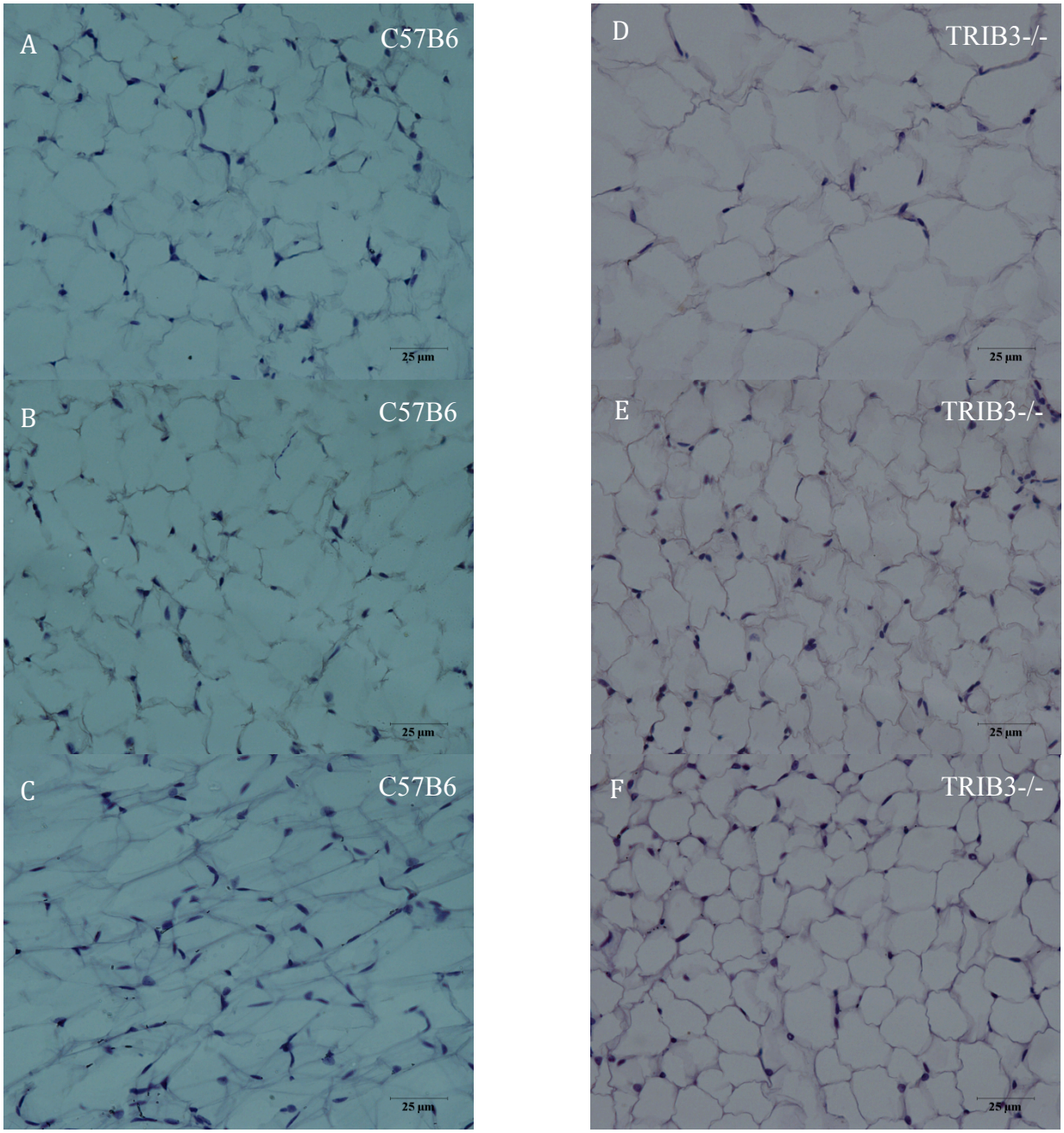
A
C57B6
25 µm
B
C57B6
25 µm
C
C57B6
25 µm
D
TRIB3-/-
25 µm
E
TRIB3-/-
25 µm
F
TRIB3-/-
25 µm

HFD

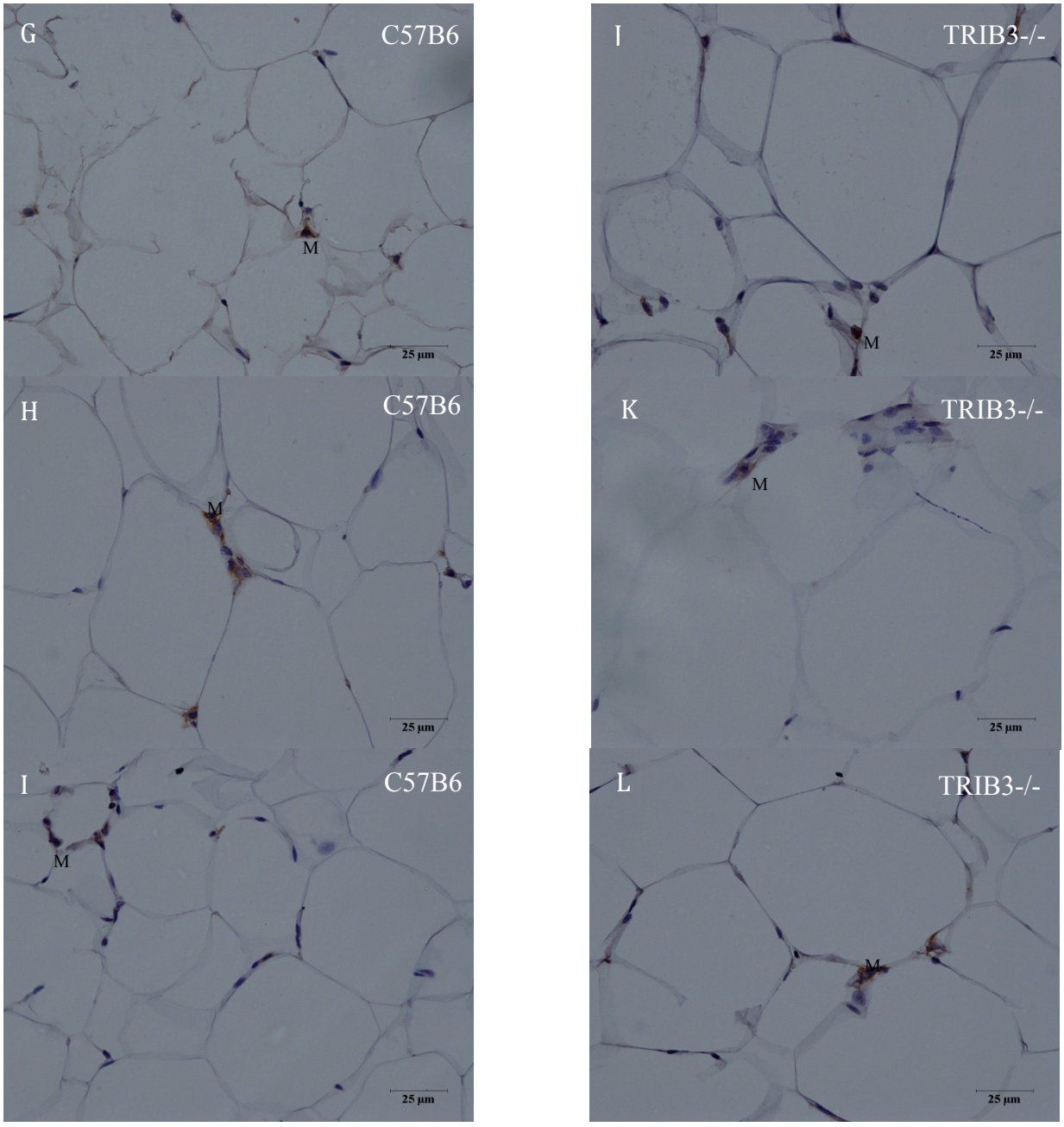

Figure 6. 14: The importance of TRIB3 in determining macrophage number in adipose tissue of mouse fed chow and 60% HFD

Histological analysis of adipose tissue of C57B6 and TRIB3-/- mice on chow and 60% HFD for 11 weeks. Three adipose tissue sections were obtained from each group incubated with F4/80 antibody (the marker of macrophages; primary antibody), biotinylated anti-rat IgG (secondary antibody), Vectastain ABC-HRP reagent and DAB before staining by haematoxylin. Images A-C are representatives of microscopic adipose of C57B6, while D-F are representatives of TRIB3-/- both on chow. Images G-I are representatives of microscopic adipose of C57B6, while J-L are representatives of TRIB3-/- both on HFD. Macrophage (M).

6.3 Discussion

The literature has described the essential regulatory role for TRIB3 in lipid homeostasis and insulin resistance. A study by Ord *et al* in 2007 demonstrated that TRIB3 has a role in protecting cells against the growth inhibitory and ATF4 cytotoxic effect [208].

Further research has looked into the role of TRIB3 in insulin resistance and its effects on diabetes. Du *et al* demonstrated that TRIB3 may act as a down-regulator of Akt activation by insulin in murine liver, by linking and interfering with Akt activation. Therefore, TRIB3 contributes to insulin resistance in individuals liable to type II diabetes [153].

This study investigated the impact of TRIB3 in various experiments in C57B6 and TRIB3-/- groups fed chow and 60% HFD for 11 weeks. When looking at its impact on weight gain, the graphs indicated that TRIB3-/- and HFD have a role in increasing murine weight gain significantly. Both groups were weighed weekly and matched with their ages (Figure 6.1A), and as the weight of TRIB3-/- mice at start point was greater than the control and remained elevated with increasing age, percentage weight gain was assessed and results plotted on a graph (Figure 6.1B). This is to ensure that the increase in mouse weight gain was due to knocking out TRIB3 in addition to feeding the mice HFD, not due to TRIB3-/- mice weighing more than the control at the start of the experiment. This project proved that the effect of TRIB3 knockout on weight was gender specific, as TRIB3-/- males on chow weighed significantly more than C57B6 mice, however, no difference was found in females (Figures 6.2A and 6.2B).

The role of TRIB3 in insulin resistance in murine blood fed chow and 60% HFD was investigated. Figure 6.5 showed that knocking out TRIB3 as well as HFD have an effect on blood glucose level as the level of glucose remained elevated significantly in TRIB3 -/- mice

on HFD, while it returned to the base line after 2 hours from injection in other groups (both C57B6 groups on chow and HFD, and TRIB3-/- group on chow). In addition to this, from 30-120 minutes and from 60-120 minutes TRIB3-/- mice on HFD showed a significantly higher glucose level compared to the TRIB3-/- mice on chow and C57B6 on HFD respectively. Therefore, TRIB3 may be required to control murine blood glucose level through regulating glucose metabolism, and TRIB3 impairment may lead to develop insulin resistance. Figure 6.6 confirmed the results of figure 6.5 by illustrating groups fed HFD (C57B6 and TRIB3-/- mice) as well as TRIB3-/- mice on chow, which showed a significant decrease in glucose level at 60 minutes after insulin injection compared to 0 minute time point. However the glucose level of C57B6 on chow returned to the normal level at starting point. In other words, TRIB3 could have a key role in maintaining normal blood glucose level, and its deficiency decreases releasing glucose from tissues to the blood.

A study by Koo *et al* in 2004 proposed that inhibition of TRIB3 may treat type II diabetes as in liver, PGC-1 promotes insulin resistance via PPAR-α-dependent induction of TRIB3 [155]. Furthermore, Okamoto *et al* (2007) documented that TRIB3 deficiency displays normal hepatic insulin signalling and glucose homeostasis in mice [169]. Also looking at insulin resistance, Weismann *et al* in 2011 proposed that *in vivo* TRIB3 inhibition improves insulin sensitivity via PPAR-γ activation and without any alteration in RAC-beta serine/threonine-protein kinase (Akt2) activity in a rat model of insulin resistance [170].

Unger *et al* in 2003 suggested that insulin resistance results secondary to lipid accumulation, which occurs due to full responsiveness to insulin-stimulated lipogenic activity [209]. Takahashi *et al* (2008) demonstrated TRIB3 down-regulates PPAR-γ, a master controller of adipocyte differentiation, and regulates adipogenesis [137]. Furthermore, Wang *et al* in 2012 recorded that TRIB3 silence in diabetic ApoE-/-/LDL receptor-/- mice suppresses

atherosclerosis and stabilises plaques [171]. Oberkofler *et al* in 2010 showed in insulin-resistant obese human's atypical hepatic TRIB3 gene expression [210]. The previous literature demonstrates the important regulatory function of TRIB3 in lipid homeostasis and insulin sensitivity.

In addition to the effect of TRIB3 on insulin resistance, its role on lipid homeostasis was studied in murine blood fed chow and 60% HFD. Graphs 6.7A and 6.7B demonstrated that diet has an influence on modulating lipid homeostasis as feeding HFD to mice for 11 weeks significantly increased cholesterol and HDL concentrations in both groups. Further to this, TRIB3-/- altered the proportion of the increase as there was a rise in cholesterol and HDL levels post feeding HFD by 2 and 2.3 fold respectively in C57B6 group, whereas by 1.3 and 1.5 fold respectively in TRIB3-/- group. TRIB3 deficiency itself did not show any significant effect on lipid homeostasis in mouse blood except if the mice were fed a HFD. Here, it decreased cholesterol and HDL concentrations significantly in murine blood on 60% HFD for 11 weeks compared to their controls fed the same diet, but not in mice on a normal diet.

The above results indicate that on a HFD TRIB3 may be involved in lipid release from tissues, such as adipose tissue, to the blood to maintain lipid homeostasis. TRIB3 deficiency may therefore lead to an increased tissue lipid storage, which results in decreased blood lipid. By contrast, figure 6.7C illustrated neither diet nor knocking out TRIB3 have an effect on TG concentration. Given the above TRIB3 may regulate lipid homeostasis in mouse blood when fed a 60% HFD, however, molecular mechanism of TRIB3 action remains unclear.

Histological analysis of liver and adipose tissue were investigated in C57B6 and TRIB3-/- mice fed chow and 60% HFD for 11 weeks. The results showed no difference between liver cells of both groups whether mice were on chow or HFD (Figures 6.10A-D). Also no difference was found in adipose cells of both groups on chow. However, feeding mice HFD increased adipose

cell size of C57B6 and TRIB3-/-. In addition to this, knocking out TRIB3 resulted in a further increase in cell size when compared to C57B6 on the same diet (Figures 6.11A-D). In other words, TRIB3 may have a role on lipid release from adipose cells to the blood and knocking it out may increase lipid storage in these cells, which in turn increase cell size. This supports the above findings. It could also be that TRIB3 deficiency leads to a decrease in cell mitosis, therefore, reducing cell numbers and increasing cell size compared to its control on the same diet, or it may be due to a combination of both.

Furthermore, the role of TRIB3 on WBC numbers in the peritoneal lavage fluid in mice fed 60% HFD was studied. It was evident that knockout TRIB3 significantly increased leukocyte numbers in peritoneum compared to C57B6 (Figure 6.3A). However, neutrophils were not observed in both groups (Figures 6.3B and C). This suggests that TRIB3 is not necessary to control the number of all WBC types in peritoneum as it has no effect on neutrophil number.

The role of TRIB3 on WBC circulating in mouse blood fed chow and 60% HFD can be seen in graph 6.4A which illustrates no significant difference in the number of leukocytes in TRIB3-/- blood compared to the control regardless of whether mice were on normal food or HFD. However, post prolonged time (11 weeks) feeding both groups 60% HFD resulted in a significantly lower leukocyte numbers than feeding them for 5 weeks. With regards to the numbers of leukocyte types that are in murine blood, lymphocytes were shown to predominate in both groups whether mice are chow or HFD fed, with the exception of C57B6 group that were fed chow as the majority were lymphocytes and neutrophils (graphs 6.4B–D).

Interestingly, figures 6.4B–D also display among leukocyte types, knocking out TRIB3 decreased only neutrophil number significantly in mice fed normal food. It is possible that the decrease in neutrophils is compensated by other type of leukocytes as in figure 6.4A there were no difference in leukocyte numbers between C57B6 and TRIB3-/- mice fed chow. However,

the impact of feeding the mice 60% HFD is seen clearly on decreasing neutrophil and monocyte numbers in both blood groups (Figures 6.4C–D), while the significant decrease in lymphocyte number was restricted to C57B6 group on diet for 11 weeks compared to 5 weeks feeding of the same group (Figure 6.4B). Furthermore, the percentage of cells in blood was measured, figures 6.4E–G displayed knocking out TRIB3 increased the percentage of lymphocytes significantly, whereas the percentage of neutrophils was apparently decreased, but no effect was seen on the percentage of monocytes in mice fed chow. In contrast, feeding TRIB3-/- mice 60% HFD for short term (5 weeks) resulted in a significant decrease in the percentage of lymphocytes compared to C57B6 group on the same diet. In addition to this, measuring the percentage demonstrates the significant impact of diet, as monocytes in addition to neutrophils were decreased, whereas lymphocytes increased considerably in both C57B6 and TRIB3-/- groups.

This study also investigated the function of TRIB3 in developing lesions on aorta and heart sinus in mice fed 60% HFD for 11 weeks and clearly found both TRIB3 and feeding the mice HFD have no influence on atherosclerosis development in both areas (Figures 6.8A–D). Furthermore, TRIB3 has no effect on the heart sinus architecture as illustrated in figures 6.9A and 6.9B.

When looking at the heart, Ti *et al* (2011) showed in a type 2 diabetic rat model TRIB3 gene silencing alleviates diabetic cardiomyopathy [138]. Gong *et al* in 2009 found people with TRIB3 functional Q84R polymorphism are at risk of metabolic syndrome and carotid atherosclerosis [206].

Data shows there were almost no macrophages present in the heart sinus and liver in C57B6 or TRIB3-/- mice on HFD, in addition to adipose tissue of both groups fed chow. This indicates that TRIB3 has no role in determining macrophage numbers in these tissues (Figures 6.12A–D

and 6.13A–F). On the other hand, this diet may have an effect on adipose tissue, as adipose in both groups fed HFD have reduced macrophage numbers compared to their controls on chow. Again, knockout TRIB3 did not have a role in determining macrophage number in adipose, as the macrophage numbers in adipose of C57B6 and TRIB3-/- mice on HFD was similar (Figures 6.14A–L).

All of the above data suggest TRIB3 deficiency and HFD in combination modulate murine weight gain significantly. It also supports the theory that TRIB3 and HFD have an impact on WBC numbers in peritoneum and blood. However, their effect varies and depends on several factors as follows: leukocyte type, the mice diet and period of HFD. In addition, gender appears to play a key role on the weight of TRIB3-/- mice, which were fed chow compared to C57B6.

TRIB3 may be required to control murine blood glucose levels through regulation of glucose metabolism and glucose release from the tissues. TRIB3 deficiency may have a role in insulin resistance. Nevertheless, TRIB3 may be involved in controlling lipid homeostasis in mouse blood fed 60% HFD; neither diet nor knocking out TRIB3 has an effect on atherosclerosis development in mice. TRIB3 could also play a part in cell mitosis, specifically adipose but showed no effect on heart sinus architecture and macrophage number in all of murine heart sinus, liver and adipose in mice fed 60% HFD as seen in this study.

Further investigations on TRIB3 need to be conducted in addition to critical questions to be addressed, assessing its function. These include the molecular mechanism of TRIB3 action on lipid homeostasis, its impact on WBC numbers as well as identification of its exact role on insulin sensitivity.

Chapter 7: General Discussion

The discussion that follows below is an analysis of the experiments conducted in view of the hypothetical propositions put forward and the aims outlined in the thesis.

It has been published by Nick *et al* in 2000 that there is greater dependence on p38 MAPK pathway in the neutrophil compared to other WBC [182]. A study by Knall *et al* demonstrated that neutrophil chemotaxis towards IL8 is PI3K-dependent [183], [184]. Our observations strongly suggest that TRIB3 does not control activation of neutrophils via p38 MAPK. Its deficiency does not alter p38 phosphorylation compared to C57B6, or it may be that its effect is minute to the extent it is undetectable by western blotting technique. Data clearly highlights no profound differences between TRIB3-/- mice and the control in neutrophil chemotaxis to KC or fMLP. However, there was a trend to an increased response to KC at 10^{-5} M in TRIB3-/- mice compared to C57B6. There was also a trend to an increased response to fMLP at 10^{-6} M and 10^{-7} M. This suggests that knockout TRIB3 increased sensitivity of neutrophil chemotaxis towards chemoattractant. Hence, TRIB3 may regulate neutrophil migration in response to different chemoattractants (KC and fMLP). To see a significant effect, the number of experiments conducted should be increased. This study also clearly indicates that different signaling cascades for various stimuli regulate neutrophil chemotaxis. For more conclusive results, it would be beneficial if further *in vitro* studies on the effect of TRIB3 on neutrophil function via different intracellular signalling cascades in response to varying chemoattractants are conducted.

Siddiqi *et al* in 2001 demonstrated CD11b expression is clearly increased in PMA-stimulated neutrophils [194]. This study would suggest that once TRIB3 is knocked out and the cells are stimulated, the effect of shedding of L-selectin from the cell surface is significant. It is clear the key in increasing CD11b expression is the stimulation of cells rather than TRIB3-/- effect, while with PSGL-1, neither removing TRIB3 nor stimulating the cells has an effect on PSGL-1 expression. These observations clearly exclude the considerable effect of TRIB3 on adhesion molecules expression on murine neutrophils. The varying results in the literature and also with the *in vitro* observations of this project may have been due to various reasons, such as possible infection of mice and technical differences. Literature studies have shown discrepancies in this area and observations in this study support these findings. Given the variations in research and the findings of this experiment, further in vitro studies on the effect of TRIB3 on adhesion molecules would be recommended.

Interestingly, the effect of TRIB3 deficiency was observed in the blood of mice with thioglycollate-induced peritonitis. Knocking out TRIB3 inhibits the increase in leukocyte number in the samples significantly, while there was no effect on leukocyte chemotaxis towards the peritoneum compared to the control. Also knockout TRIB3 in mice with thioglycollate-induced peritonitis may increase sensitivity of neutrophil migration. There was a trend of increase neutrophil chemotaxis to peritoneum at 2 hours in TRIB3-/- mice compared to C57B6. This result was confirmed by the data found when studying the effect of TRIB3 on murine neutrophil chemotaxis in response to KC and fMLP. Neutrophil influx of TRIB3-/- mice towards KC at 10^{-5} M and fMLP at 10^{-7} M and 10^{-6} M was greater than C57B6, but this was not significant. It is also clear that removing TRIB3 from mice with thioglycollate-induced peritonitis had no significant effect on neutrophil chemotaxis. Furthermore, neutrophil

chemotaxis in TRIB3-/- mice persisted and continued to increase at 24 hours compared to the control which reduced after 6 hours until a minute number migrated at 24 hours (again there was no significance); a potential explanation for this could be that TRIB3 deficiency delays neutrophil apoptosis.

It was found that the initial process occurring after introducing thioglycollate, is the increasing levels of neutrophil-attracting chemokines at the site of infection. Research has showed that IL-13 activates human neutrophils to modulate the synthesis of many neutrophil proteins [203].

There was an increase in cytokine concentrations with time for both thioglycollate-induced peritonitis groups. When TRIB3 was removed from murine cells, the effect on cytokines was more selective and time dependent i.e. GMCSF, IL-17A and MCP-1 were affected at 2 hours and IL-13 at 6 hours compared to the control. However, the findings were not statistically significant except for IL-13. It could be that TRIB3 down regulates these cytokines at a certain point in time, although this regulation has no significant effect on neutrophil chemotaxis. The mechanism by which neutrophils recruit between endothelia and migrate into the inflammatory site warrants further investigation. Clarification of the link between TRIB3 and cytokines *in vivo* is hindered by the fact that the mechanism remains unclear, although cytokines are a prerequisite for neutrophil chemotaxis and TRIB3 appears to regulate these.

Literature has looked into the role of TRIB3 in lipid homeostasis and insulin resistance. Du *et al* observed that TRIB3 may act as a down-regulator of Akt activation by insulin in murine liver. Hence, TRIB3 contributes to insulin resistance in individuals susceptible to type II diabetes [153]. The results of this study reveal that TRIB3 is possibly required for control of murine blood glucose level through regulation of glucose metabolism. It also shows that TRIB3 impairment may lead to insulin resistance. Essentially, TRIB3 could have a key role in maintaining normal levels of blood glucose. Its deficiency reduces the release of glucose from

tissues to the blood. However, a study by Koo *et al* in 2004 proposed that inhibition of TRIB3 may help in the treatment of type II diabetes [155]. A further study by Wang *et al* in 2012 supporting Koo, documented that silencing TRIB3 in diabetic ApoE-/-/LDL receptor-/- mice suppresses atherosclerosis and stabilises plaques [171]. Additionally, TRIB3 deficiency and HFD in combination increase murine weight gain. Gender also play a key role on the weight of TRIB3-/- mice fed chow compared C57B6. Furthermore, this study demonstrates that HFD has an effect on modulating lipid homeostasis. It significantly elevated cholesterol and HDL levels in both groups. Likewise, TRIB3 deficiency altered the proportion of the increase as the rise in cholesterol and HDL levels were approximately double in C57B6 compared to the TRIB3-/- group. Knocking out TRIB3 also reduced cholesterol and HDL levels significantly in murine blood on HFD. This may indicate that on a HFD TRIB3 may be involved in lipid release from tissues to the blood in maintaining lipid homeostasis. In other words, the knocking out may therefore elevate tissue lipid storage, which reduced blood lipid. Again the molecular mechanism of TRIB3 action to regulate lipid homeostasis in mouse blood when fed a HFD remains uncertain.

Feeding mice HFD led to an increase in adipose cell size in both groups; however, TRIB3 deficiency resulted in a further increase in cell size. This again suggests that TRIB3 may have a role on lipid release from adipose cells to the blood. It may be possible that removing TRIB3 leads to reduce cell mitosis, hence, decreasing cell numbers and increasing cell size compared to its control on the same diet, or it could be due to a combination of both.

Moreover, it was evident that TRIB3 deficiency significantly elevated leukocyte numbers in peritoneum of mice on 60% HFD. However, TRIB3 is not necessary to regulate numbers of all WBC types in peritoneum as it has no effect on neutrophil number. Noticeable results in this study suggest that HFD decreased blood leukocyte numbers in both groups. Interestingly,

amongst leukocyte types, removing TRIB3 only reduced neutrophil number significantly in mice fed normal food. However, the effect of feeding the mice HFD is seen clearly on reducing neutrophil and monocyte numbers in both blood groups, whereas the significant decrease in lymphocytes was restricted to C57B6 group.

This study also demonstrates clearly that both TRIB3 and feeding the mice HFD have no effect on developing lesions in aorta and heart sinus, although Gong *et al* in 2009 found people with TRIB3 functional Q84R polymorphism are at risk of metabolic syndrome and carotid atherosclerosis [206]. TRIB3 equally has no effect on the heart sinus architecture as seen in this research. In addition, there were almost no macrophages present in the heart sinus and liver of either the C57B6 or TRIB3-/- mice on HFD. In contrast, both groups showed few macrophage numbers in adipose tissue compared to their controls on chow, suggesting HFD may increase macrophage number in this tissue. However, TRIB3 deficiency did not have an effect on macrophage number in adipose.

This thesis concludes that neutrophil chemotaxis towards KC and fMLP, is dependent upon p38 MAPK and PI3K. These could be controlled by TRIB3, which regulates cytokine concentrations. Removing TRIB3 prevents the increase in circulating leukocyte count considerably, may increase neutrophil chemotaxis towards peritoneum (inflammation site) and may extend their existence in thioglycollate-induced peritonitis. This is possibly due to TRIB3 deficiency interfering with neutrophil apoptosis. Moreover, TRIB3 and HFD affect murine weight gain. Gender also has a major effect on the weight of TRIB3 deficient mice fed chow compared to C57B6.

TRIB3 and HFD have an effect on WBC numbers in peritoneum and blood. However, their effect is varied and depends on a range of factors. Furthermore, TRIB3 may regulate mitosis, blood glucose levels and lipid homeostasis. This study shows a link between TRIB3 deficiency

and susceptibility to insulin resistance. However there is no effect on atherosclerosis development and heart sinus architecture in mice nor macrophage number in murine heart sinus, liver and adipose tissue of mice fed 60% HFD.

Contribution of TRIB3 in regulating lipid homeostasis is a novel finding. The role of TRIB3 in maintaining normal blood glucose level has been established previously and this has been further confirmed in this study. There is a relationship between this protein and neutrophilic inflammation. All the above provide new evidence for the close and complex link between TRIB3, insulin resistance, hyperlipidemia and inflammation. Therefore, this thesis raises the possibility of TRIB3 in the treatment of insulin resistance, inflammatory and metabolic diseases. Thus, focusing on TRIB3 may provide alternative strategies in the prevention and treatment of cardiovascular diseases. More studies on TRIB3 need to be conducted to further explore its various functions, for instance molecular mechanisms of its action on signalling pathways, WBC chemotaxis, lipid homeostasis and insulin sensitivity.

References

[1] Guo, D, Jia, Q, Song, HY et al., Vascular endothelial cell growth factor promotes tyrosine phosphorylation of mediators of signal transduction that contain SH2 domains. Association with endothelial cell proliferation. J Biol Chem 1995;270(12):6729–33.
[2] Rosen, OM, After insulin binds. Science 1987;237(4821):1452–8.
[3] Lalli, E, Sassone-Corsi, P, Signal transduction and gene regulation: the nuclear response to cAMP. J Biol Chem 1994;269(26):17359–62.
[4] Massague, J, Gomis, RR, The logic of TGFbeta signaling. FEBS Lett 2006;580(12):2811–20.
[5] Libby, P, Theroux, P, Pathophysiology of coronary artery disease. Circulation 2005;111(25):3481–8.
[6] Cook, S, Coronary artery disease, nitric oxide and oxidative stress: the "Yin-Yang" effect--a Chinese concept for a worldwide pandemic. Swiss Med Wkly 2006;136(7-8):103–13.
[7] van Diepen, JA, Berbee, JF, Havekes, LM et al., Interactions between inflammation and lipid metabolism: relevance for efficacy of anti-inflammatory drugs in the treatment of atherosclerosis. Atherosclerosis 2013;228(2):306–15.
[8] Poole, JCF, Florey, HW, Changes in the endothelium of the aorta and the behaviour of macrophages in experimental atheroma of rabbits. J Pathol Bacteriol 1958;75(2):245–51.
[9] Libby, P, Ridker, PM, Hansson, GK, Progress and challenges in translating the biology of atherosclerosis. Nature 2011;473(7347):317–25.
[10] Hoffman, M, Blum, A, Baruch, R et al., Leukocytes and coronary heart disease. Atherosclerosis 2004;172(1):1–6.
[11] Coller, BS, Leukocytosis and Ischemic Vascular Disease Morbidity and Mortality Is It Time to Intervene? Arteriosclerosis 2005;25(4):658–70.
[12] Toor, IS, Jaumdally, RJ, Moss, MS et al., Preprocedural neutrophil count predicts outcome in patients with advanced peripheral vascular disease undergoing percutaneous transluminal angioplasty. J Vasc Surg 2008;48(6):1504–8.
[13] Shurtz-Swirski, R, Sela, S, Herskovits, AT et al., Involvement of peripheral polymorphonuclear leukocytes in oxidative stress and inflammation in type 2 diabetic patients. Diabetes Care 2001;24(1):104–10.
[14] Mazor, R, Shurtz-Swirski, R, Farah, R et al., Primed polymorphonuclear leukocytes constitute a possible link between inflammation and oxidative stress in hyperlipidemic patients. Atherosclerosis 2008;197(2):937–43.
[15] Nijhuis, J, Rensen, SS, Slaats, Y et al., Neutrophil activation in morbid obesity, chronic activation of acute inflammation. Obesity (Silver Spring) 2009;17(11):2014–8.
[16] Kristal, B, Shurtz-Swirski, R, Chezar, J et al., Participation of peripheral polymorphonuclear leukocytes in the oxidative stress and inflammation in patients with essential hypertension. Am J Hypertens 1998;11(8 Pt 1):921–8.
[17] Rudolph, TK, Rudolph, V, Baldus, S, Contribution of myeloperoxidase to smoking-dependent vascular inflammation. Proc Am Thorac Soc 2008;5(8):820–3.
[18] Naruko, T, Ueda, M, Haze, K et al., Neutrophil infiltration of culprit lesions in acute coronary syndromes. Circulation 2002;106(23):2894–900.
[19] Zernecke, A, Bot, I, Djalali-Talab, Y et al., Protective role of CXC receptor 4/CXC ligand 12 unveils the importance of neutrophils in atherosclerosis. Circ Res 2008;102(2):209–17.
[20] Baetta, R, Corsini, A, Role of polymorphonuclear neutrophils in atherosclerosis: current

state and future perspectives. Atherosclerosis 2010;210(1):1–13.
[21] Bieghs, V, Wouters, K, Gorp, PJV et al., Role of scavenger receptor A and CD36 in diet-induced nonalcoholic steatohepatitis in hyperlipidemic mice. Gastroenterology 2010;138(7):2477–86.
[22] Leonarduzzi, G, Gamba, P, Gargiulo, S et al., Inflammation-related gene expression by lipid oxidation-derived products in the progression of atherosclerosis. Free Radic Biol Med 2012;52(1):19–34.
[23] Wong, MC, Diepen, JAv, Hu, L et al., Hepatocyte-specific IKKβ expression aggravates atherosclerosis development in< i> APOE* 3-Leiden</i> mice. Atherosclerosis 2012;220(2):362–8.
[24] Lewis, KE, Kirk, EA, McDonald, TO et al., Increase in serum amyloid a evoked by dietary cholesterol is associated with increased atherosclerosis in mice. Circulation 2004;110(5):540–5.
[25] Bieghs, V, Rensen, PCN, Hofker, MH et al., NASH and atherosclerosis are two aspects of a shared disease: central role for macrophages. Atherosclerosis 2012;220(2):287–93.
[26] Maganto-García, E, Tarrio, ML, Grabie, N et al., Dynamic changes in regulatory T cells are linked to levels of diet-induced hypercholesterolemia. Circulation 2011;124(2):185–95.
[27] Weij, JdV-d, Toet, K, Zadelaar., S, Anti-inflammatory salicylate beneficially modulates pre-existing atherosclerosis through quenching of NF-κB activity and lowering of cholesterol. Atherosclerosis 2010;213(1):241–6.
[28] Patel, S, Bartolo, BAD, Nakhla, S et al., Anti-inflammatory effects of apolipoprotein AI in the rabbit. Atherosclerosis 2010;212(2):392–7.
[29] Nathan, C, Neutrophils and immunity: challenges and opportunities. Nat Rev Immunol 2006;6(3):173–82.
[30] Simon, SI, Kim, MH, A day (or 5) in a neutrophil's life. Blood 2010;116(4):511–2.
[31] Ley, K, Laudanna, C, Cybulsky., MI, Getting to the site of inflammation: the leukocyte adhesion cascade updated. Nat Rev Immunol 2007;7(9):678–89.
[32] Ley, K, Cells on the run: shear-regulated integrin activation in leukocyte rolling and arrest on endothelial cells. Curr Opin Cell Biol 2008;20(5):525–32.
[33] Eriksson, EE, Xie, X, Werr, J et al., Importance of primary capture and L-selectin-dependent secondary capture in leukocyte accumulation in inflammation and atherosclerosis in vivo. J Exp Med 2001;194(2):205–18.
[34] Hidalgo, A, Peired, AJ, Wild, MK et al., Complete identification of E-selectin ligands on neutrophils reveals distinct functions of PSGL-1, ESL-1, and CD44. Immunity 2007;26(4):477–89.
[35] Barreiro, O, Vicente-Manzanares, M, Urzainqui, A et al., Interactive protrusive structures during leukocyte adhesion and transendothelial migration. Front Biosci 2004;9:1849–63.
[36] Zarbock, A, Abram, CL, Hundt, M et al., PSGL-1 engagement by E-selectin signals through Src kinase Fgr and ITAM adapters DAP12 and FcR gamma to induce slow leukocyte rolling. J Exp Med 2008;205(10):2339–47.
[37] McEver, RP, Selectins: lectins that initiate cell adhesion under flow. Curr Opin Cell Biol 2002;14(5):581–6.
[38] McEver, RP, Cummings, RD, Perspectives series: cell adhesion in vascular biology. Role of PSGL-1 binding to selectins in leukocyte recruitment. J Clin Invest 1997;100(3):485–91.
[39] Smith, ML, Olson, TS, Ley, K, CXCR2- and E-selectin-induced neutrophil arrest during inflammation in vivo. J Exp Med 2004;200(7):935–9.
[40] Salas, A, Shimaoka, M, Kogan, AN et al., Rolling adhesion through an extended conformation of integrin alphaLbeta2 and relation to alpha I and beta I-like domain

interaction. Immunity 2004;20(4):393–406.
[41] Zarbock, A, Lowell, CA, Ley, K, Spleen tyrosine kinase Syk is necessary for E-selectin-induced alpha(L)beta(2) integrin-mediated rolling on intercellular adhesion molecule-1. Immunity 2007;26(6):773–83.
[42] Rot, A, von Andrian, UH, Chemokines in innate and adaptive host defense: basic chemokinese grammar for immune cells. Annu Rev Immunol 2004;22:891–928.
[43] Chavakis, T, Bierhaus, A, Al-Fakhri, N et al., The pattern recognition receptor (RAGE) is a counterreceptor for leukocyte integrins: a novel pathway for inflammatory cell recruitment. J Exp Med 2003;198(10):1507–15.
[44] Yonekawa, K, Harlan, JM, Targeting leukocyte integrins in human diseases. J Leukoc Biol 2005;77(2):129–40.
[45] Phillipson, M, Heit, B, Colarusso, P et al., Intraluminal crawling of neutrophils to emigration sites: a molecularly distinct process from adhesion in the recruitment cascade. J Exp Med 2006;203(12):2569–75.
[46] Carman, CV, Springer, TA, A transmigratory cup in leukocyte diapedesis both through individual vascular endothelial cells and between them. J Cell Biol 2004;167(2):377–88.
[47] Nourshargh, S, Marelli-Berg, FM, Transmigration through venular walls: a key regulator of leukocyte phenotype and function. Trends Immunol 2005;26(3):157–65.
[48] Yang, L, Froio, RM, Sciuto, TE et al., ICAM-1 regulates neutrophil adhesion and transcellular migration of TNF-alpha-activated vascular endothelium under flow. Blood 2005;106(2):584–92.
[49] Heit, B, Tavener, S, Raharjo, E et al., An intracellular signaling hierarchy determines direction of migration in opposing chemotactic gradients. J Cell Biol 2002;159(1):91–102.
[50] Luster, AD, Chemokines--chemotactic cytokines that mediate inflammation. N Engl J Med 1998;338(7):436–45.
[51] Campbell, JJ, Foxman, EF, Butcher, EC, Chemoattractant receptor cross talk as a regulatory mechanism in leukocyte adhesion and migration. Eur J Immunol 1997;27(10):2571–8.
[52] Foxman, EF, Kunkel, EJ, Butcher, EC, Integrating conflicting chemotactic signals. The role of memory in leukocyte navigation. J Cell Biol 1999;147(3):577–88.
[53] Foxman, EF, Campbell, JJ, Butcher, EC, Multistep navigation and the combinatorial control of leukocyte chemotaxis. J Cell Biol 1997;139(5):1349–60.
[54] Shen, W, Li, B, Wetzel, MA et al., Down-regulation of the chemokine receptor CCR5 by activation of chemotactic formyl peptide receptor in human monocytes. Blood 2000;96(8):2887–94.
[55] Prossnitz, ER, Gilbert, TL, Chiang, S et al., Multiple activation steps of the N-formyl peptide receptor. Biochemistry 1999;38(8):2240–7.
[56] Damaj, BB, McColl, SR, Mahana, W et al., Physical association of Gi2alpha with interleukin-8 receptors. J Biol Chem 1996;271(22):12783–9.
[57] Amatruda, TT, Dragas-Graonic, S, Holmes, R et al., Signal transduction by the formyl peptide receptor. Studies using chimeric receptors and site-directed mutagenesis define a novel domain for interaction with G-proteins. J Biol Chem 1995;270(47):28010–3.
[58] Hirsch, E, Katanaev, VL, Garlanda, C et al., Central role for G protein-coupled phosphoinositide 3-kinase gamma in inflammation. Science 2000;287(5455):1049–53.
[59] Nick, JA, Avdi, NJ, Young, SK et al., Common and distinct intracellular signaling pathways in human neutrophils utilized by platelet activating factor and FMLP. J Clin Invest 1997;99(5):975–86.
[60] Cara, DC, Kaur, J, Forster, M et al., Role of p38 mitogen-activated protein kinase in chemokine-induced emigration and chemotaxis in vivo. J Immunol 2001;167(11):6552–8.

[61] Sasaki, T, Irie-Sasaki, J, Jones, RG et al., Function of PI3Kgamma in thymocyte development, T cell activation, and neutrophil migration. Science 2000;287(5455):1040–6.
[62] El Kebir, D, Filep, JG, Modulation of Neutrophil Apoptosis and the Resolution of Inflammation through beta2 Integrins. Front Immunol 2013;4:60.
[63] Savill, J, Dransfield, I, Gregory, C et al., A blast from the past: clearance of apoptotic cells regulates immune responses. Nat Rev Immunol 2002;2(12):965–75.
[64] Nathan, C, Ding, A, Nonresolving inflammation. Cell 2010;140(6):871–82.
[65] Gilroy, DW, Lawrence, T, Perretti, M et al., Inflammatory resolution: new opportunities for drug discovery. Nat Rev Drug Discov 2004;3(5):401–16.
[66] Savill, JS, Wyllie, AH, Henson, JE et al., Macrophage phagocytosis of aging neutrophils in inflammation. Programmed cell death in the neutrophil leads to its recognition by macrophages. J Clin Invest 1989;83(3):865–75.
[67] Mehta, J, Dinerman, J, Mehta, P et al., Neutrophil function in ischemic heart disease. Circulation 1989;79(3):549–56.
[68] Price, CJ, Menon, DK, Peters, AM et al., Cerebral neutrophil recruitment, histology, and outcome in acute ischemic stroke: an imaging-based study. Stroke 2004;35(7):1659–64.
[69] Jordan, JE, Zhao, ZQ, Vinten-Johansen, J, The role of neutrophils in myocardial ischemia-reperfusion injury. Cardiovasc Res 1999;43(4):860–78.
[70] Garcia de Tena, J, Inflammation, atherosclerosis, and coronary artery disease. N Engl J Med 2005;353(4):429–30; author reply 429.
[71] Boudjeltia, KZ, Faraut, B, Stenuit, P et al., Sleep restriction increases white blood cells, mainly neutrophil count, in young healthy men: a pilot study. Vasc Health Risk Manag 2008;4(6):1467–70.
[72] van Leeuwen, M, Gijbels, MJ, Duijvestijn, A et al., Accumulation of myeloperoxidase-positive neutrophils in atherosclerotic lesions in LDLR-/- mice. Arterioscler Thromb Vasc Biol 2008;28(1):84–9.
[73] Tuttle, HA, Davis-Gorman, G, Goldman, S et al., Platelet-neutrophil conjugate formation is increased in diabetic women with cardiovascular disease. Cardiovasc Diabetol 2003;2:12.
[74] Weerasinghe, A, Taylor, KM, The platelet in cardiopulmonary bypass. Ann Thorac Surg 1998;66(6):2145–52.
[75] Belcher, PR, Muriithi, EW, Milne, EM et al., Heparin, platelet aggregation, neutrophils, and cardiopulmonary bypass. Thromb Res 2000;98(4):249–56.
[76] Okouchi, M, Okayama, N, Imai, S et al., High insulin enhances neutrophil transendothelial migration through increasing surface expression of platelet endothelial cell adhesion molecule-1 via activation of mitogen activated protein kinase. Diabetologia 2002;45(10):1449–56.
[77] Zhang, W, Liu, HT, MAPK signal pathways in the regulation of cell proliferation in mammalian cells. Cell Res 2002;12(1):9–18.
[78] Pearson, G, Robinson, F, Beers Gibson, T et al., Mitogen-activated protein (MAP) kinase pathways: regulation and physiological functions. Endocr Rev 2001;22(2):153–83.
[79] Orton, RJ, Sturm, OE, Vyshemirsky, V et al., Computational modelling of the receptor-tyrosine-kinase-activated MAPK pathway. Biochem J 2005;392(Pt 2):249–61.
[80] Farooq, A, Zhou, MM, Structure and regulation of MAPK phosphatases. Cell Signal 2004;16(7):769–79.
[81] Theodosiou, A, Ashworth, A, MAP kinase phosphatases. Genome Biol 2002;3(7):REVIEWS3009.
[82] Junttila, MR, Li, SP, Westermarck, J, Phosphatase-mediated crosstalk between MAPK signaling pathways in the regulation of cell survival. FASEB J 2008;22(4):954–65.

[83] Murphy, LO, MacKeigan, JP, Blenis, J, A network of immediate early gene products propagates subtle differences in mitogen-activated protein kinase signal amplitude and duration. Mol Cell Biol 2004;24(1):144–53.
[84] Thalhamer, T, McGrath, MA, Harnett, MM, MAPKs and their relevance to arthritis and inflammation. Rheumatology (Oxford) 2008;47(4):409–14.
[85] Liu, JO, The yins of T cell activation. Sci STKE 2005;2005(265):re1.
[86] Feng, GJ, Goodridge, HS, Harnett, MM et al., Extracellular signal-related kinase (ERK) and p38 mitogen-activated protein (MAP) kinases differentially regulate the lipopolysaccharide-mediated induction of inducible nitric oxide synthase and IL-12 in macrophages: Leishmania phosphoglycans subvert macrophage IL-12 production by targeting ERK MAP kinase. J Immunol 1999;163(12):6403–12.
[87] Johnson, GL, Lapadat, R, Mitogen-activated protein kinase pathways mediated by ERK, JNK, and p38 protein kinases. Science 2002;298(5600):1911–2.
[88] Stokoe, D, Macdonald, SG, Cadwallader, K et al., Activation of Raf as a result of recruitment to the plasma membrane. Science 1994;264(5164):1463–7.
[89] Hii, CS, Stacey, K, Moghaddami, N et al., Role of the extracellular signal-regulated protein kinase cascade in human neutrophil killing of Staphylococcus aureus and Candida albicans and in migration. Infect Immun 1999;67(3):1297–302.
[90] Katsube, M, Kato, T, Kitagawa, M et al., Calpain-mediated regulation of the distinct signaling pathways and cell migration in human neutrophils. J Leukoc Biol 2008;84(1):255–63.
[91] Ruvolo, PP, Ceramide regulates cellular homeostasis via diverse stress signaling pathways. Leukemia 2001;15(8):1153–60.
[92] Davis, RJ, Signal transduction by the JNK group of MAP kinases. Cell 2000;103(2):239–52.
[93] Shaulian, E, Karin, M, AP-1 in cell proliferation and survival. Oncogene 2001;20(19):2390–400.
[94] Karin, M, Liu, Z, Zandi, E, AP-1 function and regulation. Curr Opin Cell Biol 1997;9(2):240–6.
[95] Widmann, C, Gibson, S, Jarpe, MB et al., Mitogen-activated protein kinase: conservation of a three-kinase module from yeast to human. Physiol Rev 1999;79(1):143–80.
[96] Ip, YT, Davis, RJ, Signal transduction by the c-Jun N-terminal kinase (JNK)--from inflammation to development. Curr Opin Cell Biol 1998;10(2):205–19.
[97] O'Hagan, RC, Tozer, RG, Symons, M et al., The activity of the Ets transcription factor PEA3 is regulated by two distinct MAPK cascades. Oncogene 1996;13(6):1323–33.
[98] Kato, T, Noma, H, Kitagawa, M et al., Distinct role of c-Jun N-terminal kinase isoforms in human neutrophil apoptosis regulated by tumor necrosis factor-alpha and granulocyte-macrophage colony-stimulating factor. J Interferon Cytokine Res 2008;28(4):235–43.
[99] Goh, KC, Haque, SJ, Williams, BR, p38 MAP kinase is required for STAT1 serine phosphorylation and transcriptional activation induced by interferons. EMBO J 1999;18(20):5601–8.
[100] Wang, XZ, Ron, D, Stress-induced phosphorylation and activation of the transcription factor CHOP (GADD153) by p38 MAP Kinase. Science 1996;272(5266):1347–9.
[101] Lominadze, G, Rane, MJ, Merchant, M et al., Myeloid-related protein-14 is a p38 MAPK substrate in human neutrophils. J Immunol 2005;174(11):7257–67.
[102] Browning, DD, Windes, ND, Ye, RD, Activation of p38 mitogen-activated protein kinase by lipopolysaccharide in human neutrophils requires nitric oxide-dependent cGMP accumulation. J Biol Chem 1999;274(1):537–42.
[103] Abell, K, Watson, CJ, The Jak/Stat pathway: a novel way to regulate PI3K activity. Cell Cycle 2005;4(7):897–900.

[104] Petiot, A, Ogier-Denis, E, Blommaart, EF et al., Distinct classes of phosphatidylinositol 3'-kinases are involved in signaling pathways that control macroautophagy in HT-29 cells. J Biol Chem 2000;275(2):992–8.
[105] Rommel, C, Camps, M, Ji, H, PI3K delta and PI3K gamma: partners in crime in inflammation in rheumatoid arthritis and beyond? Nat Rev Immunol 2007;7(3):191–201.
[106] Balendran, A, Casamayor, A, Deak, M et al., PDK1 acquires PDK2 activity in the presence of a synthetic peptide derived from the carboxyl terminus of PRK2. Curr Biol 1999;9(8):393–404.
[107] Okkenhaug, K, Vanhaesebroeck, B, PI3K in lymphocyte development, differentiation and activation. Nat Rev Immunol 2003;3(4):317–30.
[108] Vander Haar, E, Lee, SI, Bandhakavi, S et al., Insulin signalling to mTOR mediated by the Akt/PKB substrate PRAS40. Nat Cell Biol 2007;9(3):316–23.
[109] Franke, TF, PI3K/Akt: getting it right matters. Oncogene 2008;27(50):6473–88.
[110] Duronio, V, The life of a cell: apoptosis regulation by the PI3K/PKB pathway. Biochem J 2008;415(3):333–44.
[111] Zoncu, R, Efeyan, A, Sabatini, DM, mTOR: from growth signal integration to cancer, diabetes and ageing. Nat Rev Mol Cell Biol 2011;12(1):21–35.
[112] Dummler, B, Hemmings, BA, Physiological roles of PKB/Akt isoforms in development and disease. Biochem Soc Trans 2007;35(Pt 2):231–5.
[113] Chen, WS, Xu, PZ, Gottlob, K et al., Growth retardation and increased apoptosis in mice with homozygous disruption of the Akt1 gene. Genes Dev 2001;15(17):2203–8.
[114] Cho, H, Thorvaldsen, JL, Chu, Q et al., Akt1/PKBalpha is required for normal growth but dispensable for maintenance of glucose homeostasis in mice. J Biol Chem 2001;276(42):38349–52.
[115] Garofalo, RS, Orena, SJ, Rafidi, K et al., Severe diabetes, age-dependent loss of adipose tissue, and mild growth deficiency in mice lacking Akt2/PKB beta. J Clin Invest 2003;112(2):197–208.
[116] Tschopp, O, Yang, ZZ, Brodbeck, D et al., Essential role of protein kinase B gamma (PKB gamma/Akt3) in postnatal brain development but not in glucose homeostasis. Development 2005;132(13):2943–54.
[117] Liu, G, Bi, Y, Wang, R et al., Kinase AKT1 negatively controls neutrophil recruitment and function in mice. J Immunol 2013;191(5):2680–90.
[118] Chen, J, Tang, H, Hay, N et al., Akt isoforms differentially regulate neutrophil functions. Blood 2010;115(21):4237–46.
[119] Fischer-Posovszky, P, Tews, D, Horenburg…, S, Differential function of Akt1 and Akt2 in human adipocytes. Mol Cell Endocrinol 2012;358(1):135–43.
[120] Schabbauer, G, Tencati, M, Pedersen, B et al., PI3K-Akt pathway suppresses coagulation and inflammation in endotoxemic mice. Arterioscler Thromb Vasc Biol 2004;24(10):1963–9.
[121] Gillooly, DJ, Simonsen, A, Stenmark, H, Phosphoinositides and phagocytosis. J Cell Biol 2001;155(1):15–7.
[122] Hidalgo, MA, Ojeda, F, Eyre, P et al., Platelet-activating factor increases pH(i) in bovine neutrophils through the PI3K-ERK1/2 pathway. Br J Pharmacol 2004;141(2):311–21.
[123] Weichhart, T, Saemann, MD, The PI3K/Akt/mTOR pathway in innate immune cells: emerging therapeutic applications. Ann Rheum Dis 2008;67 Suppl 3:iii70–4.
[124] Ghosh, S, May, MJ, Kopp, EB, NF-kappa B and Rel proteins: evolutionarily conserved mediators of immune responses. Annu Rev Immunol 1998;16:225–60.
[125] Gilmore, TD, Introduction to NF-kappaB: players, pathways, perspectives. Oncogene 2006;25(51):6680–4.
[126] Chen, F, Castranova, V, Shi, X, New insights into the role of nuclear factor-kappaB in

cell growth regulation. Am J Pathol 2001;159(2):387–97.
[127] Mohamed, MR, McFadden, G, NFkB inhibitors: strategies from poxviruses. Cell Cycle 2009;8(19):3125–32.
[128] Miskolci, V, Rollins, J, Vu, HY et al., NFkappaB is persistently activated in continuously stimulated human neutrophils. Mol Med 2007;13(3-4):134–42.
[129] Jones, MR, Quinton, LJ, Simms, BT et al., Roles of interleukin-6 in activation of STAT proteins and recruitment of neutrophils during Escherichia coli pneumonia. J Infect Dis 2006;193(3):360–9.
[130] Hegedus, Z, Czibula, A, Kiss-Toth, E, Tribbles: A family of kinase-like proteins with potent signalling regulatory function. Cell Signalling 2007;19(2):238–50.
[131] Hegedus, Z, Czibula, A, Kiss-Toth, E, Tribbles: novel regulators of cell function; evolutionary aspects. Cell Mol Life Sci 2006;63 (14):1632–41.
[132] Eder, K, Guan, H, Sung, HY et al., Tribbles-2 is a novel regulator of inflammatory activation of monocytes. Int Immunol 2008;20(12):1543–50.
[133] Wei, SC, Rosenberg, IM, Cao, Z et al., Tribbles 2 (Trib2) is a novel regulator of toll-like receptor 5 signaling. Inflamm Bowel Dis 2012;18(5):877–88.
[134] Dobens, LLJ, Bouyain, S, Developmental roles of tribbles protein family members. Dev Dyn 2012;241(8):1239–48.
[135] Ostertag, A, Jones, A, Rose, AJ et al., Control of adipose tissue inflammation through TRB1. Diabetes 2010;59(8):1991–2000.
[136] Sung, HY, Francis, SE, Arnold, ND et al., Enhanced Macrophage Tribbles-1 Expression in Murine Experimental Atherosclerosis. Biology 2012;1(1):43–57.
[137] Takahashi, Y, Ohoka, N, Hayashi, H et al., TRB3 suppresses adipocyte differentiation by negatively regulating PPARgamma transcriptional activity. J Lipid Res 2008;49(4):880–92.
[138] Ti, Y, Xie, G, Wang, Z et al., TRB3 gene silencing alleviates diabetic cardiomyopathy in a type 2 diabetic rat model. Diabetes 2011;60(11):2963–74.
[139] Prudente, S, Sesti, G, Pandolfi, A et al., The Mammalian Tribbles Homolog TRIB3, Glucose Homeostasis, and Cardiovascular Diseases. Endocr Rev 2012;33(4):526–46.
[140] Angyal, A, Kiss-Toth, E, The tribbles gene family and lipoprotein metabolism. Curr Opin Lipidol 2012;23(2):122–6.
[141] Wilkin, F, Savonet, V, Radulescu, A et al., Identification and characterization of novel genes modulated in the thyroid of dogs treated with methimazole and propylthiouracil. J Biol Chem 1996;271(45):28451–7.
[142] Ndiaye, K, Fayad, T, Silversides, DW et al., Identification of downregulated messenger RNAs in bovine granulosa cells of dominant follicles following stimulation with human chorionic gonadotropin. Biol Reprod 2005;73(2):324–33.
[143] Mayumi-Matsuda, K, Kojima, S, Suzuki, H et al., Identification of a novel kinase-like gene induced during neuronal cell death. Biochem Biophys Res Commun 1999;258(2):260–4.
[144] Klingenspor, M, Xu, P, Cohen, RD et al., Altered gene expression pattern in the fatty liver dystrophy mouse reveals impaired insulin-mediated cytoskeleton dynamics. J Biol Chem 1999;274(33):23078–84.
[145] Kiss-Toth, E, Bagstaff, SM, Sung, HY et al., Human tribbles, a protein family controlling mitogen-activated protein kinase cascades. J Biol Chem 2004;279(41):42703–8.
[146] Kiss-Toth, E, Wyllie, DH, Holland, K et al., Functional mapping and identification of novel regulators for the Toll/Interleukin-1 signalling network by transcription expression cloning. Cell Signal 2006;18(2):202–14.
[147] Grosshans, J, Wieschaus, E, A genetic link between morphogenesis and cell division during formation of the ventral furrow in Drosophila. Cell 2000;101(5):523–31.

[148] Seher, TC, Leptin, M, Tribbles, a cell-cycle brake that coordinates proliferation and morphogenesis during Drosophila gastrulation. Curr Biol 2000;10(11):623–9.
[149] Mata, J, Curado, S, Ephrussi, A et al., Tribbles coordinates mitosis and morphogenesis in Drosophila by regulating string/CDC25 proteolysis. Cell 2000;101(5):511–22.
[150] Naiki, T, Saijou, E, Miyaoka, Y et al., TRB2, a mouse Tribbles ortholog, suppresses adipocyte differentiation by inhibiting AKT and C/EBPβ. J Biol Chem 2007;282(33):24075–82.
[151] Saka, Y, Smith, JC, A Xenopus tribbles orthologue is required for the progression of mitosis and for development of the nervous system. Dev Biol 2004;273(2):210–25.
[152] Rorth, P, Szabo, K, Texido, G, The level of C/EBP protein is critical for cell migration during Drosophila oogenesis and is tightly controlled by regulated degradation. Mol Cell 2000;6(1):23–30.
[153] Du, K, Herzig, S, Kulkarni, RN et al., TRB3: a tribbles homolog that inhibits Akt/PKB activation by insulin in liver. Science 2003;300(5625):1574–7.
[154] Maddala, R, Peng, YW, Rao, PV, Selective expression of the small GTPase RhoB in the early developing mouse lens. Dev Dyn 2001;222(3):534–7.
[155] Koo, SH, Satoh, H, Herzig, S et al., PGC-1 promotes insulin resistance in liver through PPAR-alpha-dependent induction of TRB-3. Nat Med 2004;10(5):530–4.
[156] Wilkin, F, Suarez-Huerta, N, Robaye, B et al., Characterization of a phosphoprotein whose mRNA is regulated by the mitogenic pathways in dog thyroid cells. Eur J Biochem 1997;248(3):660–8.
[157] Ord, D, Ord, T, Mouse NIPK interacts with ATF4 and affects its transcriptional activity. Exp Cell Res 2003;286(2):308–20.
[158] Bowers, AJ, Scully, S, Boylan, JF, SKIP3, a novel Drosophila tribbles ortholog, is overexpressed in human tumors and is regulated by hypoxia. Oncogene 2003;22(18):2823–35.
[159] Ferrell, JEJ, What do scaffold proteins really do? Sci STKE 2000;2000(52):pe1.
[160] Carlotti, F, Chapman, R, Dower, SK et al., Activation of nuclear factor kappaB in single living cells. Dependence of nuclear translocation and anti-apoptotic function on EGFPRELA concentration. J Biol Chem 1999;274(53):37941–9.
[161] Hoffmann, A, Levchenko, A, Scott, ML et al., The IkappaB-NF-kappaB signaling module: temporal control and selective gene activation. Science 2002;298(5596):1241–5.
[162] Sveiczer, A, Csikasz-Nagy, A, Gyorffy, B et al., Modeling the fission yeast cell cycle: quantized cycle times in wee1- cdc25Delta mutant cells. Proc Natl Acad Sci U S A 2000;97(14):7865–70.
[163] Ord, T, Ord, D, Koivomagi, M et al., Human TRB3 is upregulated in stressed cells by the induction of translationally efficient mRNA containing a truncated 5'-UTR. Gene 2009;444(1-2):24–32.
[164] Ding, J, Kato, S, Du, K, PI3K activates negative and positive signals to regulate TRB3 expression in hepatic cells. Exp Cell Res 2008;314(7):1566–74.
[165] Avery, J, Etzion, S, DeBosch, BJ et al., TRB3 function in cardiac endoplasmic reticulum stress. Circ Res 2010;106(9):1516–23.
[166] Liu, J, Zhang, W, Chuang, GC et al., Role of TRIB3 in regulation of insulin sensitivity and nutrient metabolism during short-term fasting and nutrient excess. Am J Physiol Endocrinol Metab 2012;303(7):E908–16.
[167] Iynedjian, PB, Lack of evidence for a role of TRB3/NIPK as an inhibitor of PKB-mediated insulin signalling in primary hepatocytes. Biochem J 2005;386(Pt 1):113–8.
[168] Qi, L, Heredia, JE, Altarejos, JY et al., TRB3 links the E3 ubiquitin ligase COP1 to lipid metabolism. Science 2006;312(5781):1763–6.
[169] Okamoto, H, Latres, E, Liu, R et al., Genetic deletion of Trb3, the mammalian Drosophila

tribbles homolog, displays normal hepatic insulin signaling and glucose homeostasis. Diabetes 2007;56(5):1350–6.
[170] Weismann, D, Erion, DM, Ignatova-Todorava, I et al., Knockdown of the gene encoding Drosophila tribbles homologue 3 (Trib3) improves insulin sensitivity through peroxisome proliferator-activated receptor-γ (PPAR-γ) activation in a rat model of insulin resistance. Diabetologia 2011;54(4):935–44.
[171] Wang, ZH, Shang, YY, Zhang, S et al., Silence of TRIB3 suppresses atherosclerosis and stabilizes plaques in diabetic ApoE-/-/LDL receptor-/- mice. Diabetes 2012;61(2):463–73.
[172] Andreozzi, F, Formoso, G, Prudente, S et al., TRIB3 R84 variant is associated with impaired insulin-mediated nitric oxide production in human endothelial cells. Arterioscler Thromb Vasc Biol 2008;28(7):1355–60.
[173] Prudente, S, Hribal, ML, Flex, E et al., The Functional Q84R Polymorphism of Mammalian Tribbles Homolog TRB3 Is Associated With Insulin Resistance and Related Cardiovascular Risk in Caucasians From Italy. Diabetes 2005;54(9):2807–11.
[174] Zambrowicz, BP, Abuin…, A, Wnk1 kinase deficiency lowers blood pressure in mice: a gene-trap screen to identify potential targets for therapeutic intervention. Proc Natl Acad Sci U S A 2003;100(24):14109–14.
[175] Mitra, S, Abraham, E, Participation of superoxide in neutrophil activation and cytokine production. Biochim Biophys Acta 2006;1762(8):732–41.
[176] Fumagalli, L, Zhang, H, Baruzzi…, A, The Src family kinases Hck and Fgr regulate neutrophil responses to N-formyl-methionyl-leucyl-phenylalanine. J Immunol 2007;178(6):3874–85.
[177] Zu, YL, Qi, J, Gilchrist, A et al., p38 mitogen-activated protein kinase activation is required for human neutrophil function triggered by TNF-alpha or FMLP stimulation. J Immunol 1998;160(4):1982–9.
[178] Montecucco, F, Bianchi, G, Gnerre, P et al., Induction of neutrophil chemotaxis by leptin: crucial role for p38 and Src kinases. Ann N Y Acad Sci 2006;1069:463–71.
[179] Liu, L, Pharmacological inhibition of p38 mitogen-activated protein kinases affects KC/CXCL1-induced intraluminal crawling, transendothelial migration, and chemotaxis of neutrophils in vivo. Mediators Inflamm 2013;2013:290565.
[180] Heit, B, Liu, L, Colarusso, P et al., PI3K accelerates, but is not required for, neutrophil chemotaxis to fMLP. J Cell Sci 2008;121(Pt 2):205–14.
[181] Aomatsu, K, Kato, T, Fujita, H et al., Toll-like receptor agonists stimulate human neutrophil migration via activation of mitogen-activated protein kinases. Immunology 2008;123(2):171–80.
[182] Nick, JA, Young, SK, Brown, KK et al., Role of p38 mitogen-activated protein kinase in a murine model of pulmonary inflammation. J Immunol 2000;164(4):2151–9.
[183] Knall, C, Young, S, Nick, JA et al., Interleukin-8 regulation of the Ras/Raf/mitogen-activated protein kinase pathway in human neutrophils. J Biol Chem 1996;271(5):5832–8.
[184] Knall, C, Worthen, GS, Johnson, GL, Interleukin 8-stimulated phosphatidylinositol-3-kinase activity regulates the migration of human neutrophils independent of extracellular signal-regulated kinase and p38 mitogen-activated protein kinases. Proc Natl Acad Sci U S A 1997;94(7):3052–7.
[185] Liu, L, Puri, KD, Penninger, JM et al., Leukocyte PI3Kgamma and PI3Kdelta have temporally distinct roles for leukocyte recruitment in vivo. Blood 2007;110(4):1191–8.
[186] von Andrian, UH, Chambers, JD, McEvoy, LM et al., Two-step model of leukocyte-endothelial cell interaction in inflammation: distinct roles for LECAM-1 and the leukocyte beta 2 integrins in vivo. Proc Natl Acad Sci U S A 1991;88(17):7538–42.

[187] Phillips, ML, Schwartz, BR, Etzioni, A et al., Neutrophil adhesion in leukocyte adhesion deficiency syndrome type 2. J Clin Invest 1995;96(6):2898–906.
[188] Guyer, DA, Moore, KL, Lynam, EB et al., P-selectin glycoprotein ligand-1 (PSGL-1) is a ligand for L-selectin in neutrophil aggregation. Blood 1996;88(7):2415–21.
[189] Cavanagh, SP, Gough, MJ, Homer-Vanniasinkam, S, The role of the neutrophil in ischaemia-reperfusion injury: potential therapeutic interventions. Cardiovasc Surg 1998;6(2):112–8.
[190] Chen, Y, Mendoza, S, Davis-Gorman, G et al., Neutrophil activation by murine retroviral infection during chronic ethanol consumption. Alcohol Alcohol 2003;38(2):109–14.
[191] Witko-Sarsat, VRP, Descamps-Latscha B, Lesavre P, Halbwachs-Mecarelli L, Neutrophils: molecules, functions and pathophysiological aspects. Lab Invest 2000;80 (5):617–53.
[192] Davenpeck, KL, Brummet, ME, Hudson, SA et al., Activation of human leukocytes reduces surface P-selectin glycoprotein ligand-1 (PSGL-1, CD162) and adhesion to P-selectin in vitro. J Immunol 2000;165(5):2764–72.
[193] Neeley, SP, Hamann, KJ, White, SR et al., Selective regulation of expression of surface adhesion molecules Mac-1, L-selectin, and VLA-4 on human eosinophils and neutrophils. Am J Respir Cell Mol Biol 1993;8(6):633–9.
[194] Siddiqi, M, Garcia, ZC, Stein, DS et al., Relationship between oxidative burst activity and CD11b expression in neutrophils and monocytes from healthy individuals: effects of race and gender. Cytometry 2001;46(4):243–6.
[195] Harvath, L, Falk, W, Leonard, EJ, Rapid quantitation of neutrophil chemotaxis: use of a polyvinylpyrrolidone-free polycarbonate membrane in a multiwell assembly. J Immunol Methods 1980;37(1):39–45.
[196] Khajah, M, Millen, B, Cara…, DC, Granulocyte-macrophage colony-stimulating factor (GM-CSF): a chemoattractive agent for murine leukocytes in vivo. J Leukoc Biol 2011;89(6):945–53.
[197] Filippo, KD, Henderson…, RB, Neutrophil chemokines KC and macrophage-inflammatory protein-2 are newly synthesized by tissue macrophages using distinct TLR signaling pathways. J Immunol 2008;180(6):4308–15.
[198] Zlotnik, A, Yoshie, O, Chemokines: a new classification system and their role in immunity. Immunity 2000;12(2):121–7.
[199] Baron, EJ, Proctor, RA, Elicitation of peritoneal polymorphonuclear neutrophils from mice. J Immunol Methods 1982;49(3):305–13.
[200] Li, L, Huang, L, Vergis, AL et al., IL-17 produced by neutrophils regulates IFN-γ- mediated neutrophil migration in mouse kidney ischemia-reperfusion injury. J Clin Invest 2010;120(1):331–42.
[201] Chiba, K, Zhao, W, Chen, J et al., Neutrophils secrete MIP-1 beta after adhesion to laminin contained in basement membrane of blood vessels. Br J Haematol 2004;127(5):592–7.
[202] Ratthe, C, Ennaciri, J, Garces Goncalves, DM et al., Interleukin (IL)-4 induces leukocyte infiltration in vivo by an indirect mechanism. Mediators Inflamm 2009;2009:193970.
[203] Girard, D, Paquin, R, Naccache, PH et al., Effects of interleukin-13 on human neutrophil functions. J Leukoc Biol 1996;59(3):412–9.
[204] Ramos, CD, Canetti, C, Souto, JT et al., MIP-1alpha[CCL3] acting on the CCR1 receptor mediates neutrophil migration in immune inflammation via sequential release of TNF-alpha and LTB4. J Leukoc Biol 2005;78(1):167–77.
[205] Kipari, T, Watson, S, Houlberg, K et al., Lymphocytes modulate peritoneal leukocyte recruitment in peritonitis. Inflamm Res 2009;58(9):553–60.
[206] Gong, HP, Wang, ZH, Jiang, H et al., TRIB3 functional Q84R polymorphism is a risk

factor for metabolic syndrome and carotid atherosclerosis. Diabetes Care 2009;32(7):1311–3.
[207] Bhargava, P, Lee, CH, Role and function of macrophages in the metabolic syndrome. Biochem J 2012;442(2):253–62.
[208] Ord, D, Meerits, K, Ord, T, TRB3 protects cells against the growth inhibitory and cytotoxic effect of ATF4. Exp Cell Res 2007;313(16):3556–67.
[209] Unger, RH, Lipid overload and overflow: metabolic trauma and the metabolic syndrome. Trends Endocrinol Metab 2003;14(9):398–403.
[210] Oberkofler, H, Pfeifenberger, A, Soyal, S et al., Aberrant hepatic TRIB3 gene expression in insulin-resistant obese humans. Diabetologia 2010;53(9):1971–5.

Appendix 1: Chemicals and other Laboratory substances

Item	Supplier, Town, Country
100bp DNA ladder	Norgen, Thorold, Canada
4-(2-Hydroxyethyl)-1-piperazineethanesulfonic acid, HEPES	Sigma-Aldrich, Dorset, UK
96-Well EASIA plates	Sarstedt, Leicester, UK
Accu-Chek Aviva test strips	Roche, Burgess Hill, UK
Acetic acid	VWR, Lutterworth, UK
Acrylamide stock solution (30%)	Geneflow, Fradley, UK
Agarose	Bioline, London, UK
Akt Ab	New England Biolabs, Hitchin, UK
Albumin solution (7.5%)	Sigma-Aldrich, Dorset, UK
Amersham Hyperfilm^{TM} ECL	Fisher, Loughborough, UK
Ammonium persulphate, APS	Sigma-Aldrich, Dorset, UK
Anti-mouse CD115	AbD Serotec, Kidlington, UK
Anti-mouse CD2	BD, Oxford, UK
Anti-mouse CD45R	eBioscience, Hatfield, UK
Anti-mouse CD5	BD, Oxford, UK
Anti-mouse F4/80	eBioscience, Hatfield, UK
BD cytometric bead array, CBA, kit	BD Biosciences, Oxford, UK
Bio-Rad DC protein assay kit	Bio-Rad, Hemel Hempstead, UK
Biomix	Bioline, London, UK
Biotinylated anti-rat IgG	Vector Laboratories, CA, USA
Bovine serum albumin, BSA	Sigma-Aldrich, Dorset, UK
CellFIX	BD, Erembodegem, Belgium
Chemotaxis plates	Receptor Technologies, Leamington Spa
Cotton swabs	Fisher Scientific, Loughborough, UK
ddH_20 (MilliQ H_2O)	Merck-Millipore, Watford, UK
Dextran	Sigma-Aldrich, Dorset, UK
Di-sodium hydrogen orthophosphate, Na_2HPO_4	Sigma-Aldrich, Dorset, UK
Diff-Quick	BDH Merck Ltd, Poole, UK
Dimethyl sulphoxide, DMSO	Sigma-Aldrich, Dorset, UK
Disposable haemocytometers	Labtech International, Ringmer, UK
DPX mounting medium	Sigma-Aldrich, Dorset, UK
Eosin solution	Sigma-Aldrich, Dorset, UK
Erythrolyse red blood cell lysing buffer	AbD Serotec, Kidlington, UK
Ethanol	Fisher Scientific, Loughborough, UK
Ethidium bromide, EtBr	Sigma-Aldrich, Dorset, UK
Ethylenediaminetetra-acetic acid, EDTA	Sigma-Aldrich, Dorset, UK
FITC rat anti-mouse Ly-6G (1A8)	BD, Oxford, UK
Formaldehyde	Sigma-Aldrich, Dorset, UK
Formyl-methionyl-leucyl-phenylalanine, fMLP	Sigma-Aldrich, Dorset, UK
Glucose	VWR, Lutterworth, UK
Glycerol	VWR, Lutterworth, UK
Glycine	VWR, Lutterworth, UK

Goat anti-rabbit-HRP	**Dako, Ely, UK**
Goat anti-rat mircobeads	**Miltenyi Biotech, Bisley, UK**
Haematoxylin solution	**Sigma-Aldrich, Dorset, UK**
Heparin sodium 5,000 IU/ml	**Leo Laboratories Ltd., Bucks, UK**
Hydrochloric acid	**VWR, Lutterworth, UK**
Hydrogen peroxide (H_2O_2)	**Sigma-Aldrich, Dorset, UK**
Ilford universal developer	**Jessop's, Leicester, UK**
Ilford, hypam fixer	**Jessop's, Leicester, UK**
Isofluorane	**Burtons, Marden, UK**
Isopropanol (propan-2-ol)	**Sigma-Aldrich, Dorset, UK**
Lipopolysaccharide, LPS	**Sigma-Aldrich, Dorset, UK**
MACS speration columns	**Miltenyi Biotech, Bisley, UK**
Methanol	**Fisher, Loughborough, UK**
Milk powder	
Murine KC	**Peprotech EC Ltd, London, UK**
N,N,N',N'-tetramethylethylenediamine, TEMED	**Sigma-Aldrich, Dorset, UK**
Nitrocellulose protran membrane	**Geneflow, Fradley, UK**
Oil Red O	**Sigma-Aldrich, Dorset, UK**
p38 inhibitor (SB 203580)	**Cell Signaling Technology, Danvers, MA, USA**
p38 MAP kinase assay kit (nonradioactive)	**New England Biolabs, Hitchin, UK**
p38 MAPK Ab	**New England Biolabs, Hitchin, UK**
Paraformaldehyde	**Sigma-Aldrich, Dorset, UK**
PE anti-mouse CD162 (PSGL-1) (2PH1)	**BD, Oxford, UK**
PE rat anti-mouse CD11b (M1/70)	**BD, Oxford, UK**
PE rat anti-mouse CD62L (L-selectin) (MEL-14)	**BD, Oxford, UK**
PE rat IgG_1, κ isotype control	**BD, Oxford, UK**
PE rat IgG_{2a}, κ isotype control	**BD, Oxford, UK**
PE rat IgG_{2b}, κ isotype control	**BD, Oxford, UK**
Pentobarbital sodium (20%) solution	**Pharmacol Ltd., Andover, UK**
Peroxidase substrate kit (DAB)	**Vector Laboratories, CA, USA**
Phenylmethanesulphonylfluoride, PMSF	**Sigma-Aldrich, Dorset, UK**
Phorbol 12-myristate 13-acetate, PMA	**Sigma-Aldrich, Dorset, UK**
Phosphate buffered saline, PBS	**Oxoid, Basingstoke, UK**
Phospho Akt (ser473)	**New England Biolabs, Hitchin, UK**
Phospho p38 MAPK	**New England Biolabs, Hitchin, UK**
PI3K inhibitor (LY 294002)	**Cell Signaling Technology, Danvers, MA, USA**
Pierce supersignal west dura kit	**Fisher, Loughborough, UK**
Ponceau S solution	**Sigma-Aldrich, Dorset, UK**
Primers (LTR-2, LEXKO-1947-3' and LEXKO-1947-5')	**Sigma-Aldrich, Dorset, UK**
Protease inhibitor cocktail tablets	**Roche, Burgess Hill, UK**
Proteinase K	**Sigma-Aldrich, Dorset, UK**
Rainbow molecular weight markers	**Fisher, Loughborough, UK**
Reblot plus mild stripping solution	**Millipore, Watford, UK**
Reducing agent (5x)	**Invitrogen, Paisley, UK**
RM AFE 60%FAT 20%CP 20%CHO (M) 25kGy	**Special Diets Services (SDS), Witham, UK**
RPMI media	**Lonza, Wokingham, UK**
Sodium chloride	**VWR, Lutterworth, UK**

Sodium chloride (0.9%)	**Baxter, Thetford, UK**
Sodium dodecyl sulphate, SDS	**VWR, Lutterworth, UK**
Sodium fluoride, NaF	**VWR, Lutterworth, UK**
Sodium orthovanadate, Na3VO4	**Sigma-Aldrich, Dorset, UK**
Sodium phosphate, NaH_2PO_4	**Sigma-Aldrich, Dorset, UK**
Sodium pyrophosphate	**Sigma-Aldrich, Dorset, UK**
Thioglycollate	**Sigma-Aldrich, Dorset, UK**
Tri-sodium citrate	**Abcam, Cambridge, UK**
Tris (hydroxymethyl) methylamine, Tris	**VWR, Lutterworth, UK**
Tris-HCl	**Sigma-Aldrich, Dorset, UK**
Triton	**Sigma-Aldrich, Dorset, UK**
TRIzol reagent	**Life Technologies, Paisely, UK**
Tween-20	**Sigma-Aldrich, Dorset, UK**
Vectastain ABC-HRP reagent	**Vector Laboratories, CA, USA**
Whatman filter paper, grade 3	**Fisher, Loughborough, UK**
Xylene	**Sigma-Aldrich, Dorset, UK**

Appendix 2: Equipment

Avantic Centrifuge J-26 XP (Beckman, Germany)

BD Vacutainer (K2EDTA)(BD, USA)

C-Chip Disposable Hemocytometer (Digital Bio, Korea)

Chemi Genius2 Bio Imaging System (Syngene, UK)

Cytospin 2 (SHANDON, UK)

FACSCalibur (BD Bioscience, USA)

Fine insect pins (Fine Science Tools, Germany)

G-STORM (Gene Technologies, UK)

Laborlus Microscope (Leitz, Germany)

LEICA RM2135 Microtome (Leica, Germany)

Microfuge R Centrifuge (Beckman, Germany)

NanoDrop N1000 (Thermo Fisher Scientific, USA)

Nikon ECLIPSE E600 (Nikon Instruments Europe B.V., Amstelveen, The Netherlands)

Nikon SMZ1000 (Nikon Instruments Europe B.V., Amstelveen, The Netherlands)

Novex NuPAGE 4-12% Bis-Tris Gel (Life Technologies, USA)

NuPAGE Minutei-Cell Electrophoresis (Life Technologies, USA)

Plate Reader (Opsys MR, Dynex Technologies, USA)

Refrigerated Centrifuge PK 120 R (ALC, Italy)

Sysmex KX-21N Haematology analyser (Sysmex Corporation, Japan)

UW Sonicator (Ultrawave Ltd, UK)

Xcell IITM Blot Module (Life Technologies, USA)

Xcell SureLockTM Minutei-Cell (Life Technologies, USA)

Appendix 3: Software

CellQuest Pro version 3.01 (BD, USA)
GeneSnap version 7.04 (SynGene, UK)
GeneTools version 3.02 (SynGene, UK)
GraphPad PRISM software version 5.00 (GraphPad Software Inc, USA)
ND-1000 (Thermo Fisher Scientific, USA)
Nis-Elements (Nikon Instruments Europe B.V., Amstelveen, The Netherlands)
Revelation version 4.25 (Thermo Fisher Scientific, USA)